Instituto Tecnológico y de Estudios Superiores de Monterrey

Campus Estado de México

School of Engineering and Sciences

“Triborheological Analysis of Reconstituted Gastrointestinal Porcine Mucus / Chitosan:TPP Nanoparticles System for studying mucoadhesion under different pH conditions”.

A dissertation presented by

Gustavo Ruiz Pulido

Submitted to the
School of Engineering and Sciences
in partial fulfillment of the requirements for the degree of

Doctor of Philosophy

In

Nanotechnology

Mexico City, December 5th, 2022.

Dedication

This thesis work is dedicated especially to my parents, who have always been a great example of loyalty, honesty, work, and above all, they have always been there to support me in all my goals and dreams.

Also, I want to dedicate this thesis to a little boy who always dreamed about working in a lab, doing scientific experiments all day, and contributing with new knowledge to this world. I want to tell you: **We did it!**

Finally, I want to dedicate this great achievement to an old man who has lived in a roller coaster, who has suffered and worked hard to achieve his goals, but who has achieved a life full of satisfaction. To that man, I want to say: **Do you remember that this was the beginning of our journey?**

"There are only two people in this world that you need to make you proud: It's the 8 years old version of you, and the 8O years old version of you".

- Anonymous.

Acknowledgements

I would like to express my deepest gratitude to my supervisor, **Dr. Dora I. Medina**, for her guidance, encouragement, unconditional support, trust, and advice throughout the thesis project, the publications made, the conferences attended, and the entire turbulent journey that PhD implies in all aspects.

Thanks to **Dr. David Quintanar** for his support, ideas, and feedback during the project, for the access to the facilities of the 'Laboratorio de Posgrado en Tecnología Farmacéutica' (UNAM – FES Cuautitlán), and for his participation as a member of the evaluation committee.

I am infinitely grateful with **my parents** and **brother** for their unconditional support, their love, their faith, for encouraging me until the end despite the long nights and the difficult moments.

I would like to express my recognition to **my grandfather** †, who was a source of inspiration to improve myself, to pursue my dreams and to always give my best.

I would like to express my gratitude to **Dr Anai Valencia** for her advice, her valuable comments, and recommendations on this thesis project and during all the PhD path, as well as for her participation as a member of the evaluation committee.

I am thankful with **Dr. Josefina Castillo** for her loyalty, support, and faith along the development of the thesis projects, and for her participation as a member of the evaluation committee.

I would like to say thanks to **Dr. Cecilia Treviño** for her contributions to enrich the project and her support as a member of the evaluation committee.

I would like to thank my laboratory colleges and friends: **Jesús Alberto Martínez**, **Iván Avilés**, **Laura Duque**, **Katya Aguilar**, **Carolina Ramírez**, **Dilawar Hassan**, **Ayesha Sani**, **Diego Ceciliano**, and **Victoria Flores** for their help, support and contribution in the project and publications, as well as for the good, funny, stressful end memorable moments we lived throughout this adventure.

Many thanks for all the members of **Dr. Dora's Research Group** for their collaborative support during all the group meetings with the objective of enhancing the quality of this project.

Thank you for all the members of **Dr. David's Research Group** for their help and advice during the project development.

Sincere thanks to **Dr Dulce Melo** for her help and guidance for the use of different laboratory equipment, to **Ing. Mario Loperena** and **Ing. Antonio García** for his

support to carry out the Scanning Electron Microscopy, to **MSc Roberto Delgado** and biologist **Ramón Rivero** for their help during laboratory work.

I am sincerely grateful with all those people who always believed in me, who were there to encourage me and support me, who made this experience wonderful and unforgettable, who always showed me their loyalty and love, many thanks to **Nancy Orozco**, **Luis Martínez**, **Fernando Soledad**, **María Fernanda Leyva**, **Fernanda Vuga**, **Violeta Milán**, **Iñaqui Marrón**, **Juan Manuel de la Rea**, **Ximena Tomassini**, and all those people I had the fortune to meet during these four years.

I would like to express the gratitude to the **Tecnológico de Monterrey** for the support on tuition fees, the use of the facilities and academical tools required to carry out the project.

I would like to acknowledge the Mexican National Council of Science and Technology (Consejo Nacional de Ciencia y Tecnología - **CONACYT**) for their support for living expenses through the program 'Becas Nacionales'.

Finally, I want to thank life and **God** for all the opportunities, challenges, laughs, tears, learning and great memories that I take with me.

“Triborheological Analysis of Reconstituted Gastrointestinal Porcine Mucus / Chitosan:TPP Nanoparticles System for studying mucoadhesion under different pH conditions”.

by

Gustavo Ruiz Pulido

Abstract

The use of biodegradable polymers as vehicles for administration and long-term release of drugs has great relevance in the delivery of new generation therapeutic agents, such as: amino acids, peptides, proteins, antibodies, nucleic acids, among others. Because biomolecules are metabolized or excreted after short periods within the body, which are usually shorter than time required to observe their therapeutic effect or to reach the site of action. For that reason, the encapsulation of biomolecules in microspheres or nanoparticles represents a method of interest for biopharmaceuticals administration.

Additionally, the phenomenon of mucoadhesion has been studied as an alternative to increase the residence time of nanocarriers within the body and, consequently, increase the half-life and cell permeability of biomolecules, allowing them to reach the level of bioavailability necessary to carry out its therapeutic activity when administered orally.

Chitosan nanoparticles were analyzed as a possible mucoadhesive vehicle for drug delivery based on their cationic nature that exhibits a high degree of interaction with negatively charged mucus functional groups. However, chitosan presents significant changes in its surface charge throughout the gastrointestinal tract due to variations in pH, affecting its mucoadhesive properties.

This project proposed the analysis of the interaction between reconstituted gastrointestinal porcine mucus and chitosan:TPP nanoparticles under gastrointestinal pH conditions (pH = 2.0 – 7.0) from a triborheological point of view. Considering that rheological synergism represents an indirect method to evaluate the presence or absence of mucoadhesion phenomenon based on the strength of the interfacial layer between mucus and nanoparticles, which is measured by the increase of viscosity (η) or elastic modulus (G’) in the mixture of mucus-nanoparticles as a result of the interpenetration of polymeric and mucin chains through electrostatic interactions and physical entanglement, mainly.

Therefore, triborheological tests were performed to characterize the viscoelastic, viscous, and lubricating profiles of reconstituted mucus at different pH conditions to examine the variations experienced by the mucus along the gastrointestinal tract. Similarly, triborheological synergism analyzes were performed to determine under which pH values the mucoadhesion phenomenon occurs, revealing that chitosan:TPP exhibit mucoadhesiveness at conditions below its value of pKa (6.5). Whereas, under neutral environment or above to their pKa value, chitosan:TPP nanoparticles do not exhibit the mucoadhesion properties.

Keywords: *Triborheology, gastrointestinal mucus, chitosan nanoparticles, rheological synergism, mucoadhesion.*

“Análisis Triboreológico del Sistema de Mucosidad Porcina Gastrointestinal Reconstituida / Nanopartículas de Quitosano:TPP para estudiar la mucoadhesión bajo diferentes condiciones de pH”.

por

Gustavo Ruiz Pulido

Resumen

El uso de polímeros biodegradables como vehículo de administración y liberación prolongada de fármacos tiene gran relevancia en el transporte de agentes terapéuticos de nueva generación, como: aminoácidos, péptidos, proteínas, anticuerpos, ácidos nucleicos, entre otros. Debido a que, las biomoléculas son metabolizadas o excretadas tras períodos cortos dentro del organismo, que suelen ser menores que el tiempo requerido para observar su efecto terapéutico o para llegar al sitio de acción. Por ello, la encapsulación de biomoléculas en microesferas o nanopartículas representa un método de interés para la administración de biofármacos.

Adicionalmente, se ha estudiado el fenómeno de la mucoadhesión como una alternativa para aumentar el tiempo de residencia de los nanovehículos en el organismo y, en consecuencia, incrementar la vida media y la permeabilidad celular de las biomoléculas, permitiéndoles alcanzar el nivel de biodisponibilidad necesario para llevar a cabo su función, principalmente cuando se administran por vía oral.

Nanopartículas de quitosano se analizaron como un posible vehículo mucoadhesivo para la administración de fármacos en función de su naturaleza catiónica, que exhibe un alto grado de interacción con los grupos funcionales con carga negativa de la mucosidad. Sin embargo, el quitosano presenta cambios significativos en su carga superficial a lo largo del tracto gastrointestinal debido a variaciones en el pH, afectando sus propiedades mucoadhesivas.

Este proyecto propuso el análisis de la interacción entre la mucosidad gastrointestinal reconstituida y las nanopartículas de quitosano:TPP en condiciones de pH gastrointestinal (pH = 2,0 - 7,0) desde un punto de vista triborreológico. Considerando que el sinergismo reológico representa un método indirecto para evaluar la presencia o ausencia del fenómeno de mucoadhesión, basado en la fuerza de la capa interfacial entre la mucosidad y las nanopartículas, la cual se mide por el aumento de la viscosidad (η) o del módulo elástico (G') en la mezcla de mucosidad-nanopartículas como resultado de la interpenetración de cadenas poliméricas y de mucina, que se establece a través de interacciones electrostáticas y entrelazamientos físicos, principalmente.

Por lo tanto, se realizaron pruebas triborreológicas para caracterizar los perfiles viscoelástico, viscoso y lubricante de la mucosidad reconstituida en diferentes condiciones de pH para examinar las variaciones que experimenta a lo largo del tracto gastrointestinal. De igual manera, se realizaron análisis de sinergismo triboreológico para determinar bajo qué valores de pH ocurre el fenómeno de mucoadhesión, revelando que el quitosano:TPP exhibió una fuerte mucoadhesión en condiciones altamente ácidas, por debajo de su valor de pKa (6.5). Mientras que, en condiciones neutras o cercanas a su valor de pKa, la mucoadhesividad de las nanopartículas de quitosano:TPP fue insignificante.

Palabras clave: *Triboreología, mucosidad gastrointestinal, nanopartículas de quitosano, sinergismo reológico, mucoadhesión.*

List of Figures

Figure 1.1. Biopharmaceutics Classification System (BCS) **2**

Figure 1.2. Absorption of drugs through the intestinal mucus after being administered orally ... **2**

Figure 1.3. Comparison between the bioavailability of a drug at the absorption site after oral administration of a) the drug alone and 2) the drug encapsulated in nanoparticles **3**

Figure 1.4. Schematic comparison between the structure of commercial (reconstituted) and native mucus **8**

Figure 2.1. Classic frequency response for: a) solid – like behavior, b) gel – like behavior, and c) liquid – like behavior **13**

Figure 2.2. Different flow and viscosity behaviors of Newtonian and non-Newtonian behaviors (Bingham plastic, dilatant and pseudoplastic) **14**

Figure 2.3. Viscosity-shear rate characteristic curve of a polymer undergoing shear thinning . **15**

Figure 2.4. Stribeck curve showing the three different lubrication regimes: boundary lubrication, mixed lubrication, and hydrodynamic lubrication **16**

Figure 2.5. Cone and plate rheometer **17**

Figure 2.6 Schematic structure of membrane-associated mucins. **19**

Figure 2.7. A graphical representation of the thickness of firmly adherent and loosely adherent mucus layers in the rat gastrointestinal tract in vivo. **20**

Figure 2.8. Mucin is subject to conformational changes dependent on environmental pH **23**

Figure 2.9. The permeability of nanoparticles through mucus is limited by different types of barriers and physicochemical interactions, including: a) electrostatic interactions; b) formation of hydrogen bonds; c) exclusion by size; and d) hydrophobic interactions **25**

Figure 2.10 Schematic representation of a drug-loaded polymeric nanoparticles: nanocapsule and nanosphere **26**

Figure 2.11. Chemical structure of chitosan. **27**

Figure 2.12. Schematic representation of the mucoadhesion mechanism between a cationic nanoparticle and a mucus layer **29**

Figure 2.13. Schematic representation of the six main theories to explain the phenomenon of mucoadhesion: (1) the wetting theory, (2) the electronic theory, (3) diffusion theory (4) absorption theory, (5) the fracture theory, and (6) the mechanical theory **31**

Figure 2.14. Comparison between a positive and a negative synergism to determine the presence or absence of the mucoadhesion phenomenon **33**

Figure 3.1 Protocol used for preparing reconstituted gastrointestinal porcine mucus **34**

Figure 3.2 Protocol used for synthesis of chitosan:TPP nanoparticles through ionic gelation method. **35**

Figure 3.3 Malvern Zetasizer Nano ZS instrument used for measuring particle size, polydispersity index and zeta potential **36**

Figure 3.4. JEOL JSM 6360 Scanning Electron Microscope used for visualizing nanoparticles morphology **37**

Figure 3.5 Discovery Hybrid Rheometer (DHR-3) using a Cone-And-Plate geometry (0.9969°) for testing viscoelastic and viscous performance of reconstituted mucus, chitosan:TPP nanoparticles and the mixture of mucus / nanoparticles **38**

Figure 3.6. Discovery Hybrid Rheometer (DHR-3) using a Plate-And-Plate geometry for testing the lubricant profile of reconstituted mucus, chitosan:TPP nanoparticles and the mixture of mucus / nanoparticles. **40**

Figure 4.1. Rheological analysis of the viscoelastic performance of reconstituted mucus in the angular velocity range of 0.1 – 100 rad/s at 37°C under different pH conditions. **41**

Figure 4.2. Interactions related with mucin rodlike conformation and 'weak' gel behavior of mucus under acidic conditions **42**

Figure 4.3. Interaction related with mucin random coil conformation and polymeric solution behavior of mucus under neutral conditions **43**

Figure 4.4. Rheological analysis of the viscous performance of reconstituted mucus in the shear rate range of 0.1 – 1000s^{-1} at 37°C under different pH conditions: pH 2, pH 4, pH 6 and pH 7 **44**

Figure 4.5. Evaluation of the lubricant properties of reconstituted mucus by plotting an Stribeck curve in the angular velocity range 0 – 50 rad/s, at 37°C under different pH conditions..... **46**

Figure 4.6. SEM images of a) Freeze-dried chitosan:TPP nanoparticles, and b) Dispersed chitosan:TPP nanoparticles..... **48**

Figure 4.7. Evaluation of the mucoadhesion of chitosan:TPP nanoparticles by rheological synergism from the point of view of the elastic modulus (ΔG')..... **50**

Figure 4.8. Influence of pH on the solubility of chitosan..... **51**

Figure 4.9. Evaluation of the mucoadhesion of chitosan:TPP nanoparticles by rheological synergism from the point of view of the apparent viscosity (Δη). **53**

Figure 4.10. Comparative evaluation of coefficient of friction (CoF) of the reconstituted mucus alone and the mixture of reconstituted mucus – chitosan:TPP nanoparticles at 37°C under different pH conditions **55**

List of Tables

Table 2.1. Average thickness of the different layers of mucus found in the stomach and intestines **20**

Table 3.1. Mean particle size, polydispersion index (PDI) and zeta potential measurements of chitosan:TPP nanoparticles dissolved under different pH conditions **47**

Table 3.2. Comparison of the CoF values among reconstituted mucus alone and the mixture of reconstituted mucus - chitosan:TPP nanoparticles during the different lubrication regimes considering the variations in the pH conditions **54**

Contents

Declaration of Authorship i
Dedication ii
Acknowledgements iii
Abstract v
Resumen vi
List of Figures vii
List of Tables ix
Table of Contents x

1 Introduction 1
1.1 Motivation 4
1.2 Problem Statement and Context 5
1.3 Hypothesis 6
1.4 Research Questions 6
1.5 Objectives 7
2.3.1 General Objective 7
2.3.1 Specific Objective 7
1.6 Scope and Limitations 7
1.7 Solution Overview 9
1.8 Main Contribution 9

2 Theoretical Framework 11
2.1 Triborheology 11
2.2 Rheology 11
2.3 Tribology 15
2.4 Cone-And-Plate Geometry 17
2.5 Gastrointestinal Mucus 18
2.6 Mucus Rheological Properties 21
2.7 Mucus Structural Changes Influenced by pH 22
2.8 Transmucosal Drug Delivery 24
2.9 Polymeric Nanoparticles 25
2.9.1 Chitosan Nanoparticles 27
2.10 Mucoadhesion Phenomenon 28
2.11 Rheological Synergism 32

3 Materials and Methodology 34
3.1 Materials 34
3.2 Preparation of Reconstituted Mucus (5% Mucin Solutions) 34
3.3 Synthesis of Chitosan:TPP Nanoparticles by Ionic Gelation Method 35
3.4 Characterization of Chitosan:TPP Nanoparticles 36

3.4.1 Nanoparticle Size, Polydispersity Index and Zeta Potential Measurement .. 36
3.4.2 Scanning Electron Microscopy (SEM)..... 37
3.5 Rheological Profiling of Reconstituted Mucus 37
3.6 Rheological Synergism..... 38
3.7 Triborheological Profiling of Reconstituted Mucus 39
3.8 Statistical Analysis 40

4 Results and Discussions 41
4.1 Triborheological Analysis of the Reconstituted Mucus Samples at Different Gastrointestinal pH Values 41
4.2 Chitosan:TPP Nanoparticles Synthesis and Characterization 46
4.2.1 Particle Size, Polydispersity Index and Zeta Potential Measurement 47
4.2.2 Morphological Characterization..... 48
4.3 Assessment of Chitosan Nanoparticle – Mucus Interaction through Rheological Synergism 49
4.3.1 Rheological Synergism..... 49
4.3.2 Triborheological Synergism..... 53

5 Conclusions..... 56

Bibliography..... 58

Published Papers 79

Curriculum Vitae 81

Chapter 1. Introduction.

During last thirty years, the development of drugs has grown significantly with the appearance of drugs of new generation and biopharmaceuticals, such as: amino acids, peptides, recombinant proteins, nucleic acids, monoclonal antibodies, enzymes, among others. This new class of drugs offers advantages of high selectivity and therapeutic efficacy, showing fewer side effects, in comparison with small molecules [1].

However, the conversion of drugs and active compounds into medicines frequently is delayed because the delivery process of a drug can considerably affect its therapeutic activity. As well, drug delivery systems should cross several biological barriers before reaching the site of action [2]. Highlighting that biopharmaceutical drugs face critical problems during administration and storage, producing loss of activity in response to exposure to light, humidity, pH or temperature changes [3], [4]. For that reason, the research of new kind of drug delivery vehicles have acquired extreme relevance. Since oral delivery represent one of the main targets for designing drug delivery nanocarriers because it represent the preferred administration route since it allows self-medication, which is highly convenient, easy and comfortable for the patients [5].

Otherwise, most drugs need to reach the systemic circulation for achieving the bioavailability required for developing their therapeutic activity [1]. The main challenges for oral administration of drugs is the presence of mucus, which represents a complex biological barrier that acts as selective permeable barrier to protect the wet epithelium of the gastrointestinal tract and the entrance to the systemic circulation, as well as, the acidic pH of the stomach which can degrade therapeutic agents [6].

As well, mucus acts as a lubricant for the epithelium allowing the passage of food through the tract, as a moisturizing layer for the epithelium, even, as a filter that protects tissues and blood against pathogens and external substances while it mediates the exchange of nutrients and gases. So, its properties reduce the effectiveness of the therapeutic agents by affecting drug delivery methodology [7]–[9]. Highlighting the poor oral bioavailability which sometimes is limited > 1% as a result of the low absorption and rapid clearance within the gastrointestinal tract [10].

Emphasizing the importance of the correlation between aqueous solubility and intestinal permeability in order to identify possible absorption problems after oral administration [11], the biopharmaceutical classification system (BCS) was proposed in 1995 with the purpose to classify drugs in four classes based on their in vitro solubility and intestinal permeability [12], [13], as Figure 1.1 shows. Moreover, BCS acquires a key role in the improvement and development of drug delivery

carriers, considering that approximately between 70 and 90% of new generation drugs belong to classes II and IV (low solubility) [14].

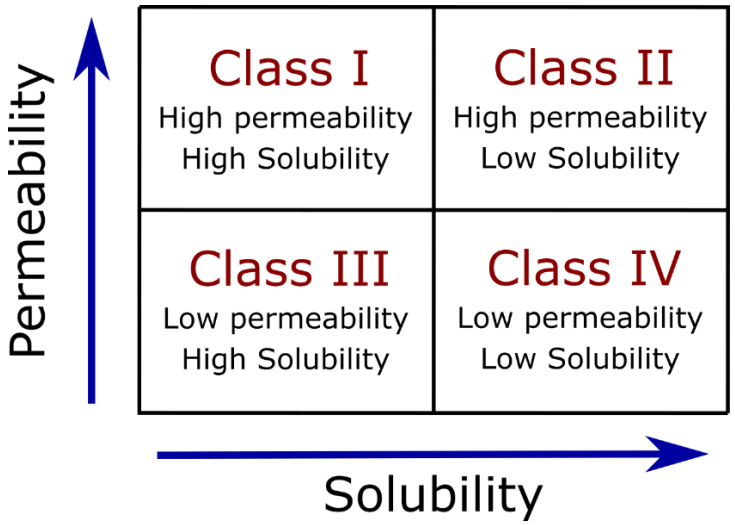

Figure 1.1. Biopharmaceutics Classification System (BCS).

Therefore, new and promising formulations have been emerged to optimize the efficiency of drug delivery by improving the stability, solubility, therapeutic concentration, permeability and drug absorption through the mucus of the small intestine, to be subsequently absorbed by the enterocytes and transported to the bloodstream (Figure 1.2), from where it can reach the site of action. While, they reduce the effects produced by drug toxicity, and even allow long-term release of the active pharmaceutical compound [1], [15]–[17].

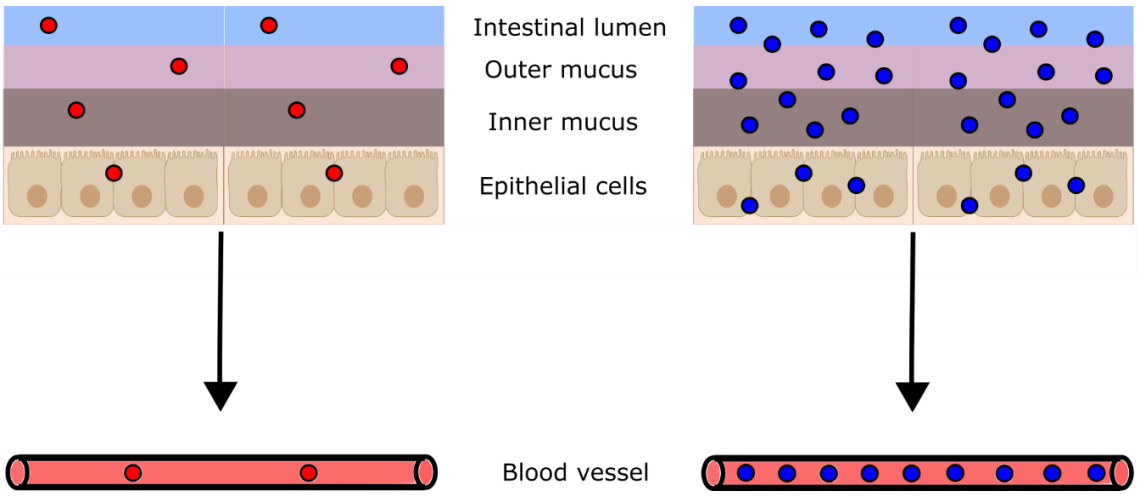

Figure 1.2. Absorption of drugs through the intestinal mucus after being administered orally. a) Drug with low permeability (red dots) through mucus and rapid clearance within the gastrointestinal tract, and b) drug with a high degree of penetration through mucus (blue dots), reaching high bioavailability in the blood flow, and adequate efficacy.

Among these drug delivery methods, polymeric nanoparticles have emerged as a strategy with great potential (Figure 1.3) to deliver drugs across mucus [18], based on their particular properties, such as biocompatibility, the ability to protect the drug from degradation due to environmental conditions, excellent encapsulation efficiency, longer duration in blood circulation, improved bioavailability, reduced toxicity, design flexibility based on functionalization (to control particle size, adjust solubility, improve stability or enhance site specific targeting properties), and controlled release [19]–[22]

Chitosan-based nanoparticles has been widely explored as an appropriate nanocarrier for mucosal routes due to its low toxicity, tunable physical properties, small particle size and mucoadhesive characteristics. Additionally, chitosan has been approved by the US FDA for various applications, including drug delivery due to its biocompatibility [23], [24].

Nonetheless, chitosan possesses high amount of primary amino groups, which are protonated under its pKa value (~6.5) and are intimately related with chitosan charge and physicochemical properties, including solubility and mucoadhesion profile [25]. So, chitosan stability represents a critical factor to consider during pharmaceutical applications [26]. Since, chitosan would be exposed to significant fluctuations in the pH along the gastrointestinal tract, which plays a critical role in its stability because as the pH approaches neutral values (mainly in the intestine), the size of chitosan nanoparticle suddenly increases [27] and the mucoadhesive potential of the nanoparticles is reduced [28], [29].

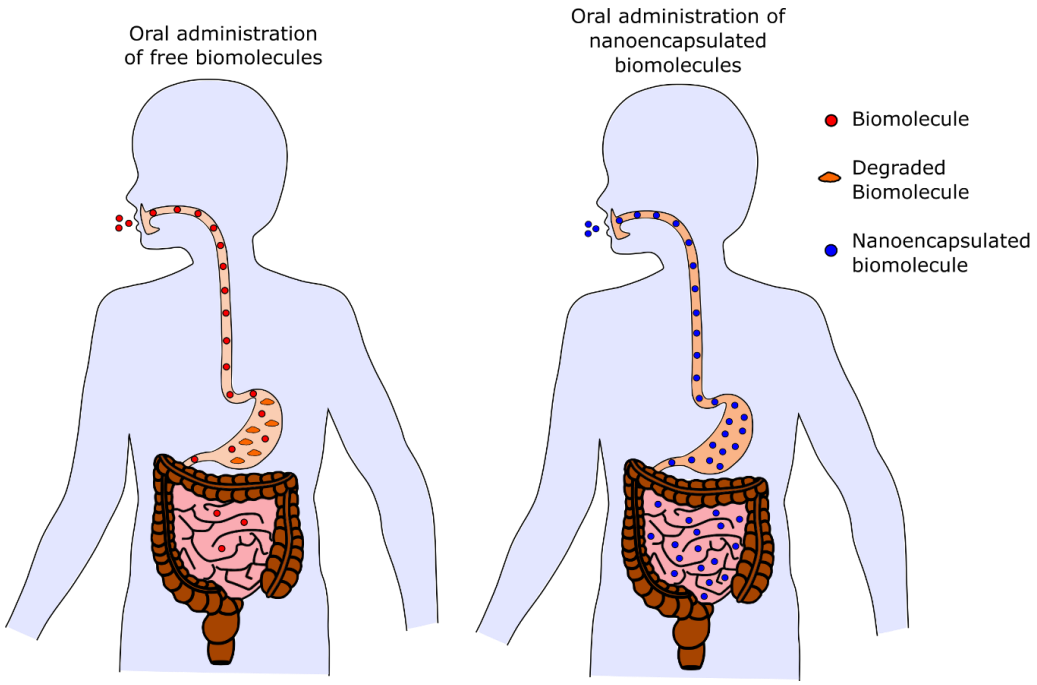

Figure 1.3. Comparison between the bioavailability of a drug at the absorption site (small intestine) after oral administration of a) the drug alone and 2) the drug encapsulated in nanoparticles.

For that reason, the project focus on analyzing the mucoadhesion properties of chitosan under the fluctuating pH conditions of the gastrointestinal tract, considering pH values in the range 2.0 – 7.0 to mimic body conditions. Thus, rheological synergism represents a useful in vitro parameter to establish the presence of the mucoadhesive phenomenon based on the strength of the mucoadhesive interaction [2], [30], [31] by calculating the rheological synergism parameter (Δη) after measuring the variations in the viscosity between mucin solutions, chitosan nanoparticles solution and the mixture mucin – chitosan nanoparticles [32]. A positive rheological synergism indicates a significant interaction between mucin and the nanoparticles [33]; while, a negative rheological synergism is related with not functional adhesion [30].

Also, chitosan nanoparticles should interact with mucus without affecting its main properties, so it still protects the body from potentially damaging environmental agents or shear rate forces during digestion [34]. Because mucus tends to exhibit a shear thinning pseudoplastic behavior regarding the pH [35], which is associated with a reduction in the coefficient of friction (CoF) [36]. Therefore, the apparent viscosity and frictional behavior (CoF) of the mucoadhesive mixtures were evaluated under different gastrointestinal pH conditions to analyze if the bio-tribological properties of gastrointestinal mucus are affected by mucoadhesion phenomenon.

1.1 Motivation

Gastrointestinal tract (mainly upper small intestine) represents the best absorption place for many drugs because of microvilli [37], so developing specific oral drug delivery vehicles for targeting the stomach or intestines would improve the efficacy of the medicine in a significant way. Additionally, oral delivery offers substantial advantages over other routes based on its high patient acceptability and painless administration [38]. However, a mucus layer covers all the wet epithelium of gastrointestinal tract, acting as a physiological barrier with different biological functions, including protection against foreign molecules and particles [39].

Thus, the study of mucus is determinant to deeply understand the drug delivery through gastrointestinal tract (GIT) for optimizing drugs distribution vehicles without affecting mucus fundamental protective, cleaning, and lubricant properties [40]. Because any particle that reaches the GIT can establish different non-covalent interactions with mucus, such as size exclusion [9], hydrogen bond formation [1], electrostatic [8] and hydrophobic interactions [10]. The presence of those interactions modify the physicochemical properties of mucus, and consequently, its viscoelastic properties [1], [10], which are intimately related with the protective and lubricant properties provided to the epithelial surfaces [41]. Therefore, the gastrointestinal tract can be considered as a complex triborheological apparatus that

involves the flow of layers of mucus, different liquids, and food elements with very different consistencies, textures, and frictional behaviors that undergoes viscoelastic, viscous and lubricant variations along the tract [42].

Otherwise, polymeric nanoparticles have been widely investigated for drug delivery purposes based on their properties, such as small size and the capability to protect drugs from degradation [1] with low toxicity and high biocompatibility [43]. Emphasizing that the use of some biopolymers as delivering active agents have acquired a lot of attention for administering therapeutic molecules via mucosal membranes due to their mucoadhesive properties, which are related with a prolonged gastrointestinal retention, enhanced bioavailability, and increased duration of drug release [47]. Chitosan represents one of the most studied mucoadhesive polymers [44], representing an attractive alternative for non-invasive drug administration routes, such as: nasal, oral, ocular, and pulmonary delivery [79].

Therefore, the use of chitosan nanoparticles as possible oral administration vehicle for new generation biomolecules, represents a great opportunity to improve their bioavailability. However, the mucoadhesive profile of chitosan nanoparticles must be evaluated under the different acidic conditions of the gastrointestinal tract (pH = 1.0 – 8.0) to know the feasibility for the use of this nanocarrier for oral delivery, and the site within the gastrointestinal tract where it exhibits better mucoadhesiveness, considering that the pH can alter its properties. So, rheological tests are useful for evaluating the strength of the interactions established between gastrointestinal mucus and particles of interest (in this case: chitosan:TPP nanoparticles) through rheological synergism method, which is based mainly in the changes of viscosity ($\Delta\eta$) and viscoelastic modulus ($\Delta G' / \Delta G''$) [45].

1.2 Problem Statement and Context

Since thirty years ago, the development of novel drugs has grown significantly with the emergence of biopharmaceuticals [43]. Nonetheless, the approval and use of new molecules for therapeutic purposes has recently decreased due to the complexity of formulation, storage, and administration of these biomolecules [46]. Consequently, the research of drug delivery alternatives has focused on countering the different challenges that new generation drugs face, including: large size, high molecular weight, complexity, sensibility to degradation, limited absorption, poor bioavailability, reduced aqueous solubility, restricted permeability across mucosal surfaces, short half-life, and first-pass metabolism by the liver [47].

Otherwise, the most studied vias for targeting drug delivery vehicles are ocular, nasal, gastrointestinal and upper airways because they represent easy and comfortable methods of drug administration for the patients [48]. Emphasizing that the administration of drugs through oral route is considered the most convenient and

accepted way, mainly when constant administrations are required due to it is low invasive, less painful, easy to administrate, it does not require the intervention of a specialist and low-cost manufacturing [7], [49].

However, intravenous administration remains the most effective route of administration, as it enters directly into the blood circulation, allowing higher concentration and enhanced bioavailability of the drug [50], [51]. Whereas, the oral administration of various therapeutic agents presents significant disadvantages due to the hostile environment that the gastrointestinal tract represents, where the large amount of proteolytic enzymes and the high levels of acidity tend to degrade the therapeutic agents [28], [52]. In addition, the tight junctions (TJ) and efflux pumps (such as P-glycoprotein) present in the intestinal enterocytes restrict the paracellular and transcellular transport of drugs, decreasing drug bioavailability [53]. Even, the short and unpredictable gastric retention time represents a major problem because the effectiveness of the administered drugs can be decreases by an incomplete release at the absorption site, which could be the stomach or the small intestine depending on the molecules properties [54].

1.3 Hypothesis

Chitosan:TPP nanoparticles represent promising alternatives for the oral administration of biopharmaceuticals because they allow the drug to reach the site of absorption (stomach or intestine) and adhere for a long time for a sustained drug release of the drug, without affecting or damaging the structure of the mucus.

1.4 Research Questions

The thesis proposes the following research questions:

- How do pH variations along the gastrointestinal tract affects the viscoelastic, viscous and lubricant profile of reconstituted mucus?

- Do chitosan:TPP nanoparticles affect the viscoelastic, viscous or lubricating properties of reconstituted mucus?

- Do chitosan:TPP nanoparticles exhibit mucoadhesion phenomenon under gastrointestinal tract pH conditions?

- How does gastrointestinal tract pH affect chitosan:TPP mucoadhesion properties?

- Do chitosan:TPP nanoparticles represent a feasible nanocarrier for oral drug delivery?

1.5 Objectives

1.5.1 General objective.

To analyze the interactions between the reconstituted gastrointestinal mucus and chitosan:TPP nanoparticles through triborheological synergism tests under acid conditions that mimic the human gastrointestinal tract to determine the degree of mucoadhesion of chitosan:TPP nanoparticles with the purpose of evaluating their potential as an alternative during the oral administration of different biomolecules.

1.5.2 Specific objectives.

- To study the viscoelastic, viscous, and lubricant profiles of reconstituted mucus under different pH conditions.

- To characterize physicochemical properties of chitosan:TPP nanoparticles.

- To evaluate mucoadhesive interactions between chitosan:TPP nanoparticles and reconstituted mucus under different pH values.

- To determine how mucoadhesion phenomenon alters the triborheological profile of reconstituted mucus – chitosan:TPP system.

1.6 Scope and Limitations

Rheology measurements are commonly used for evaluating and comparing the viscoelastic features of biopolymers, such as mucus. As well, rheology allows to analyze the mucoadhesive profile of several polymers. However, the use of rheology alone for mucoadhesive measurements is limited [55], since rheology tests must be complemented with other characterization techniques, including Atomic Force Microscopy (AFM)y, tensile force measurements or flow-through method [56], [57], among others techniques. Because the presence of the mucoadhesive phenomenon is intimately related with the origin (native or commercial), the concentration and the preparation method of the mucus [41].

Additionally, the characterization of mucus rheological properties is difficult because any minimal modification in its constituents, significantly alters

physicochemical properties and performance. Thus, the rheological behavior of mucus is affected by: variations between organisms (batches), purification methodologies, and characterization techniques [7], [58], [59].

Native mucus exhibit poor reproducibility due to the great variability between batches because their exact composition differs among organisms [2], since mucus properties are dependent on diet, age, sex, or disease state of the organism. As well, isolation techniques directly affect mucus properties through protein denaturation and the elimination of salts or other minor elements that are intimately associated with mucus viscoelastic characteristics and gel formation properties [60]. Consequently, isolation techniques produces high polydispersity among mucus samples, representing a critical issue in the obtention of representative mucus samples [59] by altering the proportion of soluble and insoluble mucins through modifications in their charge distribution and molecular weight [61].

Whereas, reconstituted mucus is prepared with commercial mucin (obtained from SIGMA-ALDRICH®), presenting low variability between batches and allowing the obtention of standardized results [62]. Nevertheless, reconstituted mucus is unable to replicate the exact rheological and filtering properties of native mucus [63], even in concentrations above the physiological values (5% wt) [58]. Mainly, because the purification procedures alter the physicochemical properties of mucin, probably as a consequence of chemical purification or fragmentation with proteases, resulting in irreversible changes and loss of essential elements of the mucus (Figure 1.4), which limits the reconstruction of the primary structure of the mucin chains after rehydration [35], [64].

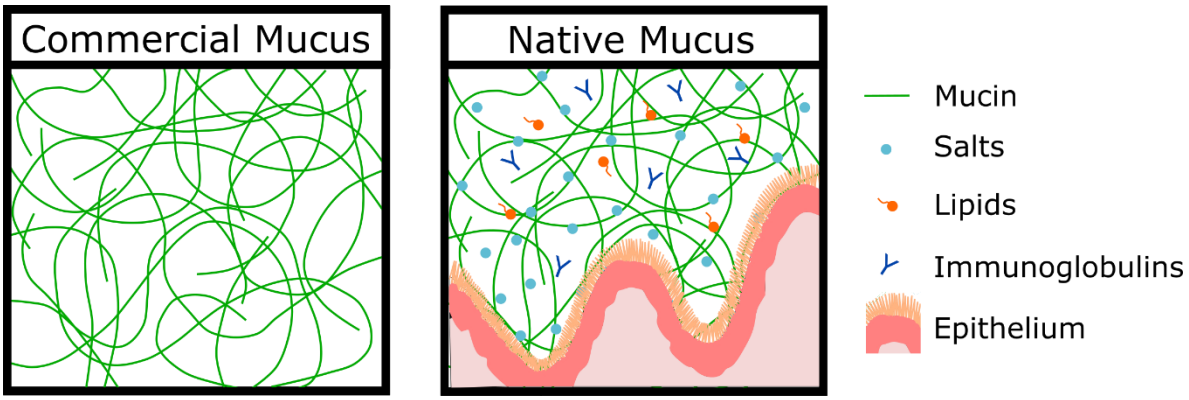

Figure 1.4. Schematic comparison between the structure of commercial (reconstituted) and native mucus. The reconstituted mucus mainly corresponds to a mucin solution, since during the aggressive mucus isolation procedures several molecular components are lost, resulting in irreversible changes that limit the reconstruction of the primary structure of the mucosal chains after rehydration. In contrast, the native mucosa largely maintains its natural components intact due to it is obtained directly from organism [65].

Otherwise, the interactions that are intimately associated with mucoadhesion phenomenon are not well understood. Since, cationic molecules usually present an important interaction with negatively charged mucin [34]. But different studies have shown that molecules with both positive and negative charges on their surface tend to exhibit stronger interactions than those molecules with a single charge (even if it is positive) [66]. Therefore, rheological synergism has emerged as an useful methodology for studying mucoadhesion in vitro, independently of the variations between mucus samples, since higher rheological synergism is associated with stronger interactions between mucus and polymeric nanoparticles [2].

Nevertheless, the interpretations of rheological synergism depend on the concentrations of mucus and mucoadhesive polymer [55], because a concentration of the polymer above the critical value presents high viscosity, which can mask the rheological synergism with the rheological properties of the polymer alone [67].

1.7 Solution overview

The study of the mucoadhesion phenomenon that occurs between the chitosan nanoparticles and the gastrointestinal mucosa allows optimizing the use of this nanovehicles for the oral administration of drugs, considering the conditions to ensure a proper delivery of the drugs. Due to there are parts of the gastrointestinal tract that exhibit mucoadhesion (acidic environment), and parts in which nanoparticles tend to collapse (neutral or alkaline environment). Moreover, the triborheological analysis allows us to visualize how the nanoparticles adhesive performance alters the lubricating profile of the mucus, a situation that must be considered when using the nanoparticles to administer drugs in order to avoid damaging mucus protective properties or to reduce side effects during drug administration.

1.8 Main Contribution

The mucoadhesive profile of chitosan:TPP nanoparticles has been analyzed in an general way through rheological synergism, and it has been established that chitosan is a mucoadhesive material. However, this project studies in more detail the mucoadhesive behavior of chitosan throughout the gastrointestinal tract, identifying that variations in pH conditions can be limiting in the use of chitosan nanoparticles for oral administration. Since the intestine reaches neutral or slightly alkaline environmental conditions, causing the loss of mucoadhesiveness, and the collapse of the nanoparticles.

In addition, a triborheological analysis was carried out to complement the study and provide a more complete characterization by identifying how

mucoadhesion phenomeno established by chitosan:TPP nanoparticles and gastrointestinal pH alter the lubricating properties of mucus. This knowledge allows a deeper understanding of the behavior of this nanovehicle in terms of improving its properties, while reducing weaknesses so that in the future it will be a viable alternative for oral administration of different biomolecules.

Chapter 2. Theoretical Framework

2.1 Triborheology

Triborheology is a new science that involves a multi-variate approach by coupling two complementary sciences: tribology and rheology, providing a more complete and robust analysis of the mechanical properties of a specific material [68]–[70]. Even triborheology has been suggested as a possible technique to deeply characterize various systems (including industrial and biological systems), which are not fully explained by rheological properties. Since, multiple systems also imply behaviors of surface tension, wear and friction-lubrication due to the textures and roughness present in the interacting surfaces [71].

In addition, various studies have established that the apparent viscosity performance of viscoelastic materials is particularly correlated with lubrication regimes, mainly with the hydrodynamic regime [72]. Since, the samples are evaluated under not constant combinations of applied force and sliding speed, they present a variable flow behavior which is closely related to the large-scale sample response and deformation [73], [74], affecting the friction, wear and lubrication among surfaces that are in relative motion [75], [76]. Considering that increasing shear rate and temperature variations (caused by friction), modifies the properties of samples (mainly fluidic samples) and alters its viscosity and viscoelastic properties [77].

Therefore, triborheology can be described as the study of the relative motion of two surfaces separated by viscoelastic fluid between them, considering the friction and wear generated under a load applied at a certain sliding speed [78].

2.2 Rheology

Rheology comes from the Greek word *rheos* which means ‘to flow’, and it is based on Heraclitus quote ‘everything flows’. Certainly, every material flows but at different proportion depending on how much force, in which direction, and for how long it is applied [79]. So, rheology is focused on studying how matter flows (solids, liquids, and gases) and how it deforms or change its shape under the influence of specific stresses or forces, showing a characteristic mix of elastic, viscous and plastic behavior for each material [45], [80].

Thus, the purpose of rheology is to predict how material will deform as a function of force, time, and spatial orientation [79]. To study rheological phenomena, "rheological state equations" or "constitutive equations" have been established in

order to evaluate the mathematical relationship between forces and the geometric effects induced by those said forces [44].

One of the simplest constitutive equations for describing the relation among force and deformation is Hooke's law:

$$\tau = G\,\gamma \tag{2.1}$$

where τ is the force per unit of area (stress), γ is the relative length change (strain), and G is the constant of proportionality (elastic modulus), which is an intrinsic property of solid materials [46].

Instead, the simple constitutive equation used for representing liquids behavior is Newton's law of viscosity:

$$\tau = \eta\,\dot{\gamma} \tag{2.2}$$

where τ represents the force per unit of area (stress), $\dot{\gamma}$ is the relative length change (strain), and η is the constant of proportionality (Newton viscosity), which represents an intrinsic property of liquids [46].

Hooke's and Newton's laws describe ideal elastic behavior for solids (mainly metals and ceramics) and viscous behavior for liquids (water and some oils), respectively. However, real soft materials are unable to behave as ideal solids or liquids, since they usually present both elastic and viscous responses, so they are called viscoelastic materials, such as colloidal suspensions, emulsions, polymeric networks, among others [81].

Thus, for understanding more about real soft materials that shows a non-ideal performance, is essential to perform dynamic rheological analysis, which evaluate the viscoelastic properties of the sample through two dynamic moduli: storage modulus (G') and loss modulus (G'') [82].

The storage or elastic modulus (G′) measures the deformation energy stored in the material during the shear process. Whereas the loss or viscous modulus (G″) measures the deformation energy consumed in the material during the shear and lost in the sample due to dissipation.

In this case, if G' is greater than G'', the sample exhibits a solid-like behavior with the ability to recover its shape. Instead, if G'' is greater than G', the sample presents a liquid-like performance with low resistance to flow [83]. Emphasizing that in case G' dominates throughout the test without showing frequency dependence, the behavior of the sample is considered a gel-like performance [84], as Figure 2.1 shows [85].

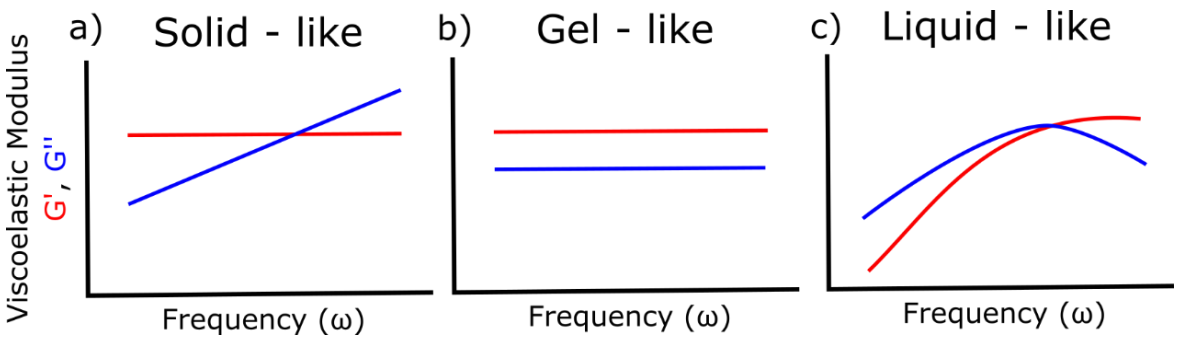

Figure 2.1. Classic frequency response for: a) solid – like behavior, the sample exhibits the ability to recover its initial shape (initial G' > G''), b) gel – like behavior, the sample presents a frequency dependence (dominant G' > G''), and c) liquid – like behavior, the sample shows low resistance to flow (initial G'' > G'). Red lines correspond to the elastic modulus (G'), and blue lines corresponds to the viscous modulus (G'').

Moreover, the rheological properties of the polymers are closely associated to their chemical structures. Because the viscosity of a polymer is proportional to its molecular weight or its concentration, since a high molecular weight or a concentration above the critical value is associated to a more complex entanglement of the polymeric chains, and therefore, the polymer presents a high viscoelastic profile [86] due to polymer chains take a longer time to separate and flow [87].

On the other hand, viscosity represents a critical parameter to classify fluids according to their flow properties under an externally applied pressure or under the action of shear stress. Based on their viscous behavior, fluids are classified as Newtonian and non-Newtonian (Figure 2.2) [88]. Newtonian fluids exhibit a direct proportionality between stress (τ) and strain rate (γ) in laminar flow:

$$\boldsymbol{\tau = \mu \dot{\gamma}} \tag{2.3}$$

where $\boldsymbol{\mu}$ is the viscosity constant, which is independent of the strain rate [89].

Instead, the behavior of non-Newtonian fluids is neither linear nor constant, but which is dependent on the flow conditions (geometry, shear rate, temperature or applied pressure) [90]. Non-Newtonian fluids are classified into three general groups based on their flow behavior:

1) Viscoplastic behavior (Bingham plastic) describes a fluid that deforms or flows upon exceeding a stress limit (called yield stress, σ_0). The sample tends to exhibit an elastic solid behavior when the applied external stress is lower than the yield stress, σ_0. In contrast, when the external applied stress exceeds the

value of σ_0, the fluid acquires a Newtonian performance with a constant value of viscosity (η), or shear thinning properties, $\eta(\gamma)$ [90], [91].

2) Shear-thickening (dilatant) behavior refers to those solutions that exhibited an abrupt increase in their viscosity as shear rate or applied stress is increasing as a result of an order-disorder transition that leads to an aggregation phenomenon, such as starch dispersions, silica suspensions or multi-walled carbon nanotubes [92].

3) Shear-thinning (pseudoplastic) behavior corresponds to a decrease in viscosity with increasing shear rate. Because during shear-induced motion, the crosslinked polymeric molecules stretch, partially disentangle, and orient themselves in the shear direction, exhibiting less flow resistance and hence, lower viscosity [93].

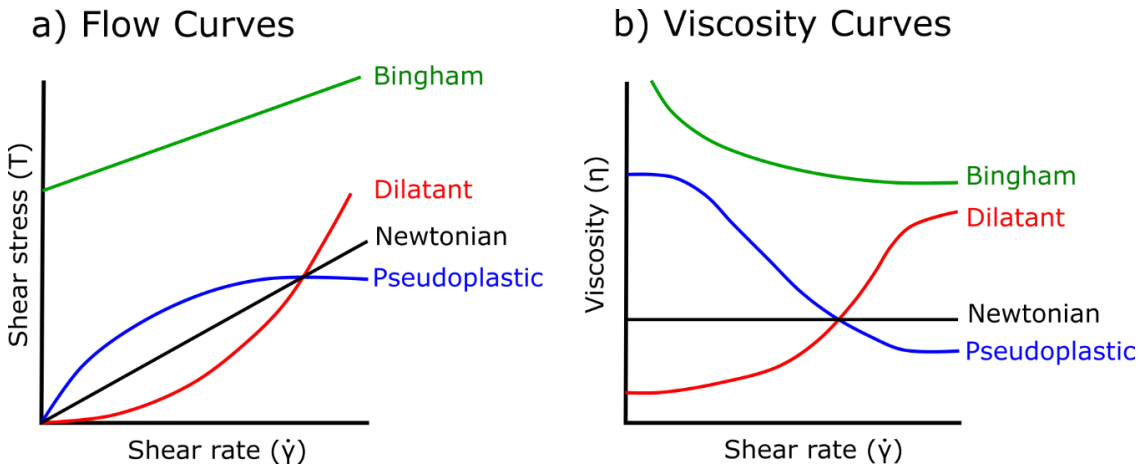

Figure 2.2. Different flow and viscosity behaviors of Newtonian and non-Newtonian behaviors (Bingham plastic, dilatant and pseudoplastic). Newtonian fluids exhibit a constant viscosity no matter the amount of the shear applied. Bingham plastic (viscoplastic) behaves as a rigid solid at low shear rate but flows as a viscous fluid at high shear rate. Dilatant (shear-thickening) exhibit a sudden increase in its viscosity as shear rate increases. Pseudoplastic (shar-thinning) presents a decreasing viscosity as shear rate in increasing.

Otherwise, polymers often manifest shear thinning behavior due to polymer are entangled mesh networks that tends to disentangle and orient along the flow direction when enough deformation force is applied, as Figure 2.3 shows. Nevertheless, the second Newtonian Plateau is rarely observed experimentally because the required shear values are very high and usually outside the measurement range [94], [95].

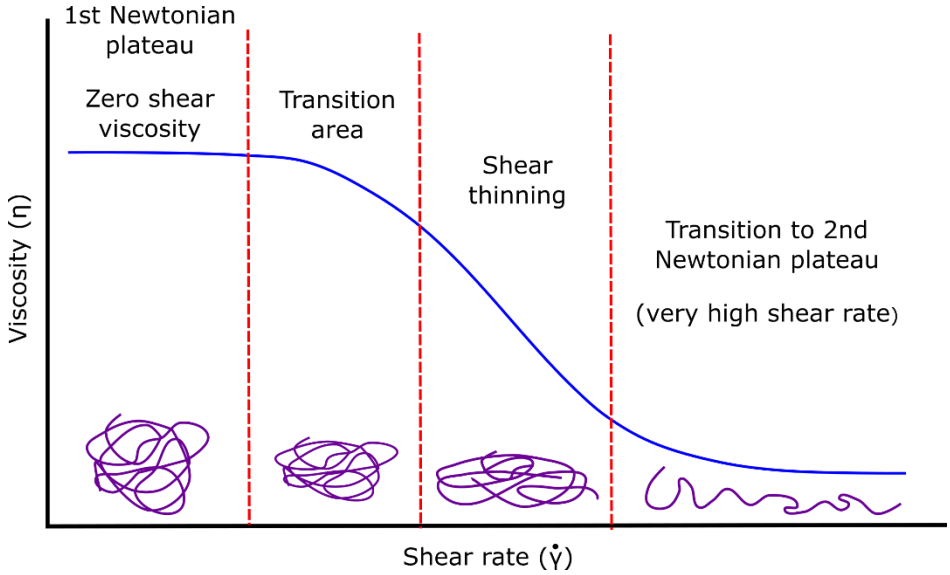

Figure 2.3. Viscosity-shear rate characteristic curve of a polymer undergoing shear thinning. Emphasizing that the second Newtonian plateau is generally only detectable for dilute polymer solutions, because in concentrated solutions it needs very high shear rates (commonly outside the range of measuring instruments). Also, the image illustrates the disentanglement and orientation of the polymeric molecules as the shear rate increases.

2.3 Tribology

Tribology comes from the greek word *tribos* which means 'rubbing', so tribology could be described as a science that analyzes interacting surfaces in relative motion, focusing on the study of the coefficient of friction, wear and lubrication [96], [97]. Friction refers to the force of resistance to relative motion between two surfaces that are in contact, representing a classical tribological system that is found everywhere in our daily life. However, friction causes energy loss and material damage effects through wear processes between the surfaces that are in contact [98], [99]. So, it is critical to understand the tribological properties of different systems in order to reduce friction and wear [100], considering the influence of surface roughness and topography, because perfectly smooth surfaces do not exist [101].

Moreover, friction can be described (equation 2.4) through a quantitative parameter called coefficient of friction (CoF), μ. CoF is a dimensionless scalar value that describes the ratio of tangential friction force (*F*) to the normal load force (*N*), since the friction force is proportional to the normal applied load [102].

$$\boldsymbol{\mu} = \frac{\boldsymbol{F}}{\boldsymbol{N}} \tag{2.4}$$

On the other hand, lubrication represents the most important component of applied tribology, since it represents the most used method for reducing friction and wear through the application of a thin layer with low resistance to shear, between two rubbing surfaces. This friction-reducing layer could be a softer material than the rubbing surfaces, a liquid lubricant or an entrained gas [103], [104].

For the study of tribological systems, Stribeck curves (Figure 2.4) plays an important role in the experimental characterization of the friction behavior of a tribological system and in the identification of its lubrication regimes: boundary lubrication, mixed lubrication and hydrodynamic lubrication [105]–[108]. This curve describes the dependence among the CoF and the dimensionless product of the sliding speed and viscosity divided by the applied load [109].

Boundary lubrication indicates that the applied load is mainly supported by the contact between the asperities of the two contacting surfaces, so the viscosity of the liquid lubricant do not play a major role and the coefficient of friction stays constant [110]. While mixed lubrication describes the transition from boundary lubrication to full hydrodynamic lubrication, because the applied load is supported partly by the lubricant fluid and partly by surface asperities [111], [112]. Finally, hydrodynamic lubrication is achieved when the pressure exerted by the lubricant is sufficient to support the applied normal load, and therefore, the contact surfaces separate completely [113].

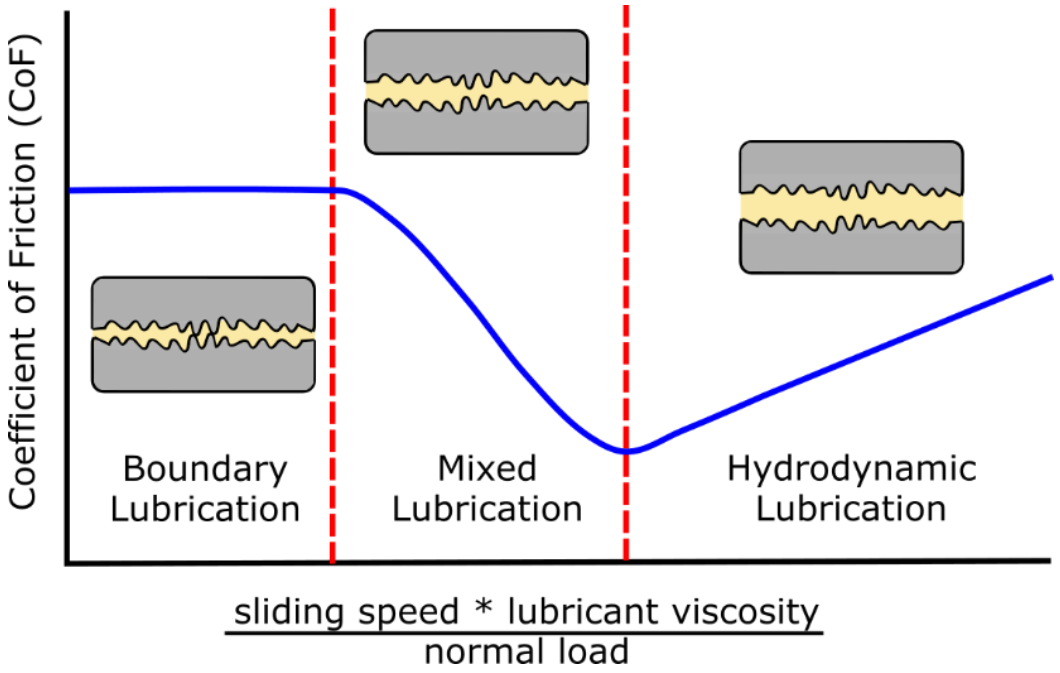

Figure 2.4. Stribeck curve showing the three different lubrication regimes: boundary lubrication, mixed lubrication, and hydrodynamic lubrication.

Moreover, tribology is commonly associated with the surface interaction of mechanical systems, however the concepts of tribology have also been important in the study of several biological systems. Biotribology has emerged as a branch of tribology with the objective of analyzing biological systems, allowing a better understanding of the functioning of different natural systems [114]. Around 70% of biotribology studies focus on joint tribology, skin tribology and oral tribology, while the rest of the research seems to be associated with the tribology of other human tissues (including mucosal surfaces) [115].

2.4 Cone-And-Plate Geometry

The cone-and-plate geometry is commonly used for viscosity measurements of non-Newtonian solutions, as it is a simple, easy-to-use device that requires low sample volume, and allows rapid measurements that do not need tedious correction calculations [116]. Moreover, in this measuring system, the fluid sample is placed between an upper rotating cone and a stationary flat plate, as Figure 2.5 exemplifies.

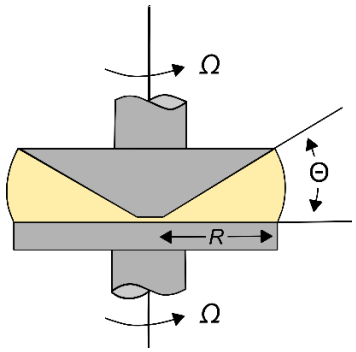

Figure 2.5. Cone and plate rheometer. The small-angle cone rotates at angular velocity Ω while the plate is stationary [47].

The cone geometry should exhibit a small cone angle (< 4°) to ensure a constant shear rate along the shearing gap due to the linear velocity and the gap among the cone-and-plate system increases as the distance from the axis increases [117]. However, cone-and-plate geometry is not adequate for suspensions with large-size particles, since these particles tends to disturb the flow in the narrow gap region of the cone-and-plate system [118], [119].

The viscosity calculated using cone-and-plate geometry is described by:

$$\boldsymbol{\eta} = \frac{\mathbf{3\ T\ \Theta}}{\mathbf{2\ \pi\ R^3 \Omega}} \tag{2.5}$$

where η is the viscosity, T corresponds to the torque on the cone, Θ refers to the angle of the space between the plate and the cone, Ω is the angular velocity and *R* is the radius of the plate [120].

2.5 Gastrointestinal Mucus

Mucus is a viscoelastic hydrogel that covers all the wet epithelial surfaces of the gastrointestinal tract (GIT) [34], acting as a protective barrier that performs different essential biological functions, such as trapping viruses and avoids bacterial surface adhesion through steric obstruction and binding interactions [9], [10], [121], [122], lubricating luminal contents for minimizing friction and shear-induced damage by the mechanical forces associated with peristaltic movements along the GIT during food bolus or chyme digestion [8], [34], [123], keeping a proper hydration of the gastrointestinal organs which should be around 90-98% [61], and controlling exchange of gases, nutrients and elemental biomolecules with the epithelium through selective physicochemical filter activity [7], [124]. Emphasizing the specific role of mucus in the stomach, which is focused on protecting the epithelium against gastric acid and high enzymatic activity [63].

Therefore, gastrointestinal mucus gel is rapidly and constantly renew with a clearance period varying between 4-6 hours by secretion of fresh mucin from goblet cells [10] [55] with the purpose of preserving mucus homeostasis intact to prevent the entrance of potentially damaging agents into the body or the dysregulation in its filtering properties, compromising its protective activity and causing inflammation along the gastrointestinal lumen [125], [126]. In the same way, mucus is continuously shifted and removed by the peristaltic movements in the gastrointestinal tract for displacing luminal food or fecal material [127], [128], which decreases the residence time of the drug delivery vehicles that fails to penetrate mucus [129].

On the other hand, mucus detail composition is still unknow and varies depending on different physiological conditions, including age [130], diet [131], alcohol [132], smoking [133], drugs [134], sex [135], health/disease state [136], among other. Nonetheless, mucus general composition contains around 95% w/w of water with the remaining 5% w/w corresponding to biopolymeric mesh network that includes a set of molecules, such as immunoglobulins, globular proteins, lysozyme, salt, DNA, lipids, cells and mucin, which is a family of high molecular weight (200 kDa - 200 MDa) and densely glycosylated proteins [7], [137]–[139] that are secreted by specialized goblet cells along the GIT epithelium [140].

Mucus mesh network is formed by the polymerization of mucin individual subunits through disulfide bonding among C and N terminal regions that are non-glycosylated and rich in cysteine [62]. Meanwhile, each mucin subunit contains a protein core composed of a large tandem of repeating regions rich in proline, serine, and threonine that allow the interlocking of O-linked glycan chains and mucin stabilization through covalent and noncovalent interactions, such as hydrophobic interactions, electrostatic repulsion between negative charge polysaccharide side chains and hydrogen bonding, resulting into bottlebrush-like molecular structure [39],

[62], [138], as Figure 2.6 shows. In addition, these interactions act as a first mechanism of filtration or union (mucoadhesion) of the particles that could interact with the mucus [34].

Besides, mucin glycosylation includes mainly sialic acid, N-acetylgalactosamine, N-acetylglucosamine, galactose, fucose, mannose and sialic acids [141]. Highlighting the function of the N-acetylgalactosamine residues by contributing to the expanded structure of the mucin by establishing steric interactions with the protein core [7]. However, mucin tends to exhibit a polyanionic nature due to the different negative residues present on its structure, including aspartic and glutamic acid residues (pKa ~ 4) in the protein core, and sialic acid (pKa ~ 2.6) in the oligosaccharide side chains [142]–[144].

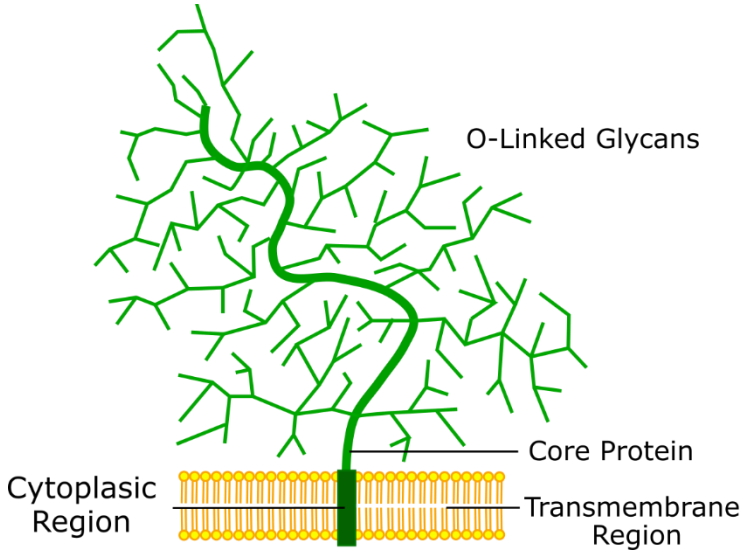

Figure 2.6 Schematic structure of membrane-associated mucins, which are formed by a core protein with O-linked glycans [48].

Moreover, mucin contains hydrated hydroxyl groups to protect epithelium from dehydration due to about 95% of mucus mass should be water to preserve complete mucus lubrication and avoid damage derived from shear rate that emerges from swallowing food [121]. Even, mucus presents some viscoelastic properties due to its capacity of stretching and reorienting in response to external forces of deformation, which can be regulated in vivo through variation in the pH or salt concentration, as well as, by the manipulation of the identity and density of mucin glycoproteins [34].

Otherwise, mucus mesh network presents heterogenous pore size from 10-200 nm [145] and a mean thickness around 100-900μm [7] as Figure 2.7 and Table 2.1 shows. Mucus overall thickness is determined by a balance among mucus secretion rate and degradation/removal rate [55] that varies along the gastrointestinal tract, exhibiting the thickest mucus in the colon and rectum in order

to protect the epithelium from the high concentration of bacteria in the colon lumen [146].

In the same way, stomach and colon mucus exhibits two thick mucus layers (Figure 2.7): 1) a loosely adherent and thick superficial mucus layer that could be easily dispersed, and 2) an underlying firmly adherent and sterile mucus layer attached to the epithelium, due to the harsh conditions in those organs; whilst, the rest of the tract only contains a loosely adherent layer [127]. The single loosely mucus layer of the small intestine represents the main way of absorption of molecules (including carbohydrates, proteins, lipids, water, vitamins, minerals and drugs) by up taking around 90% of them, while the stomach and large intestine absorb the remaining 10% [7].

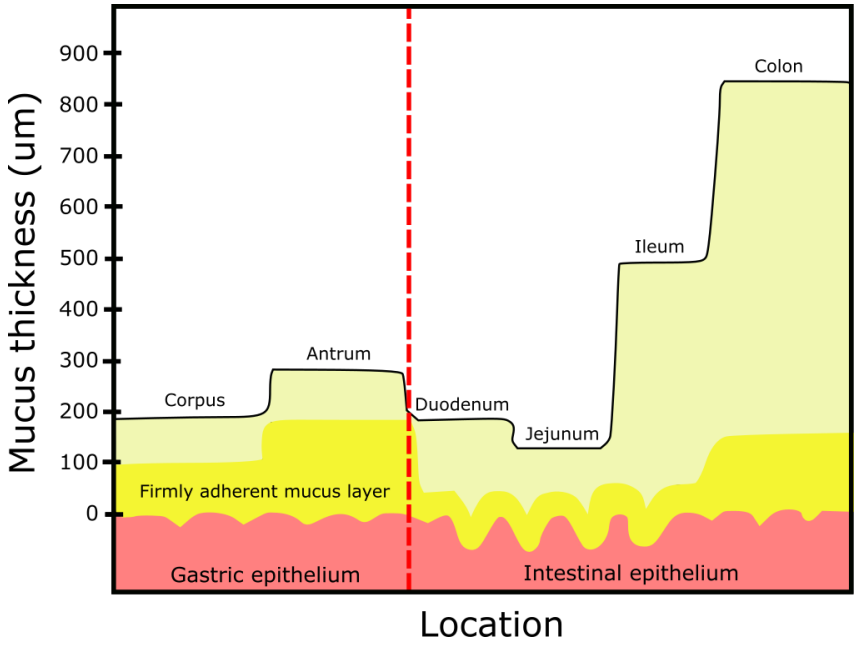

Figure 2.7. A graphical representation of the thickness of firmly adherent and loosely adherent mucus layers in the rat gastrointestinal tract in vivo.

Table 2.1. Average thickness (μm) of the different layers of mucus found in the stomach (corpus and antrum), and intestines (duodenum, jejunum, ileum and colon) [129].

	Corpus (μm)	Antrum (μm)	Duodenum (μm)	Jejunum (μm)	Ileum (μm)	Colon (μm)
Total	189 ± 11	274 ± 41	170 ± 38	123 ± 4	480 ± 47	830 ± 110
Firmly adherent	80 ± 5	154 ± 16	16 ± 3	15 ± 2	29 ± 8	116 ± 51
Loosely adherent	109 ± 12	120 ± 38	154 ± 39	108 ± 5	447 ± 47	714 ± 109

Therefore, the presence of mucus restricts the uptake of drugs and other molecules by forming a physical barrier that regulates their permeability through different mechanisms, such as exclusion by size, formation of hydrogen bonds, electrostatic and hydrophobic interactions, which are mainly driven by mucus physicochemical properties, including pore size (20 - 200 nm), viscoelasticity, ionic strength, surface charge, among other properties that impact directly in drug delivery through mucosal tissues [7], [139].

2.6 Mucus Rheological Properties.

The high degree of viscoelasticity and effective porosity that mucus gel network presents results from the various intermolecular interactions that occur between the mucin monomers, coupled with the high degree of physical entanglement that occurs among the mucus elements [35], [138], [147]. Emphasizing that changes in mucus viscoelastic properties directly affect its essential protective and lubricant properties [129].

Moreover, mucin represents the main element involved in mucus rheological characteristics, since the degree of mucin glycosylation and its composition affect the viscoelastic properties of mucus [148] due to the limited flexibility and disruption of the interlocking network structure produced by a high concentration of negative charges associated with the mucin sugar side chains [34]. As well, mucin glycan domains exhibits high water-holding capacity, which is determinant in the typical gel-like properties of mucus [136], [149]. Even, osmotic pressure changes could modify water and ions distribution, modifying the degree of swelling of mucus and hence its rheological properties [34]

Therefore, rheological measurements are used to analyze mucus consistency, which varies between a viscous liquid and an elastic solid [150]. The viscoelastic behavior is evaluated through two dynamic modules: 1) a storage or elastic modulus (G') that describes the ability of a gel to recover its initial shape, and 2) a loss or viscous modulus (G'') that estimates the resistance of a gel to flow [82]. In this case, mucus exhibits a predominantly solid elastic behavior with a storage modulus (G') > loss modulus (G'') under small-amplitude oscillatory shear conditions, representing a complex non-Newtonian, thixotropic gel that recovers its shape over the time [46]. Instead, mucus tends to acquire a viscous liquid behavior with an eventually irreversible deformation under high shear rate [150].

However, frequency measurements represent a more appropriated method than oscillatory shear tests to maintain mucus structure intact during the experiment [87]. Additionally, frequency tests can differentiate between liquid-like and solid-like behaviors based on the chain disentanglement during a single oscillation at low frequency. Because in the liquid-like behavior (G'' > G'), mucus chains have enough

time to separate and flow, while in the solid-like (G' > G") there is not enough time for proper disentanglement of the chains, which limits the flow [151].

Considering that the viscoelastic behavior of mucus could be affected by increasing shear stress, time rate of shearing or conformational changes produced by pH and salt ions concentration modifications [2] [34]. It is important to guarantee the equilibrium among liquid-like (viscous) and solid-like (elastic) behaviors represent a determinant element in human health, since the balance ensures a proper physiological function of gastrointestinal mucus [152]. A significant reduction in the viscosity of the gastrointestinal mucosa facilitates the adhesion of bacteria within the tract [153]. Instead, the hyperviscosity of the mucus makes it less transportable, triggering an accumulation of mucus due to defective clearance [142].

Moreover, mucus exhibits the property of shear thinning (non-Newtonian), which means that mucus viscosity decreases as the shear rate increases, resulting in a progressive disentanglement of o-glycan chains that tend to align in the direction of flow [143], [154]. These shear thinning properties of the mucus secreted in the gastrointestinal tract allow the bolus to pass through the tract without disturbing the tightly adherent layer and epithelium [129]. Moreover, mucus exhibited solid elastic performance with viscosity values that could be around 100 to 10,000 times higher than the viscosity of water at low shear rates. In contrast, at maximum physiological shear rate values, mucus acquired a viscous liquid performance with a viscosity similar to the viscosity values of water, providing excellent low-viscosity lubricant properties [7], [39].

2.7 Mucus Structural Changes Influenced by pH.

Gastrointestinal tract exhibits pH variation among 1.0 and 8.0. Highlighting that the hardest challenge for mucus is the highly acid environment of the stomach, which can reach a pH around 1.0 or 2.0 during active digestion, depending on various factors including diet, diseases, presence of gases, fatty acids and fermentation products [155].

Nevertheless, it has been noticed that mucus is resistant to extremely acidic pH conditions to prolong its lifetime under those harsh conditions [156]. This resistance is produced due to mucus is subjected to a pH-dependent sol-gel transition as a result of changes in pH and ionic concentration [157], which promotes conformational changes and aggregation in mucin, resulting in the formation a highly viscous hydrogel as a protective barrier to restrict the passage of hydrogen ions from gastric juices in order to prevent the stomach from being digested by its own acids [60], [158], [159].

Furthermore, high sialic acid and sulfate residues on mucin confer a net-negative surface charge to mucus at physiological pH with a pKa around 2.6. [7],

[160]. So, its conformational change is found at pH between 2 and 3, where it is the isoelectric point, indicating a change of charge of mucin proteins as the pH decreases [60], as Figure 2.8 shows.

At neutral pH, mucus shows a random coil conformation of glycosylated chains due to the electrostatic interactions between polysaccharide side chains and disulfide (S-S) linkages in the cysteine terminals of mucin molecules [156]. While, at low pH, mucin acquires an extended conformation through complex interactions among hydrophilic and hydrophobic regions of the glycoproteins, including the protein core, after salt and disulfide bridges break, inducing the formation of non-covalent crosslinking between non-glycosylated domains, allowing the stabilization of water molecules by the hydrophilic groups, leading to the formation of a protective gel [60], [156].

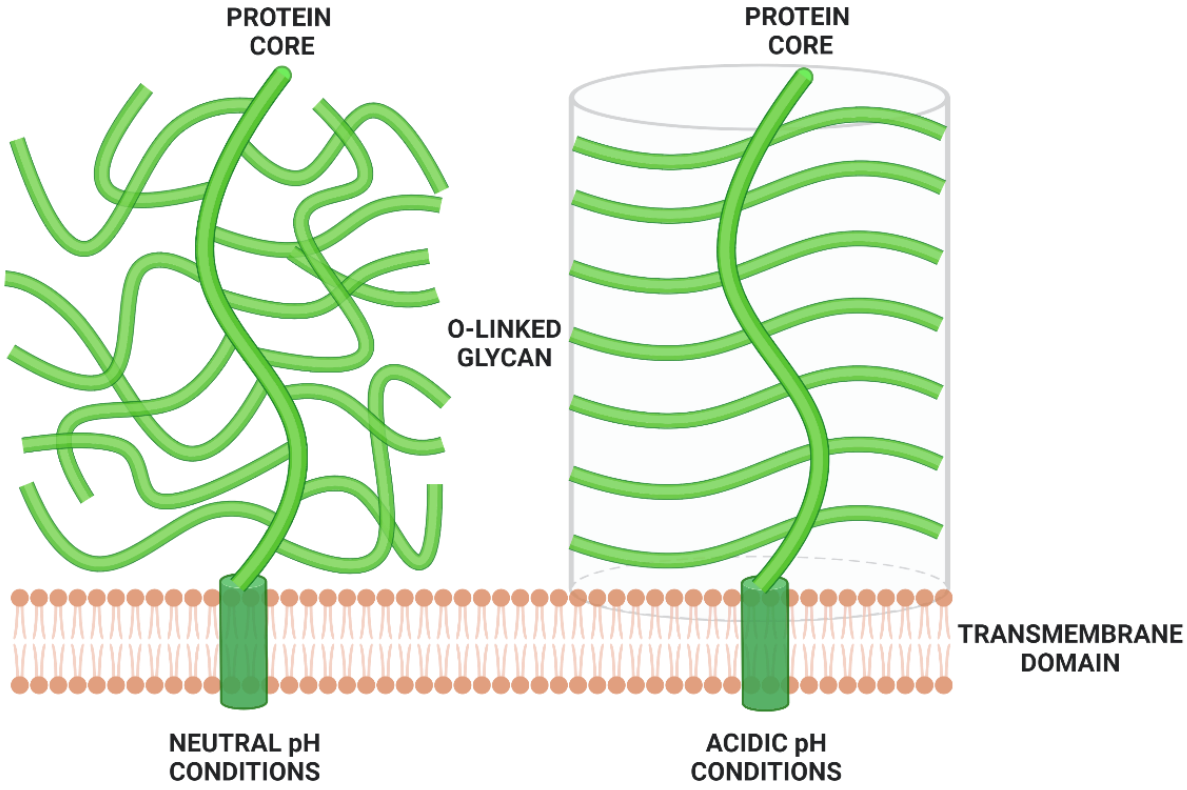

Figure 2.8. Mucin is subject to conformational changes dependent on environmental pH. At neutral conditions, (left), mucin exhibits a random coil structure as a result of the electrostatic interactions established between polysaccharide side chains that induce entanglement. In contrast, at high acid conditions (right), mucin exhibits a rodlike structure due to complex interactions between exposed hydrophilic and hydrophobic glycoprotein domains [39]. **Created with BioRender.com**

However, the gelation mechanism experienced by mucus is not yet fully understood, so the most accepted theory contemplates an aggregation of mucin

molecules produced by the association between domains of the C-terminal region that are not glycosylated in a similar way to the triblock copolymer gelation [158].

Consequently, an important correlation between structural and viscoelastic properties of mucin and pH can be established [158]. Moreover, some previous studies have shown that in a pH > 4, the viscous modulus (G") acquires higher values that the elastic modulus (G'), which is representative of polymeric dispersions, as long as, in acidic media, it shows a characteristic elastic behavior of gel with G' > G" [60].

2.8 Transmucosal Drug Delivery

The administration of biomolecules through the gastrointestinal mucosa is an alternative of great interest to achieve a systemic distribution of drugs. However, it is essential that drug delivery vehicles interact with the mucosal barrier and penetrate it without affecting it, to guarantee an adequate bioavailability of the therapeutic molecule. Thus, it is required to learn about the physicochemical characteristics of the nanocarrier (such as molecular weight, size, hydrophobicity, charge, stability, among other) in order to design highly effective drug delivery systems [161].

Particle permeation, including nanoparticles, through the mucus is limited by different kind of physicochemical barriers and interactions (Figure 2.9), such as size exclusion by mucus polymeric network, physical entanglement, electrostatic or hydrophobic interactions, which traps particles and eliminate them by a rapid mucus clearance [2], [162]. Molecular weight of the delivery vehicle generally exhibits an inverse correlation against diffusion coefficient, as well as the size significantly affects the diffusion of large molecules no matter if they are hydrophilic or hydrophobic.

However, hydrophobic molecules tend to interact with the multiple low-affinity interactions efficiently formed by the negative charges of carboxyl and sulfate groups on the mucin glycoproteins and lipids, displaying higher affinity and slower diffusion than hydrophilic drugs, which results in a lower bioavailability [7] [10].

Moreover, steric hindrance could restrict particle movement across the porous and water-filtered channel of the mucosal network, or the cohesive and repulsive electrostatic contacts between particles and mucus glycans [163]. Even some drug delivery vehicles exhibit poor capability to diffuse rapidly through mucus, establishing very strong interactions or presenting degradation before reaching the epithelium for absorption. For this reason, the ability to permeate the mucosa represents an essential requirement for delivery vehicles that target mucosal areas [164].

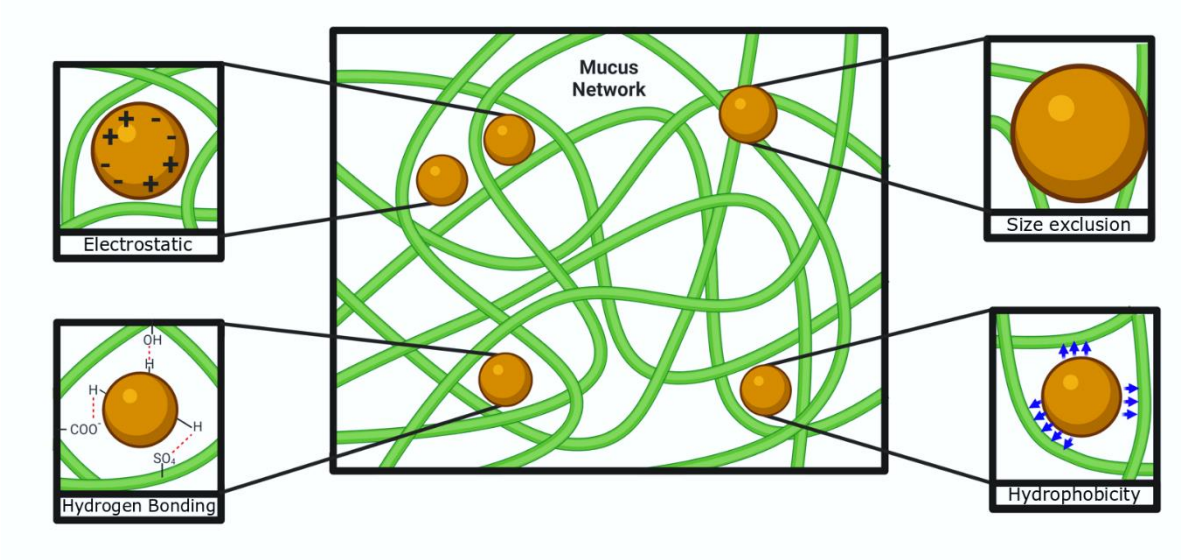

Figure 2.9. The permeability of nanoparticles (orange) through mucus (green) is limited by different types of barriers and physicochemical interactions, including: a) electrostatic interactions between positively (attraction) or negatively (repulsion) charged nanoparticles and negatively charged mucin chains; b) formation of hydrogen bonds between the hydroxyl, carboxylic, and sulfate groups of the mucus with the different hydrogenated functional groups present on the surface of the nanoparticle; c) exclusion by size of those nanoparticles that exceed the pore size of the mucus (20-200 nm); and d) hydrophobic interactions between the non-polar regions of the O-glycan chains and the hydrophobic groups present in the surface of the nanoparticles [39]. **Created with BioRender.com**

Therefore, different delivery strategies have been studied for improving the permeability through the mucosal membrane, including polymeric nanovehicles, such as nanoparticles, nanoemulsions, permeation enhancers, mucoadhesive and mucopenetrating adjuvants. Because, fast mucus penetration avoids rapid clearance and degradation, which ensure an interaction with the epithelial surface with a subsequent cellular uptake and possible transcytosis that results in a high drug bioavailability [7], [165]. For this reason, the use of mucoadhesive polymers has gained great interest to improve the efficiency in the administration of many drugs that interact with mucus layers [166]. Nevertheless, some mucoadhesive biomolecules tend to get trapped in the poorly adherent mucus layer and are rapidly eliminated without reaching adsorption sites, since mucus is continually secreted, leading to early removal of those molecules that adhere strongly to the mucus surface [167].

2.9 Polymeric Nanoparticles

Nanoparticle-sized systems have been widely studied as a delivery vehicles due to their convenient size and protective properties against drug degradation [7]. Among the most used materials for the formulation of nanocarriers for therapeutic

purposes, are lipids, polymers and metals [168]. The diameter of nanocarriers is an important variable in drug delivery in order to avoid possible embolism due to several pharmaceutical drugs achieve the systemic circulation, which smallest blood capillaries have a diameter around 4μm [169]. As well, hydrophilicity and electrical charge of nanoparticles surface are intimately related with particle trapping and mucus permeability [10].

Nanoparticles are commonly used as a delivery nanovehicle for controlled bioavailability and lifetime of different biomolecules inside the body, including DNA, RNA, amino acids, peptides, proteins, vitamins, and several different kind of therapeutic agents [1], [170]. Moreover, they can offer sustained release of drugs by modifying drug pharmacokinetics in a non-linear and dose-dependent way [169], [170] through increasing surface of contact and magnetic properties [171]. As well, nanoparticles small size allows them to cross through the mucosal barriers, unless they exhibit strong hydrophobic, electrostatic or hydrogen bond interactions with mucus, leading to entrapment inside the mucus network [9]. Moreover, nanoparticles coating with a hydrophilic polymers represents an attractive alternative to adjust their surface charge density for increasing mucus permeability and cellular uptake [10].

Polymeric nanoparticles have gained great relevance in drug delivery applications, since their structure and surface can be easily modified to protect and deliver molecules at specific sites of action, or even, these nanoparticles can be design with the ability to respond to specific stimuli (physiological or external) with the purpose of achieving a specific and controlled release [172]. Besides, the preparation mode and the composition of the organic phase play a critical role in the formulation of polymeric nanoparticles, since nanocapsules or nanospheres can be obtained, as Figure 2.10 exemplifies. Nanocapsules are composed of an aqueous or oily core that encloses the active compounds, which is covered by a protective polymer shell. Instead, nanospheres have a structure similar to a disordered matrix in which the active compounds and the polymer are well dispersed [21], [173].

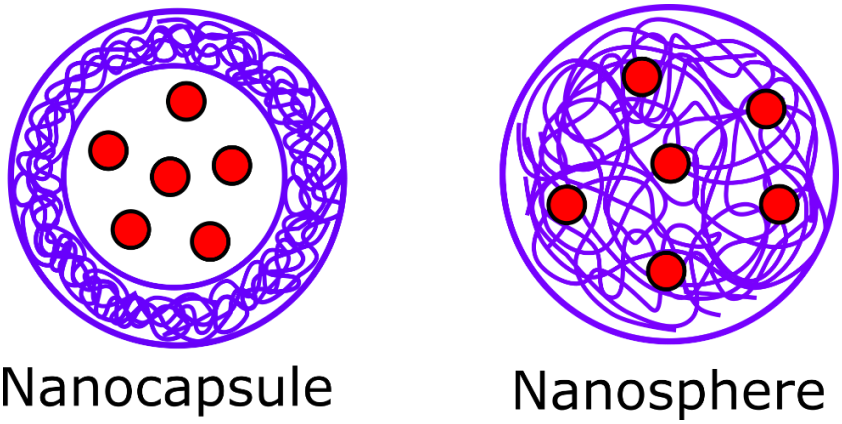

Figure 2.10 Schematic representation of a drug-loaded polymeric nanoparticles: nanocapsule (left) and nanosphere (right).

Otherwise, polymeric nanoparticles exhibit several advantages, including simple preparation, good biocompatibility, high drug loading, controlled drug release kinetics, easy surface modification with different ligands, bio-imitative characteristics, drug protection against degradation, improved bioavailability, enhanced reactivity, among others [19], [174], [175].

2.9.1 Chitosan Nanoparticles

One of the most common ligands used is chitosan, which is a biopolymer obtained from the partial N-deacetylation of chitin under alkaline conditions, which is a molecule collected from crustacean shells (prawns or crabs), mollusks or from fungi cell walls [23], [176]. Moreover, chitosan is a cationic, mucoadhesive, biodegradable, biocompatible polysaccharide conformed by a chain of repeating units of N-glucosamine and N-acetyl-glucosamine linked by β-(1'4)-glycosidic bonds, which proportion depends on the deacetylation degree of the biopolymer [7], [139], as Figure 2.11 displays. As well, chitosan is considered nontoxic with an oral LD50, similar to sugar or table salt doses. Even, it is degraded inside the body by lysozyme hydrolytic action on the acetylated residues depending on its degree of crystallinity (caused by deacetylation) [51].

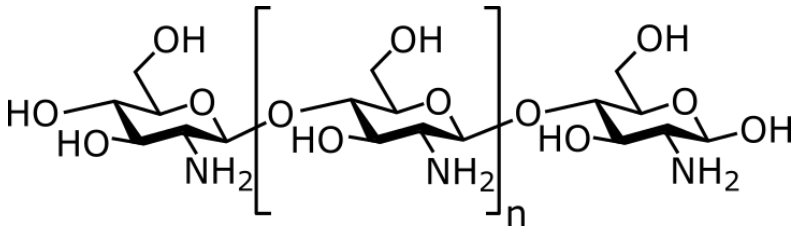

Figure 2.11. Chemical structure of chitosan.

Chitosan exhibits several advantages, such as: 1) increasing drug carrier potential through its positive charge, 2) offering controlled drug release at acidic environments since it appropriately dissolves at pH around 5.0, 3) highly reactive surface, 4) reducing opsonization by phagocytic mononuclear cells in blood decreasing nanoparticles accumulation in liver and spleen, 5) preventing drug oxidation or denaturation, 6) facilitated transmucosal drug delivery, 7) mucoadhesive properties, 8) developing an antibacterial, antifungal and wound-healing activity, and 9) free of toxic organic reagents formulation process [51], [139], [169], [177], [178].

Moreover, U.S. FDA have approved chitosan as a drug delivery carrier modifier for enhancing nanoparticles permeability and mucoadhesive properties through complex ionic, hydrogen bonding and hydrophobic interactions with mucosal surfaces (negative charged), as long as, prolonging nanoparticles residence time at the gastrointestinal tract [23], [139], [170].

However, chitosan presents an approximated pKa at 6.5, so pH values are determinant for chitosan activity during drug release due to the amino group of chitosan is protonated at low pH, enhancing its mucosal adhesion and solubility. While, at pH higher than 6.5, the amino group is deprotonated, forming an insoluble biopolymer shell reducing its release efficiency. So, it is important to consider absorption target site because human body presents different pH values depending on the region [179].

Moreover, the functional groups of chitosan surface, including hydroxyl (-OH) and amine (-NH2) are highly reactive, allowing an easy surface modification by different chemical reactions, including alkylation, o-acetylation, quaternization, and cross-linking with different ligands [16], [51]. As well, chitosan deacetylation is useful for modifying chitosan solubility, degradation speed, hydrophobicity, and electrostatic interactions [139].

2.10 Mucoadhesion Phenomenon

Mucoadhesive polymers are hydrophilic macromolecules with the ability to adhere to mucous membranes through different physicochemical interactions [180], with the objective of boosting the contact time with mucus and, consequently, improving the bioavailability of drugs by combining an enhanced absorption, targeted administration, reduced drug degradation, longer interaction times and sustained release [181], [182].

Mucoadhesive nanoparticle and microparticle formulations have been associated with a significant improvement in the efficacy during the delivery of various biomolecules into the GI tract, compared to drugs that are delivered without an encapsulation system [183].

Moreover, the characteristics of the mucoadhesive polymers (including size, shape, morphology, hydrophobicity, molecular weight, concentration, surface functional groups and charge) and environmental properties (such as pH conditions and mucus flow rate) plays a critical role in the interactions established among polymer and mucus chains [184]–[188]. Because the mucoadhesive phenomenon is the result of the formation of different types of bonds and interactions, including: hydrogen bonding [144], electrostatic interactions [82], hydrophobic interactions [7], [34], van der Waal forces [18], covalent bonds [189], and physical entanglement [190].

Mucoadhesion is a complex process that could be divided into two main stages to understand the phenomenon in a simple way, as Figure 2.12 exemplifies: 1) The contact stage, where the mucoadhesive polymer approaches the mucosa, and an initial strong or weak contact is established, depending on the capacity of the material polymer to hydrate and spread, as well as by the interfacial forces between

the adhesive material and the mucosa, such as electrostatic attraction, and van der Waals forces. 2) The consolidation stage is characterized by various physicochemical interactions that stimulates the physical entanglement and the formation of different chemical bonds between the mucus and polymer chains [191]–[194].

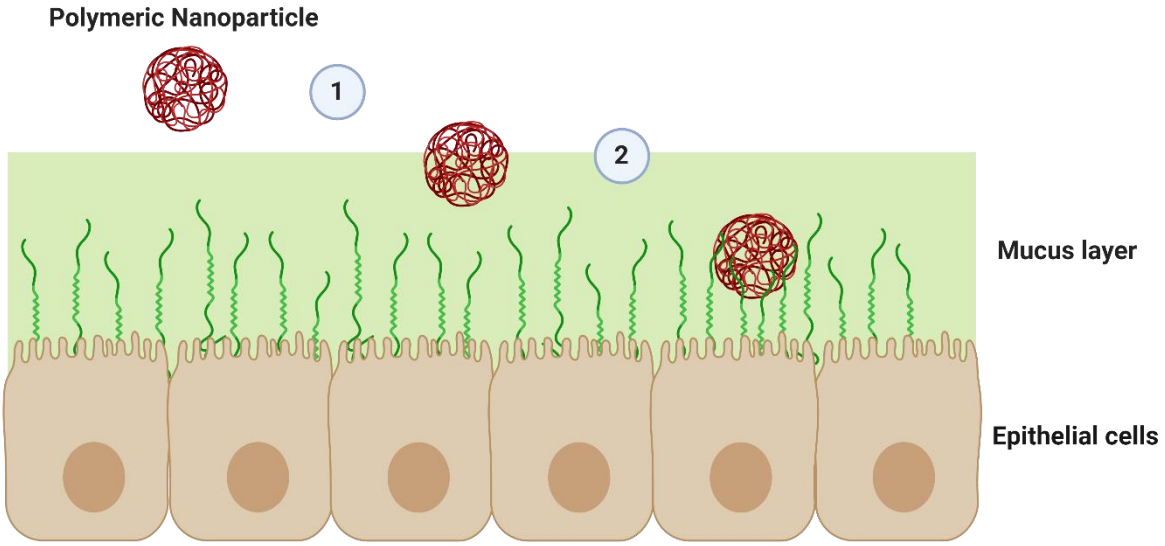

Figure 2.12. Schematic representation of the mucoadhesion mechanism between a cationic nanoparticle (red) and a mucus layer (light green). 1) Contact stage, the nanoparticle is attracted to the surface of the mucus layer due to the opposite charges. 2) Consolidation stage, the polymeric chains of the nanoparticle are intertwined with the glycoprotein chains of the mucin. **Created with BioRender.com**

Nevertheless, mucoadhesion has not been fully understood, so several theories (Figure 2.13) have been developed to describe the phenomenon [195]. Among the most accepted theories are:

1) **Wetting theory** represents the first theory formulated to describe the mucoadhesive phenomenon and generally represents the first step when an interaction between the adhesive polymer and mucus is established [185]. This theory describes mucoadhesion as a phenomenon in which the polymer extends along the mucus, developing an intimate contact [196], in which the microagents of the adhesive material penetrate the irregularities of mucus surface, and harden into adhesive anchors as a result of the drastic changes in interfacial energies [197], [198]. Moreover, wetting theory mainly applies to low-viscosity liquids or polymers, because hydrophobic materials show greater affinity for mucus than hydrophilic ones, exhibiting favorable conditions for adequate and spontaneous propagation which results in increased interfacial contact and allows a stronger mucoadhesive interaction

[199]. For this reason, the contact angle represents a very useful tool to determine the different degrees of wetting [200], since a contact angle close to zero indicates a favorable contact among the liquid and the mucosal surface, while a contact angle similar to 90° or greater indicates unfavorable contact [56], [186].

2) **Electronic theory** states that adhesive polymers and mucosal surfaces exhibit adhesion based on the differences between their electrical charges. Therefore, when both surfaces come into contact, a transfer of electrons occurs in an effort to balance the Fermi levels, leading to the formation of an electrically charged double layer at the polymer-mucin interface [198], [201].

3) **Diffusion theory** establishes that the adhesion is caused by the entanglement and interpenetration between the polymeric chains and the glycoprotein chains of the mucus, resulting in the formation of a semi-permanent mesh network matrix. The adhesion inside the matrix is governed by the concentration gradient, molecular weight, chain flexibility, hydrodynamic size, crosslinking density, contact time, and diffusion coefficient of the mucoadhesive polymer [202]–[204].

4) **Adsorption theory** suggests that the attachment of adhesive materials on mucosal membranes results primarily through hydrogen bonding and van der Waals forces. However, the chemisorption theory mentions that in the second instance, an interaction interface formed by covalent and ionic bonds is established to strengthen the adhesion [196], [205]. Although covalent and ionic bonds are stronger, hydrogen and van deer Waals bonds are desirable for drug delivery purposes [206].

5) **Fracture theory** describes the adhesive strength as the force required to detach two surfaces after adhesion is established. This theory is commonly used in rigid or semi-rigid adhesive polymers, in which the interpenetration or diffusion of the polymeric chains into the mucosal substrate is negligible [207], because it assumes that adhesive bonds fail at the interface among both surfaces, but commonly a failure in the cohesive forces happens in one of the adhering surfaces [205]. Additionally, the work fracture tends to be greater when the polymeric chains are longer or the crosslinking degree is reduced [203]. The fracture strength (σ) is calculated by:

$$\boldsymbol{\sigma} = \sqrt{\frac{\boldsymbol{E} * \boldsymbol{\varepsilon}}{\boldsymbol{L}}} \tag{2.6}$$

where *E* corresponds to the Young's modulus of elasticity, *ε* refers to the fracture energy, and *L* describes the critical length [191].

6) **Mechanical theory** considers the effect of surface roughness as the main element of adhesion, since adhesion arises from the interlocking of a liquid adhesive in the irregularities of mucus rough surface. In addition, the irregularities in the adhesive biomaterials favor the accessible interfacial area, and consequently, an increased surface area is available for interaction under greater viscoelastic and plastic energy dissipation during joint failure [55], [190], [198], [208].

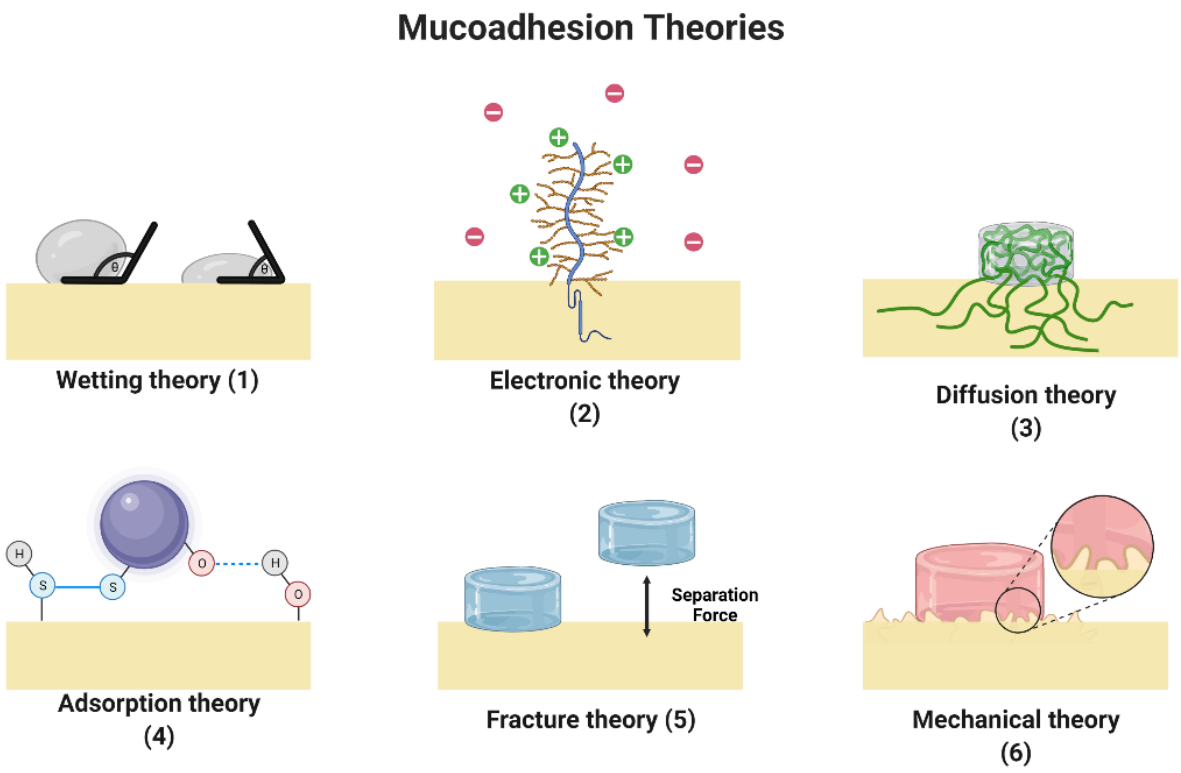

Figure 2.13. Schematic representation of the six main theories to explain the phenomenon of mucoadhesion: (1) the wetting theory is based on the hydrophobicity (contact angle) of a mucoadhesive solution, (2) the electronic theory describes the formation of a double electron shell, (3) diffusion theory occurs when physical entanglement occurs between polymer and mucus chains, (4) absorption theory describes the formation of hydrogen bonds and covalent bonds (disulfide bonds) between the mucoadhesive polymer and the mucosity, (5) the fracture theory considers the force required to separate the mucoadhesive polymer from the mucosal surface, and (6) the mechanical theory is represented by the accumulation of the polymer in the irregularities of the surface mucous membrane. **Created with BioRender.com**

2.11 Rheological Synergism

Several researchers have proposed rheology as an indirect method to evaluate the phenomenon of mucoadhesion among mucus and mucoadhesive polymers under moist conditions. Since, the comparison between the rheological profile of the mucus-polymer mixtures and the elements separately can function as an in vitro analytical parameter to predict the degree of mucoadhesiveness of the polymer in vivo by analyzing the rheological synergism of the mixture [67], [209], which evaluates the strength of mucoadhesion from the viscosity changes produced when a mucoadhesive polymer interacts with a mucin solution [2], [31].

On the other hand, the rheological synergism presented by polymer-mucus mixtures is highly influenced by the interpenetration or interdiffusion of polymeric chains in the glycoprotein chains of the mucus, which promotes physical entanglements, conformational changes, and functional group interactions among both elements, resulting in the phenomenon of adhesion [210], [211]. Moreover, this rearrangement of the macromolecules induces variations in the viscoelastic and viscous profile of the mixture, so the polymer-mucin mixture tends to exhibit an increase in the viscoelastic modulus or viscosity with respect to the single-component solutions [212], [213].

Therefore, the rheological synergism can be calculated as a function of the dynamic modulus (G' and G''), considering a positive synergism when the experimental response of the polymer-mucin mixture presents values higher than the theoretical response, which corresponds to the sum of the individual contributions of the polymeric gel and the mucin responses, and consequently, the presence of a mucoadhesive interaction is established. While a negative rheological synergism indicates a very low or negligible adhesive interaction among mucus and the polymeric material [214], [215]. In this case, the rheological synergism is described by equations 2.7 and 2.8:

$$\Delta G' = G'_{mix} - (G'_{polymer} + G'_{mucus}) \quad (2.7)$$

$$\Delta G'' = G''_{mix} - (G''_{polymer} + G''_{mucus}) \quad (2.8)$$

where $\Delta G'$ / $\Delta G''$ corresponds to the mucoadhesive interaction (or rheological synergism) term, G'_{mix} / G''_{mix} refers to the viscoelastic modulus of the mix polymer – mucin, $G'_{polymer}$ / $G''_{polymer}$ describes the viscoelastic response of the polymeric sample, and G'_{mucus} / G''_{mucus} represents the viscoelastic response of mucus sample [39], [209].

However, mucoadhesive analysis through viscoelastic synergism parameters present a limitation, since polymer:mucus concentration ratio plays a key role in the interpretation due to the interactions exhibit a maximum stoichiometry [30], [214]. So, reliable mucoadhesive comparison only can be achieved by using appropriate

concentrations of polymer, because a concentration of polymer over the stoichiometric equilibrium could exhibit a synergy masked by the rheological performance of the polymer alone, resulting in highly positive synergism values when the adhesive interaction is low [67], [216], [217].

Furthermore, the degree of synergism is intimately related to the surface charge of the polymers due to cationic polymers can establish electrostatic interactions with negatively charged mucus, instead anionic polymers exhibit poorer and less frequent interactions due to the repulsion forces. Even though, polyanionic polymers commonly display higher ΔG' values than neutral polymers, evidencing the fundamental role of electrostatic charge in mucoadhesion phenomenon [211], [218].

Otherwise, rheological synergism tends to exhibit a frequency-dependence because mucus acquires a solid behavior at low frequencies, which influences a positive synergistic value. While mucus shows a predominantly liquid behavior at high frequencies, resulting in negative synergy. For this reason, rheological synergism must be assessed at low frequencies to prevent false positive results [219].

Additionally, rheological synergism can assess the ability of the polymer to adhere to mucus through viscosity measurements (Figure 2.14), considering that the increase in viscosity values are a result of interactions and chain entanglement between the polymer and mucin, which represent the main contributors to the mucoadhesive phenomenon [33], [220].

$$\Delta \boldsymbol{\eta} = \boldsymbol{\eta_{mix}} - (\boldsymbol{\eta}_{\boldsymbol{polymer}} + \boldsymbol{\eta}_{\boldsymbol{mucus}}) \tag{2.8}$$

where $\Delta\eta$ corresponds to the rheological synergism parameter, η_{mix} refers to the mix polymer – mucin viscosity, $\eta_{polymer}$ describes the viscosity the polymeric solution, and η_{mucus} represents the viscosity of the mucus [32].

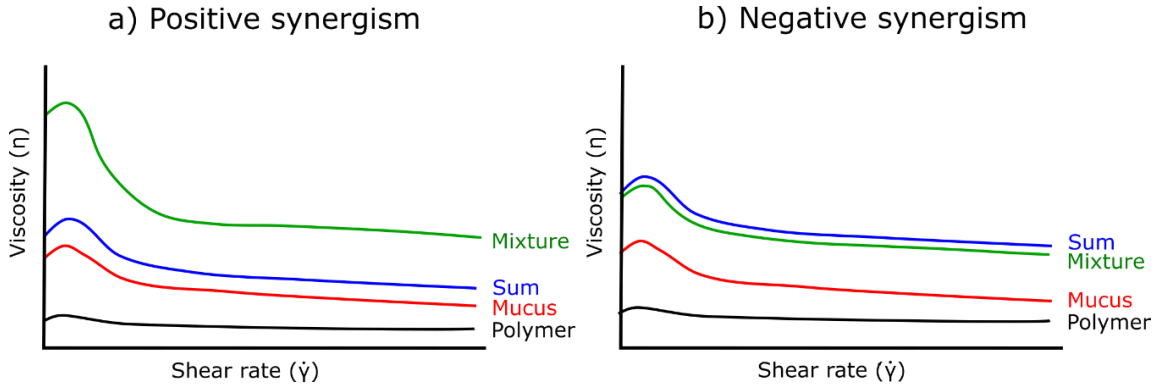

Figure 2.14. Comparison between a positive and a negative synergism to determine the presence or absence of the mucoadhesion phenomenon. a) The graph shows a positive synergism because the viscosity of the mixture (green) is much greater than the sum (blue) of the viscosities of the mucus (red) and the mucoadhesive polymer (black) individually. b) The graph exhibits a negative synergism since the viscosity of the mixture (green) is lower than the viscosity of the sum (blue) of the viscosities of the mucus (red) and the mucoadhesive polymer (black) individually.

Chapter 3. Materials and Methodology.

3.1 Materials

Mucin from porcine stomach type III, bound sialic acid 0.5-1.5%, partially purified powder and Chitosan, low molecular weight (75-85% deacetylated) were obtained from Sigma-Aldrich. Simulated Intestinal Fluid TS was obtained from RICCA Chemical. Sodium Tripolyphosphate (TPP), technical grade, 85% was acquired from Merck. All the other reagents were of analytical grade.

3.2 Preparation of Reconstituted Mucus (5% Mucin Solutions).

Each sample of reconstituted mucus was prepared by diluting 500 mg of purified mucin powder in 10 mL of simulated intestinal fluid (SIF), and it was manually agitated until obtaining a partially homogenized cream-colored solution. The solution was incubated for 24 hours under constant stirring (200 rpm) at 37°C to obtain a completely homogenized solution that mimic gastrointestinal mucus. Subsequently, the pH of reconstituted mucus solution was adjusted to perform all the different analysis and characterizations.

The pH of each sample was adjusted to one of the following values: 2.0, 4.0, 6.0 or 7.0, to mimic the different pH environments along the gastrointestinal tract. The pH adjustment was performed by adding the appropriate volumes of 1M HCL or 1M NaOH until the expected pH was achieved.

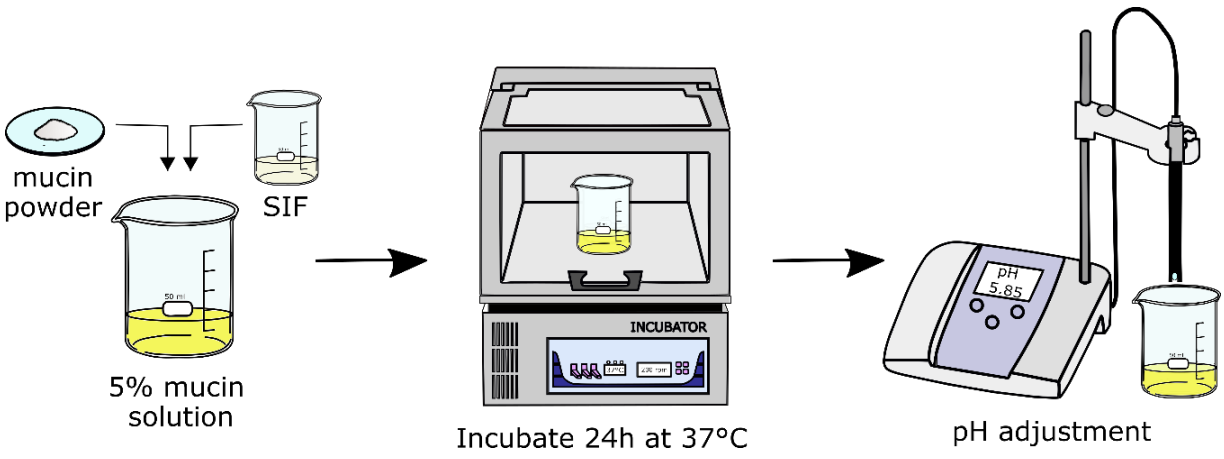

Figure 3.1 Protocol used for preparing reconstituted gastrointestinal porcine mucus (5% mucin solution).

3.3 Synthesis of Chitosan:TPP Nanoparticles by Ionic Gelation Method

Ionic gelation methodology was performed using two different solutions: a chitosan and sodium tripolyphosphate. A 3 mg/mL solution of chitosan was prepared by the addition of 300 mg of chitosan into 100 mL of diluted acetic acid solution (1%). Simultaneously, a 1mg/mL solution of sodium tripolyphosphate (TPP) was prepared by adding 50 mg of TPP into 50 mL of 1% acetic acid solution. The pH of both solutions was adjusted to 5.0 using 1M NaOH for chitosan solution, and 1M HCL for TPP solution. Chitosan solution was stirred at 800 rpm for 60 min, while TPP solution was stirred for 30 minutes.

After that, TPP solution was added dropwise to the chitosan solution, which was under magnetic stirring at 800 rpm. The mixture was stirred for 60 min at 800 rpm. Then, the mixture was sonicated during 30 min at 40 kHz. Finally, the nanoparticle solution was frozen at -20°C and placed inside the freeze dryer for 48 hours.

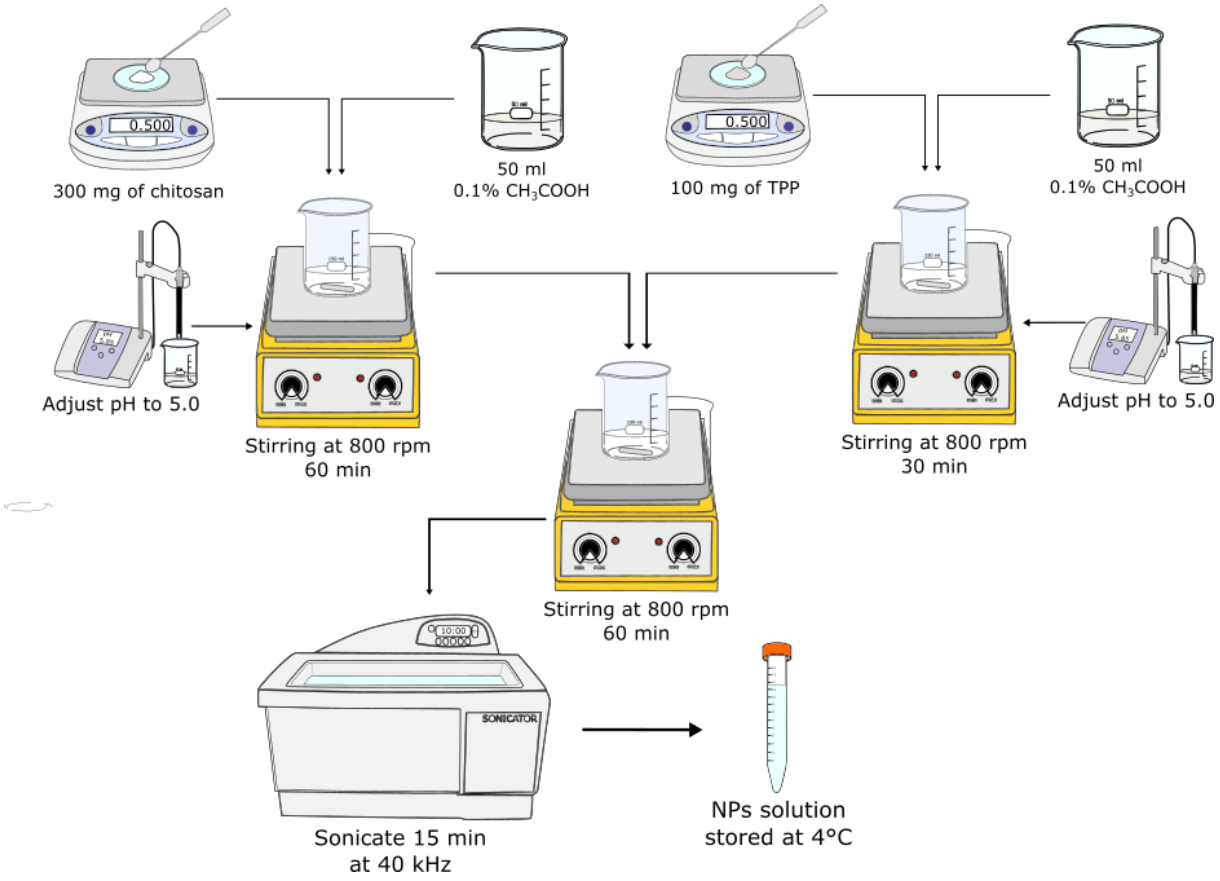

Figure 3.2 Protocol used for synthesis of chitosan:TPP nanoparticles through ionic gelation method.

Note.- Before some characterization methodologies (such as size, polydispersity index and zeta potential measurements), and triborheological tests (including rheological synergism), the lyophilized nanoparticles were diluted in distilled water at 3 mg/mL concentration and sonicated during 20 minutes at 40 kHz to obtain a well dispersed solution. Then, the pH of each solution of nanoparticles were adjusted to 2.0, 4.0, 6.0 or 7.0, respectively

3.4 Characterization of Chitosan:TPP Nanoparticles.

3.4.1 Nanoparticle Size, Polydispersity Index and Zeta Potential measurement.

Mean hydrodynamic diameter and polydispersity index (PDI) of the chitosan:TPP nanoparticles were measured by Dynamic Light Scattering (DLS) at 25°C with 2 min of equilibrium, a laser wavelength of 633 nm and a 173° detection angle, inside of DTS0012 disposable cuvettes using a Malvern Zetasizer Nano ZS. Meanwhile, zeta potential measurements were performed through Electrophoretic Light Scattering (ELS) with 2 min of equilibrium at 25°C inside of DTS1070 disposable cuvettes using a Malvern Zetasizer Nano ZS. The samples were prepared at a concentration of 3 mg/mL in distilled water, and the pH was adjusted with 1M HCL or 1M NaOH to the conditions required (pH = 2.0, 4.0, 6.0 or 7.0). The measurements were carried out in triplicate for each pH value.

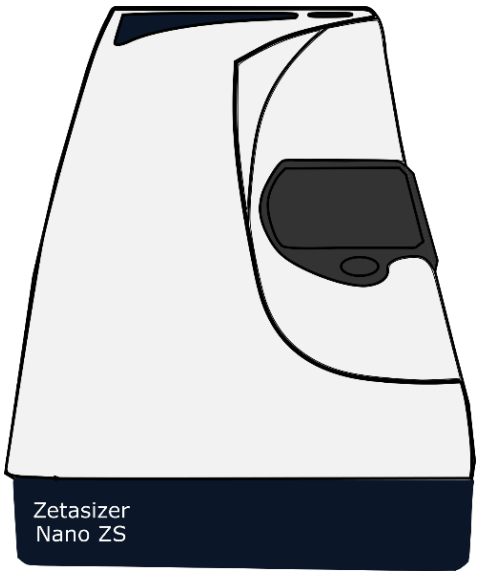

Figure 3.3 Malvern Zetasizer Nano ZS instrument used for measuring particle size, polydispersity index and zeta potential.

3.4.2 Scanning Electron Microscopy (SEM)

Lyophilized chitosan:TPP nanoparticles were analyzed using a JEOL JSM 6360 scanning electron microscope operated at an applied voltage of 15 kV using high vacuum of the beam diameter and secondary electrons at magnification of 5000X. The freeze-dried samples were placed in the sample holder and coated with gold on a JEOL JFC-1100E before the analysis to improve their conductivity properties with the objective of achieving a better quality in the images.

Furthermore, freeze dried nanoparticles were diluted in distilled water in a concentration of 3 mg/mL and sonicated during 20 minutes at 40 kHz. One drop of the solution of nanoparticles was placed on the sample holder and dried during 48 hours under vacuum at room temperature. The dried sample was gold sputtered on a JEOL JFC-1100E, and analyzed in the SEM at applied voltage of 20 kV using high vacuum of the beam diameter and secondary electrons at magnifications of 1,600X.

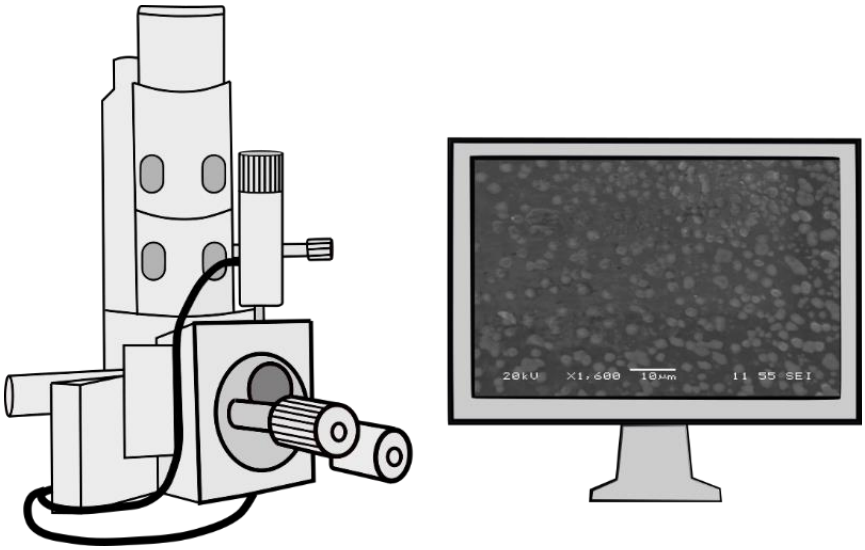

Figure 3.4. JEOL JSM 6360 Scanning Electron Microscope used for visualizing nanoparticles morphology.

3.5 Rheological Profiling of Reconstituted Mucus

Rheology was performed using a Discovery Hybrid Rheometer DHR-3 (TA Instruments) with Cone-And-Plate configuration formed by a 60 mm diameter stainless steel cone geometry (0.9969°) and a Peltier system acting as a lower plate that controls the sample temperature at 37°C to mimic human body conditions. The characterization of reconstituted mucus rheological properties at different pH conditions (pH = 2.0, 4.0, 6.0 or 7.0) included an oscillation frequency and flow sweep tests.

The oscillation frequency test was performed inside the angular frequency range of 0.1-100 rad/s at a strain 1% to identify the variation of reconstituted mucus viscoelastic modulus: storage (G') and loss (G") modulus. While the flow sweep test was carried out in the shear rate range of 0.1-1000 s^{-1} to determine the viscosity behavior of reconstituted mucus. Each experiment was run by triplicate to ensure reproducibility.

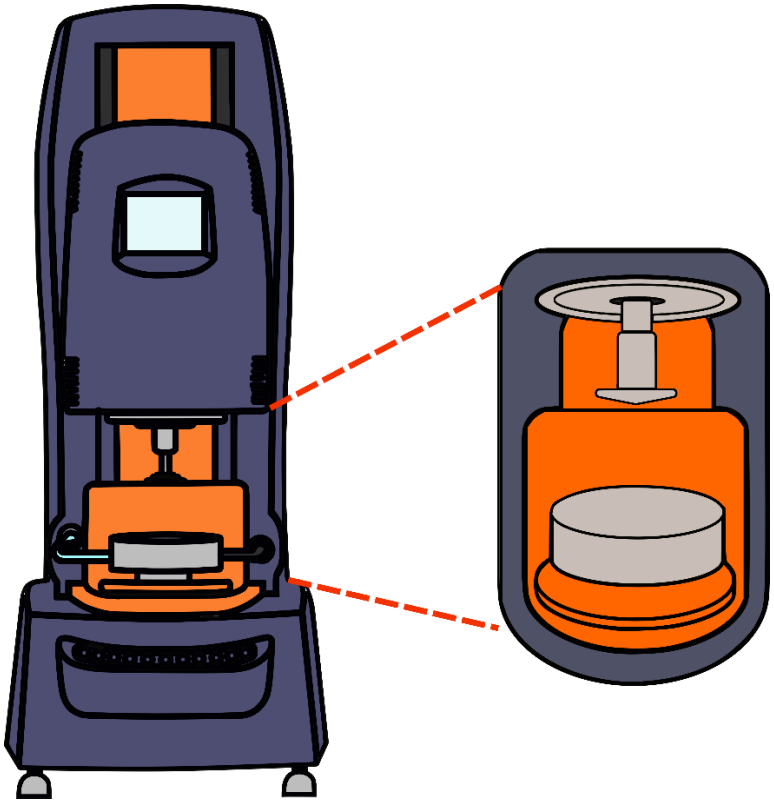

Figure 3.5 Discovery Hybrid Rheometer (DHR-3) using a Cone-And-Plate geometry (0.9969°) for testing viscoelastic and viscous performance of reconstituted mucus, chitosan:TPP nanoparticles and the mixture of mucus / nanoparticles.

3.6 Rheological Synergism

Rheological experiments performed in the subsection 3.4 (oscillation frequency and flow sweep tests) were repeated under the same conditions, but using as samples: a solution of chitosan:TPP nanoparticles (3 mg/mL), and the mixture of reconstituted mucus with chitosan:TPP nanoparticles (1:1). The collected results were compared with reconstituted mucus a) viscoelastic and b) viscous profiles to determine the existence of mucoadhesion phenomenon between reconstituted mucus and chitosan:TPP nanoparticles under different pH environments.

a) The values of the elastic modulus (G') of the reconstituted mucus, chitosan:TPP nanoparticles and the mixture were compared to evaluate the presence of mucoadhesive interactions. The evaluation was calculated as $\Delta G'$ using the Equation 3.1:

$$\Delta G' = G'_{mix} - (G'_{muc} + G'_{np}) \quad (3.1)$$

where $\Delta G'$ refers to the mucoadhesive interaction term (the elastic component is interpreted as the interaction between the mucus and the nanoparticles), G'_{mix} refers to the elastic modulus of the mixture, G'_{muc} refers to the elastic modulus of the reconstituted mucus, and G'_{np} refers to the elastic modulus of the chitosan:TPP nanoparticles.

b) The viscosity values of the reconstituted mucus, chitosan:TPP nanoparticles and the mixture were contrasted to corroborate the existence of mucoadhesion through Equation 3.2:

$$\Delta \eta' = \eta'_{mix} - (\eta'_{muc} + \eta'_{np}) \quad (3.2)$$

where $\Delta \eta'$ refers to the viscosity due to mucoadhesive interaction, η'_{mix} refers to the viscosity of the mixture, η'_{muc} refers to the viscosity of the reconstituted mucus, and η'_{np} refers to the viscosity of the chitosan:TPP nanoparticles.

3.7 Triborheological Profiling of Reconstituted Mucus.

Triborheology of reconstituted mucus under different pH conditions was evaluated using the Discovery Hybrid Rheometer DHR-3 (TA Instruments) using a plate-and-plate configuration conformed by a 40 mm diameter stainless steel plate and the Peltier system that acts as a lower plate and a temperature controller (37°C) during the tests. The coefficient of friction (CoF) was measured through a flow sweep test in the range of 0.1 to 50 rad/s, applying a normal force of 1N.

Moreover, the triborheological behavior of the mixture (reconstituted mucus – chitosan:TPP nanoparticles) was characterized and compared with the reconstituted mucus performance to observe the alterations produced in the coefficient of friction due to the mucoadhesive interaction. Each experiment was run by triplicate to ensure reproducibility.

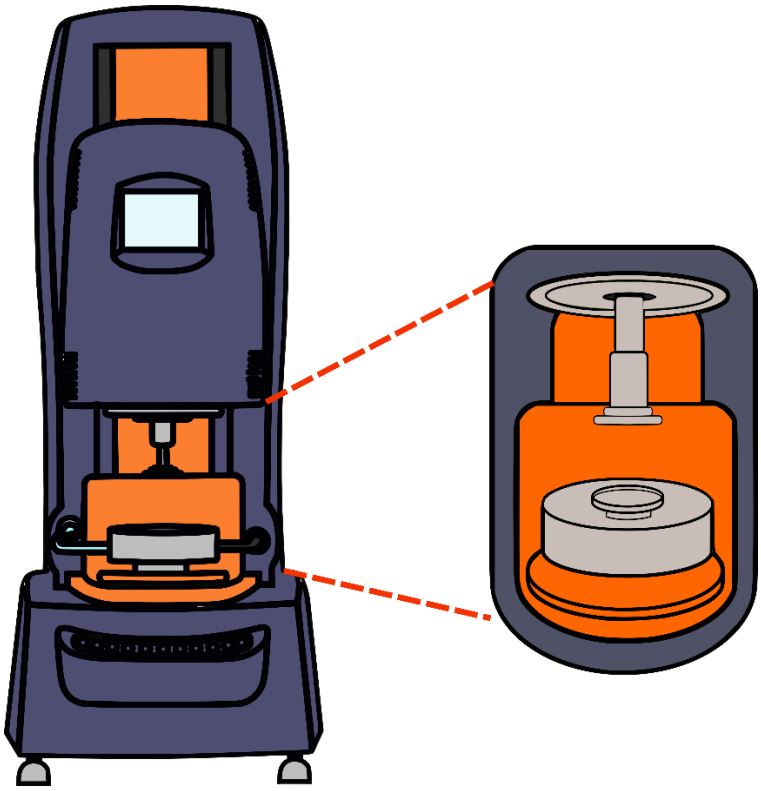

Figure 3.6. Discovery Hybrid Rheometer (DHR-3) using a Plate-And-Plate geometry for testing the lubricant profile of reconstituted mucus, chitosan:TPP nanoparticles and the mixture of mucus / nanoparticles.

3.8 Statistical Analysis

Each experiment was performed at least in triplicate to ensure reproducibility. The data shown is expressed as mean ± standard deviation. One-way analysis of variance (ANOVA) and Tukey's *post hoc* tests were calculated at the significant level of $p < 0.05$ using Minitab 19 software.

Chapter 4. Results and Discussions.

4.1 Triborheological Analysis of the Reconstituted Mucus Samples at Different Gastrointestinal pH Values.

Different triborheological tests were performed to analyze the effect of gastrointestinal pH (pH = 2, 4, 6 and 7) in the viscoelastic, viscous, and lubricating properties of the reconstituted mucus, applying a temperature of 37°C with the purpose of mimicking human body conditions.

The analysis of the viscoelastic behavior was performed through oscillation frequency tests, which demonstrated that the pH directly influences the viscoelastic behavior of the mucus, as Figure 4.1 shows. These variations in the viscoelastic behavior of mucus are closely related to the isoelectric point of mucin (pKa = 4.0) and the structural changes that it undergoes as a consequence of pH changes within the tract [158], [221]. The oscillatory frequency test was performed in an angular velocity range of 0.1 - 100 rad/s, considering the analysis of the linear viscoelastic region (LVR), because the structure of the mucus is stable along this region, and hence, the evaluation of the viscoelastic behavior of mucus is more reliable [143].

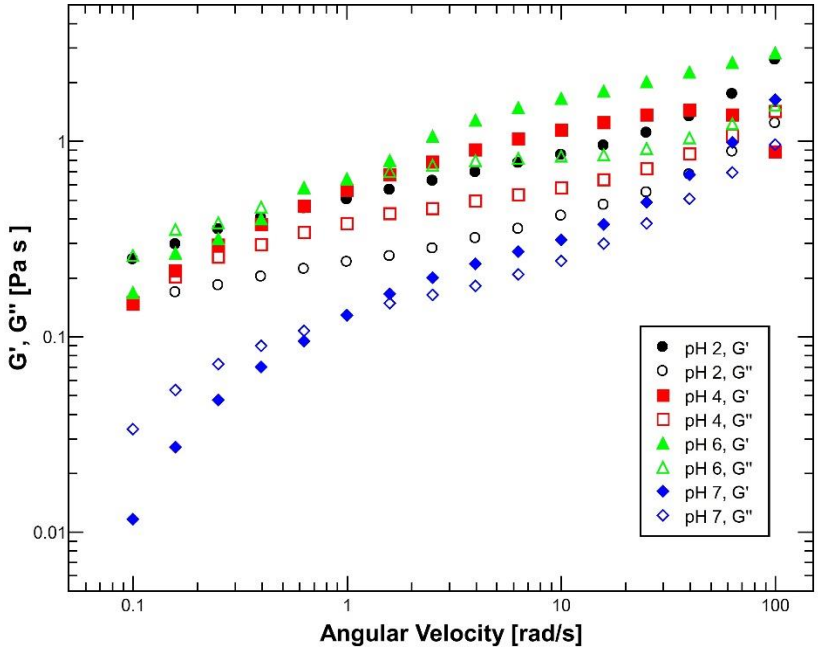

Figure 4.1. Rheological analysis of the viscoelastic performance of reconstituted mucus in the angular velocity range of 0.1 – 100 rad/s at 37°C under different pH conditions. At pH 2 (black dots), mucus exhibited a significant dominance of the elastic modulus (G' > G'). In a similar way, at pH 4 (red squares), mucus presented an initial elastic behavior (G' < G'') with a crossover at high angular velocity (~80 rad/s). In contrast, at pH 6 (green triangles) and pH 7 (blue diamonds), mucus initially behaves viscously (G'' > G') until crosslink occurred around 1 – 1.5 rad/s, in a typical polymeric solution performance. N=5

In the highly acidic stomach conditions (pH = 2), the storage modulus (G') of the mucus kept predominance over the loss modulus (G'') throughout the entire experiment, in a clear gel-like behavior (Figure 4.1). This performance is provoked by the high degree of protonation of the carboxylic groups, the breaking of the disulfide bridges and the repulsion caused by the negative charge of the sialic acid residues, inducing the unfolding and exposure of the hydrophobic domains of the glycoprotein chains [39].

Consequently, these complex interactions among the hydrophilic and the hydrophobic regions of mucin glycoproteins (including its protein core), and the repulsive electrostatic forces between mucin chains, induce an extended rodlike conformational structure [222] as Figure 4.2 shows. This structural configuration stimulates the formation of non-covalent crosslinking of chains, favoring the stabilization of water molecules by the hydrophilic groups of the mucin, resulting in the formation of a protective gel [60], [156] that covers all the stomach epithelium with the objective to restrict the passage of gastric acids and prevent self-digestion of the stomach due to the highly acidic environment [155], [157].

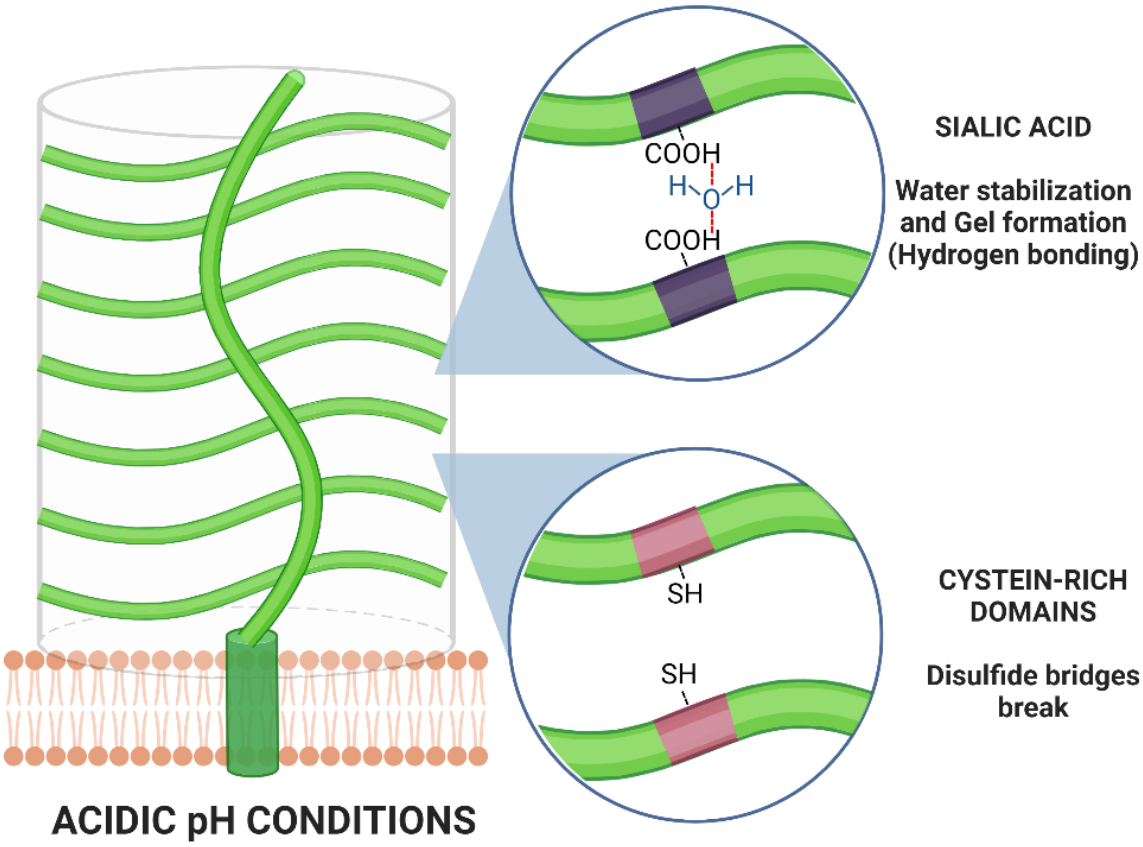

Figure 4.2. Interactions related with mucin rodlike conformation and 'weak' gel behavior of mucus under acidic conditions. Sialic acid exhibits protonation in its carboxylic groups, which interacts with water molecules for achieving the gel formation. While disulfide bridges break allowing the separation and ordering of the mucin o-glycan chains. **Created with BioRender.com**

In contrast, at pH conditions close to neutrality (pH = 6 and 7), the mucus behaves similarly to a viscous polymer solution because the viscous modulus (G') is predominant at very low frequencies, followed by a transition around the angular frequency value of 1 rad/s, in which the elastic modulus (G'') becomes dominant, as Figure 4.1 shows. This change in viscoelastic behavior is a consequence of the various electrostatic interactions that occur between the side chains of the polysaccharides and the formation of disulfide (S-S) bonds among the cysteine terminals of the mucin molecules, which promotes an increase in the entanglement of the strands, and thus, leads to a random coil conformational change of the mucin molecules (Figure 4.3), resulting in higher viscosity [41], [143], [223], [224].

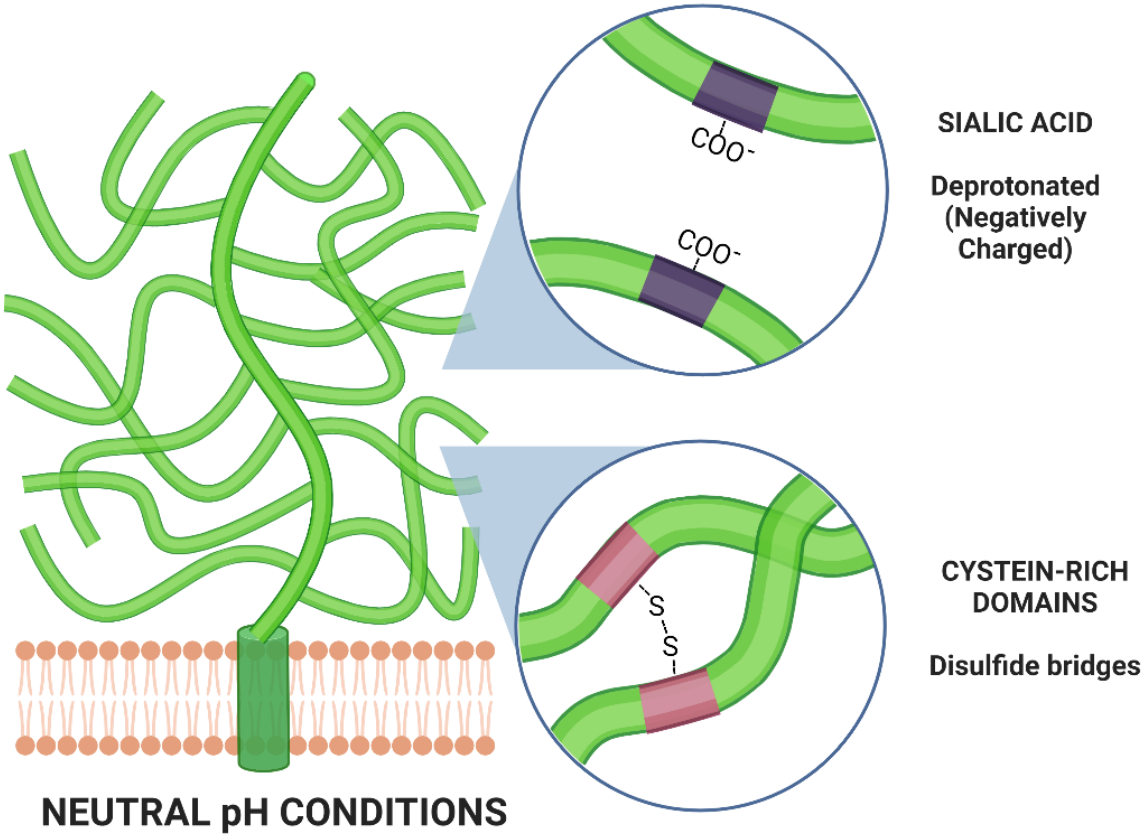

Figure 4.3. Interaction related with mucin random coil conformation and polymeric solution behavior of mucus under neutral conditions. Sialic acid undergoes deprotonation of its carboxylic groups, resulting in repulsion among the chain due to the negative charges. Whereas the disulfide bridges among cysteine-rich regions are formed, causing disorder end entanglement of the chains. **Created with BioRender.com**

Finally, under moderately acidic conditions (pH = 4), reconstituted mucus undergoes a transition stage from a weak gel behavior (high acidity conditions) to a polymeric solution (neutral conditions), since the gap between the elastic (G') and the viscous (G'') modulus initially increase, resembling a gel behavior. When the gap approaches to a maximum separation at an angular velocity ~ 9 rad/s, it begins to

gradually reduce until reaching the crossover point between modules, ~ 82 rad/s. This transition in viscoelastic behavior (at pH = 4) is closely related to the proximity to the isoelectric point of the mucus (IEP = 2.0 - 3.0), which represents a critical point because the mucus undergoes a charge shift, and consequently, its conformational structure changes [55], [60] , as shown in Figure 2.8.

Additionally, flow sweep tests were carried out to establish the viscous properties of the reconstituted mucus. Experiments confirmed that mucus exhibits a typical non-Newtonian shear thinning nature regardless of pH conditions. This non-Newtonian essence is critical for the proper functioning of mucus, which constitutes an unstirred aqueous layer that protects the gastrointestinal tract from the entry of pathogens and provides lubrication to prevent damage caused by shear forces during swallowing and digestion processes [129], [141].

Otherwise, the variation experienced by mucus in viscosity values between different pH environments is minimal, as shown in Figure 4.4. This behavior is characteristic in reconstituted mucus, since partially purified mucin loss some components during isolation methodologies, leading to a decrease in physical crosslinks among mucin molecules [60]. Emphasizing that mucus exhibited the highest viscosity values at pH 4, which corresponds to the intermediate degree of acidity, where the mucus undergoes a significant change in its conformational structure from a rodlike conformation (elastic behavior) to a random coil conformation (viscous behavior) [225].

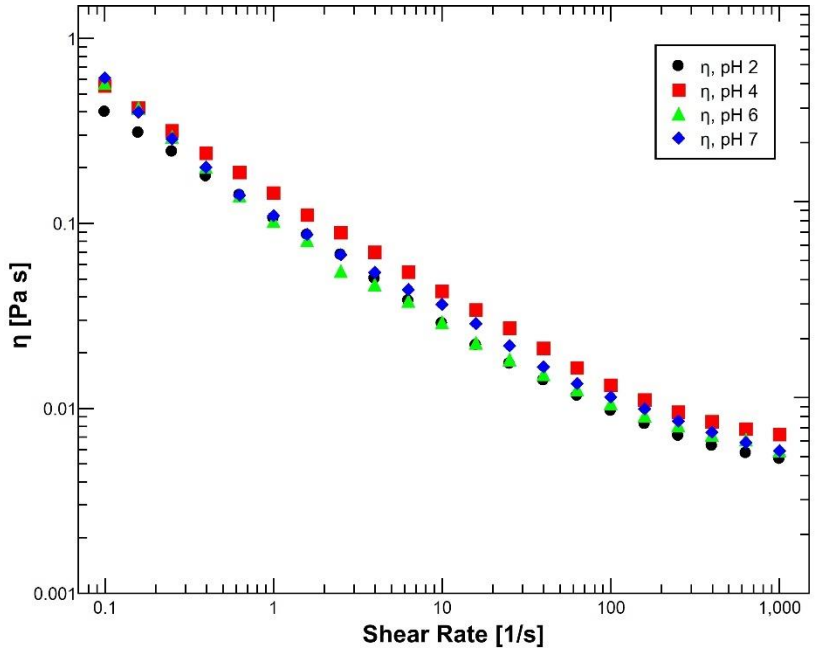

Figure 4.4. Rheological analysis of the viscous performance of reconstituted mucus in the shear rate range of 0.1 – 1000s^{-1} at 37°C under different pH conditions: pH 2 (black dots), pH 4 (red squares), pH 6 (green triangles) and pH 7 (blue diamonds). Despite the variation in the pH conditions, the apparent viscosity (η) showed similar behaviors with a negative slope which is typical in non-Newtonian shear thinning materials.

In the same way, triborheological studies have shown that variations in acidic conditions show minimal influence on the lubricating properties of mucus at low velocities, which corresponds to the frontier lubrication regime. On the contrary, when the mucus is studied under the hydrodynamic lubrication regime, the pH change significantly alters the coefficient of friction (CoF), mainly in the most acidic sample (pH = 2), which exhibit a sudden increase compared to the other samples, as shown by the Stribeck curves in Figure 4.5. This behavior is closely linked to the isoelectric point and the conformational changes around it. Since, the mucus gel-like behavior tends to present a lower lubricating activity due to the great number of water molecules accumulated in the ordered structure increases the contact area, while the polymeric solution behavior allows a greater degree of lubrication to exist as a consequence of high mobility of chains due to their disordered state that allows their flow [60], [226]–[228].

During the boundary lubrication regime, the reconstituted mucus showed CoF values of around 0.16 +/- 0.017 within the angular velocity range of 0.01 - 0.6 rad/s, followed by a sudden reduction in CoF values at 0.04 +/- 0.008 during the mixed lubrication regime, which was reached within the angular velocity range of 0.6- 3.9 rad/s. Regardless of the degree of acidity, the mucus exhibited a good lubricating profile in boundary and mixed lubrication regimes with very low CoF values (around 0.01). Because during the application of shear force, friction decreases as a result of the energy dissipation by the movements of the water molecules found in the mucus layer [64]. Nonetheless, variations in the negative charge density of the mucus along the different pH environments studied did not exhibit an observable variation in mucus lubricating properties, suggesting that in the boundary and mixed regimes, lubrication depends primarily on other factors [229]. Moreover, the lubricant profile of the reconstituted mucus demonstrated a very poor performance (mainly in the boundary regime) due to the deglycosylation of mucin during purification methodologies, which affects the hydration that the mucin achieves on a molecular scale and, consequently, its lubricating properties [121].

Eventually, the reconstituted mucus reached hydrodynamic lubrication regime, in which pH acquired an important influence in the lubrication profile of the mucus. Since, the mucus exhibited a critical increase in CoF, reaching a value of 0.26 +/- 0.027 under highly acidic conditions (pH = 2). In contrast, the slightly acid (pH = 4 and 6) and neutral (pH = 7) samples showed a more controlled increase in their CoF values: 0.23 +/- 0.036, 0.23 +/- 0.038 and 0.19 +/- 0.031, respectively. This behavior is mainly associated to the viscoelastic profile of the mucus, which is dependent on pH. Since the high viscosity of mucus under neutral conditions allows the formation of fluid films at lower angular velocities, which reduces friction in comparison to elastic mucus samples (under acidic pH), as a result of hydrodynamic drag at high angular velocities [226], [230], [231].

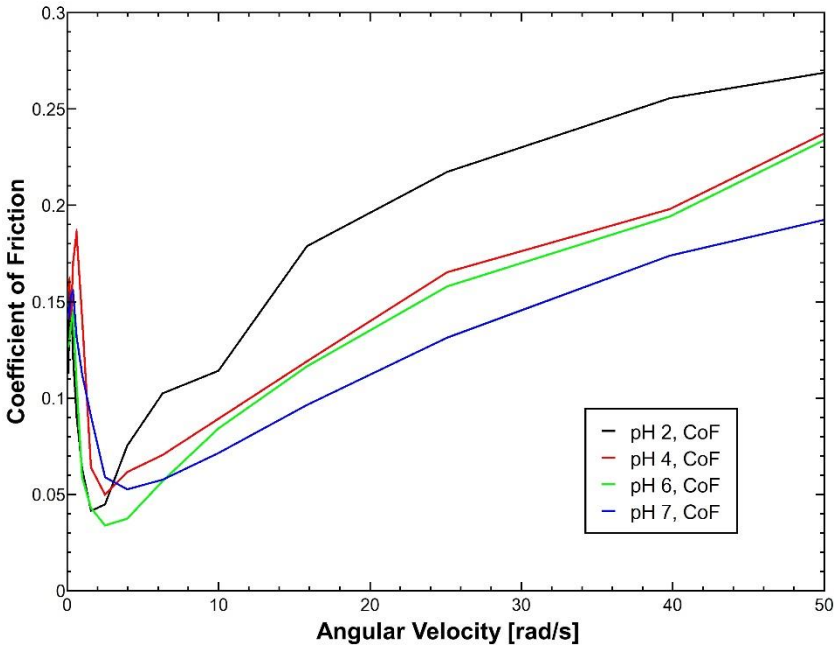

Figure 4.5. Evaluation of the lubricant properties of reconstituted mucus by plotting an Stribeck curve in the angular velocity range 0 – 50 rad/s, at 37°C under different pH conditions: pH 2 (black), pH 4 (red), pH 6 (green) and pH 7 (blue). Results showed that regardless of the pH, mucus samples showed a similar behavior during the boundary and mixed lubrication regimes. Meanwhile, the more acidic sample showed a significant increase in its CoF during the hydrodynamic regime, since the conformational change that mucus undergoes in the pH range 2.0 - 3.0 (isoelectric point) alters its lubricant properties. N=5

4.2 Chitosan:TPP Nanoparticles Synthesis and Characterization.

Chitosan:TPP nanoparticles synthesis were achieved through ionic gelation methodology, which is based on the difference in charges between cationic chitosan molecules and anionic TPP molecules. Therefore, polymeric nanoparticles were formed through ionic crosslinking when the phosphate groups of TPP were attracted to the amino groups of chitosan molecules [232]. In order to corroborate the successful synthesis of the nanoparticles, various analyzes were performed: particle size, polydispersion index, zeta potential, and morphology visualization.

Moreover, the chitosan:TPP nanoparticles were analyzed at different acidity conditions (pH = 2.0, 4.0, 6.0 and 7.0) to study how the pH of the gastrointestinal tract alter their size, polydispersity index (PDI) and zeta potential. Considering the wide range of pH variation within the gastrointestinal tract, which represents a significant challenge for all molecules that enter in this very hostile environment, which can vary from pH 1.0 - 3.0 in the stomach up to pH 6.0 - 7.5 in the intestine (duodenum, jejunum and ileum) [233].

4.2.1 Particle Size, Polydispersity Index and Zeta Potential Measurements.

The synthesis of chitosan:TPP nanoparticles was accomplished by the capability of chitosan molecules to gel spontaneously on contact with a solution of polyanionic TPP, due to the intramolecular and intermolecular crosslinking interaction among the cationic amino groups of chitosan and anionic phosphate groups of TPP [234]. Nonetheless, the mean size of chitosan:TPP nanoparticles is affected by pH conditions. Since, chitosan is usually protonated in acid solution, allowing a high degree of solubility. While, in a neutral environment, chitosan loses its cationic properties due to deprotonation, and tends to precipitate, which limits its interaction with TPP [235]. For this reason, the particle size, the polydispersion index (PDI), and the zeta potential of the nanoparticles were measured under different acidity conditions (pH = 2.0, 4.0, 6.0 and 7.0), as Table 3.1 shows.

Table 3.1. Mean particle size, polydispersion index (PDI) and zeta potential measurements of chitosan:TPP nanoparticles dissolved under different pH conditions. **N = 3**

pH	Size (nm)	PDI	Zeta Potential (mV)
2.0	171.01 ± 21.86	0.29 ± 0.03	23.55 ± 0.84
4.0	297.53 ± 31.95	0.41 ± 0.11	19.69 ± 0.21
6.0	350. 03 ± 38.84	0.42 ± 0.06	16.23 ± 1.95
7.0	506.23 ± 49.98	0.61 ± 0.04	3.87 ± 0.79

The results in Table 3.1 showed the great influence of the acidity degree of the medium on the final particle size and on the PDI of the chitosan:TPP nanoparticles. These variations are due to the fact that chitosan is a weak polyelectrolyte that has a pKa value ~ 6.5, so it is susceptible to significant changes in its degree of protonation throughout the gastrointestinal tract as a consequence of the pH variations [236]. In an acidic environment, the high amount of hydrogen ions present in the medium induces the protonation of the primary amino groups (NH_3^+) of the chitosan molecule, providing a high charge density to the molecular surface of chitosan, which generates repulsion between molecules and increases the amount of cationic amino groups exposed to interact with the polyanionic groups of TPP, resulting in the spontaneous formation of small chitosan nanoparticles with a high positive surface charge [237], [238]. On the contrary, when the environment tends to neutrality (pH similar to or above the pKa value of chitosan), the amino groups gradually deprotonate and lose their positive charge, causing the folding of the polymeric chains and chitosan insolubility problems. Consequently, the exposure of the amino groups to the phosphate groups of the TPP decreases, resulting in less

crosslinking and a larger particle size with a slightly positive surface charge, which significantly increase the tendency of nanoparticles to agglomerate [234], [239], [240].

Otherwise, the zeta potential allows to measure the electrostatic charges of the nanoparticles and, therefore, it is associated with the stability of nanoparticle solutions. Since zeta potential is a determining factor in some phenomena such as dispersion, flocculation or aggregation of polymeric solutions [241]. In the case of chitosan, the zeta potential of the synthesized nanoparticles showed a dependence related to pH due to the sensitivity of chitosan to variations in the acidity of the medium, as shown in Table 3.1. These variations in zeta potential are result of changes experienced by chitosan nanoparticles in surface charge density, since at low pH the amino groups are charged, providing a highly cationic charge to the particle. However, when the pH approaches neutral values, the deprotonation of the amino groups causes the zeta potential to decrease, favoring the establishment of hydrogen bonds and hydrophobic interactions between particles, inducing a higher rate of aggregation [242], [243].

4.2.2 Morphological Characterization

The morphology of the synthesized chitosan:TPP nanoparticles was examined with a Scanning Electron Microscope (SEM), as shown in Figure 4.6. The images of the lyophilized chitosan:TPP nanoparticles (Figure 4.6a) presented amorphous shapes, and exhibited a high degree of agglomeration due to the intermolecular and intramolecular hydrogen bonds produced between the -OH groups of the chitosan molecules during drying by lyophilization [244]. Whereas, Figure 4.6b presents spherical and well dispersed particles as a result of particle hydration effects and ultrasonic cavitation produced by 20 minutes of appropriate sonication conditions to break down the agglomerates of resuspended lyophilized nanoparticles [245].

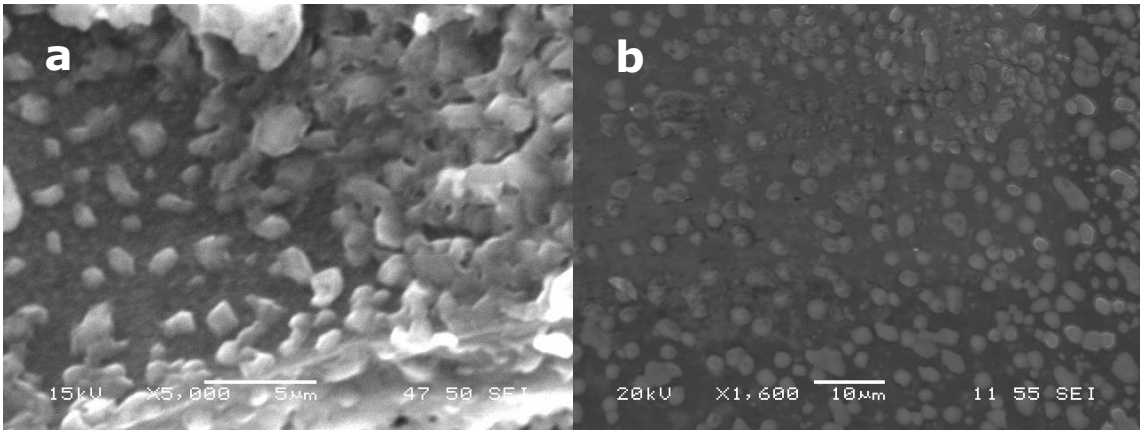

Figure 4.6. SEM images of a) Freeze-dried chitosan:TPP nanoparticles (15kV, 5000x, secondary electrons), and b) Dispersed chitosan:TPP nanoparticles (20kV, 1600x, secondary electrons).

4.3 Assessment of Chitosan Nanoparticle - Mucus Interaction through Rheological Synergism.

4.3.1 Rheological Synergism

Mucoadhesion is a phenomenon that describes the adhesive interactions among a mucoadhesive material and a mucosal surface due to the physical chain interlocking and the formation of different chemical bonds (including ionic interactions, hydrophobic interactions, hydrogen bonding, and van der Waals forces) between them [219], [246]. Considering the benefits of mucoadhesion for the development of new drug delivery systems, the evaluation of the mucoadhesive performance of different materials has acquired great relevance [247].

Among the different techniques for determining the mucoadhesive properties of polymers are ellipsometry, tensile strength, flow-through method, atomic force microscopy, and rheology [248]. Emphasizing that one of the most used in vitro approaches to assess the presence of the mucoadhesive phenomenon is based on measurements of the viscoelastic moduli or viscosity through rheological synergism [32]. Since, the rheological properties of the mixture reflect the degree of interaction, for example, high values of viscoelasticity or viscosity in the measurements of the mucus - polymer mixture indicate the presence of mucoadhesion [249]. In addition, rheology presents a significant advantage over other methods based on the measurement of the detachment force, because it is easy to evaluate diluted solutions and dispersions through rheological synergism [250], as in the case of solutions of chitosan nanoparticles: TPP. In this project, the mucoadhesive properties of chitosan:TPP nanoparticles were evaluated under the different acidity conditions that occur throughout the gastrointestinal tract (pH = 2.0, 4.0, 6.0 and 7.0), considering body temperature (37°C) to mimic the conditions of the human body.

The results of the oscillation frequency tests indicate that under acidic conditions (pH = 2, 4 and 6), the rheological synergism (ΔG') is positive since the elastic moduli (G') show higher values in the mixture of mucin – polymeric nanoparticles than in the individual curves (of mucus and nanoparticle solution) and in the sum curve (mucus + nanoparticle solution), as shown in Figures 4.7a, 4.7b and 4.7c.

The positive synergism shown in the results is an indicator of the high affinity of chitosan:TPP nanoparticles for the reconstituted mucus, which is mainly due to the interaction generated by the opposite charges among the biopolymers induces a physical entanglement between the polymeric and mucin chains [30], causing the formation of a polymeric network that exhibits a significant increase in the elastic modulus (G') of the mixture in comparison with the sum of the values of the elastic

modulus (G') of the individual components [251]. Instead, the results visualized in Figure 4.7d indicate that mucoadhesion of chitosan nanoparticles is limited under neutral conditions (pH = 7), since the values corresponding to the rheological synergism of the mixture and the values calculated with the sum of the elastic modulus (G') of the mucus and the nanoparticle solution are not significantly different (p < 0.05). This very low levels of mucoadhesion, almost negligible, are a consequence of the deprotonation of the chitosan amino groups under neutral conditions, inducing the formation of an insoluble polymer layer that makes it difficult for the chitosan and mucin chains to interpenetrate [179], [247].

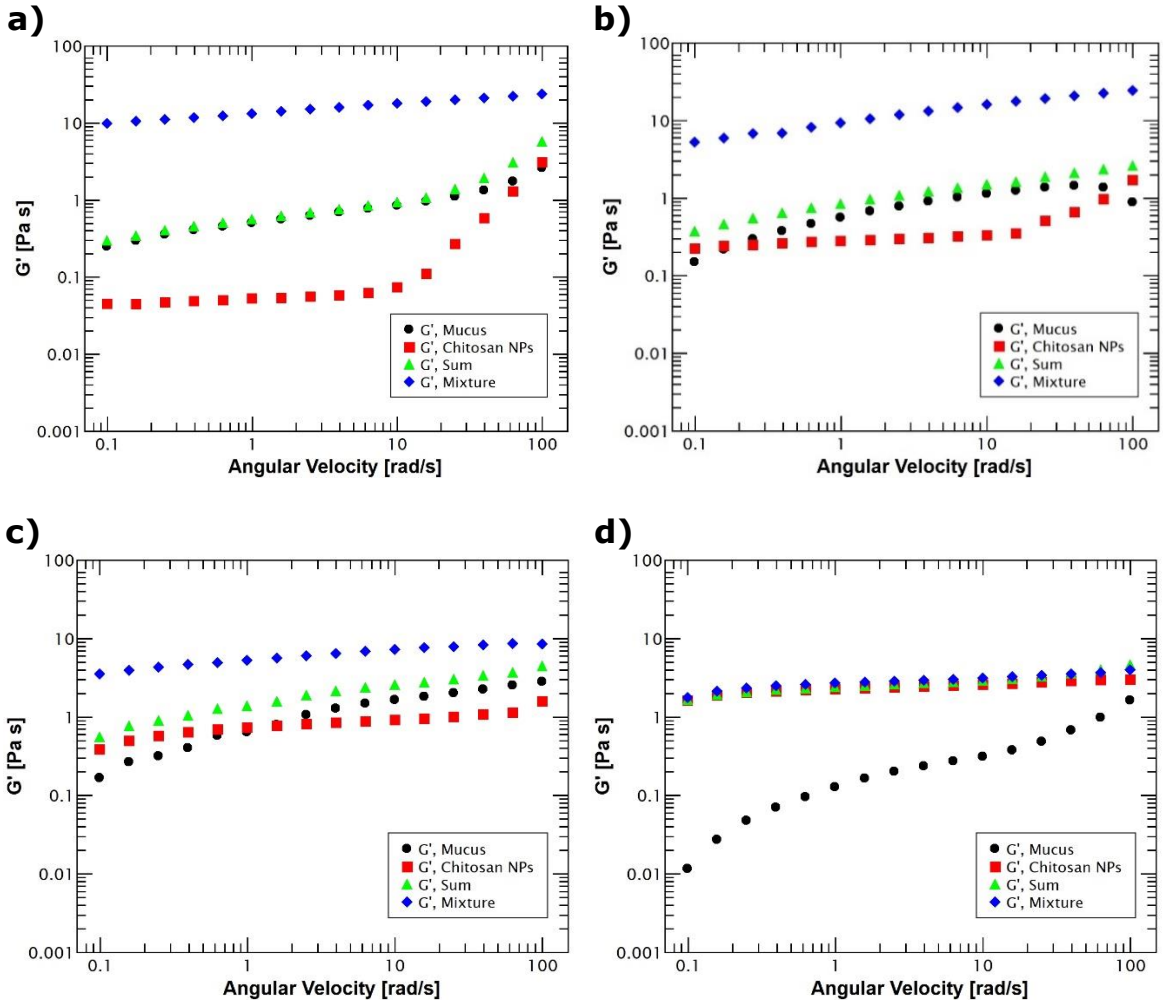

Figure 4.7. Evaluation of the mucoadhesion of chitosan:TPP nanoparticles by rheological synergism from the point of view of the elastic modulus (ΔG'). Elastic modulus (G') of the reconstituted mucus (black dots), the chitosan:TPP nanoparticles solution (red squares), the summation of reconstituted mucus - chitosan:TPP nanoparticles (green triangles), and the mixture of chitosan:TPP nanoparticles - reconstituted mucus (blue diamonds). The mixtures under acidic conditions (pH = 2, 4 and 6) showed a strong polymeric mucoadhesion because they showed higher values in their elastic modulus than the sums. In contrast, the mixture in neutral conditions (pH = 7) exhibited negligible mucoadhesion as it did not show significant differences with the sum. **N=5**

The mucoadhesive behavior of chitosan:TPP nanoparticles is a result of secondary bonds formation and electrostatic interactions among the cationic amino groups of chitosan and the anionic sialic and sulfonic acid residues of mucus [225], [252], [253]. However, the interactions are closely dependent on the protonation state of the functional groups of the polymer, and therefore, on the acidity conditions of the medium [254], [255], as Figure 4.8 illustrates. For this reason, the chitosan:TPP nanoparticles present a high amount of interactions with the compounds of the mucosa through the formation of polyelectrolyte complexes that improve adhesion, as the acidity of the environment is increasing during the interaction [256], [257]. While, under neutral or alkaline conditions, chitosan deprotonates, forming an insoluble layer that tends to precipitate (Figure 4.6), and limits its mucoadhesive properties [29], [179], [258].

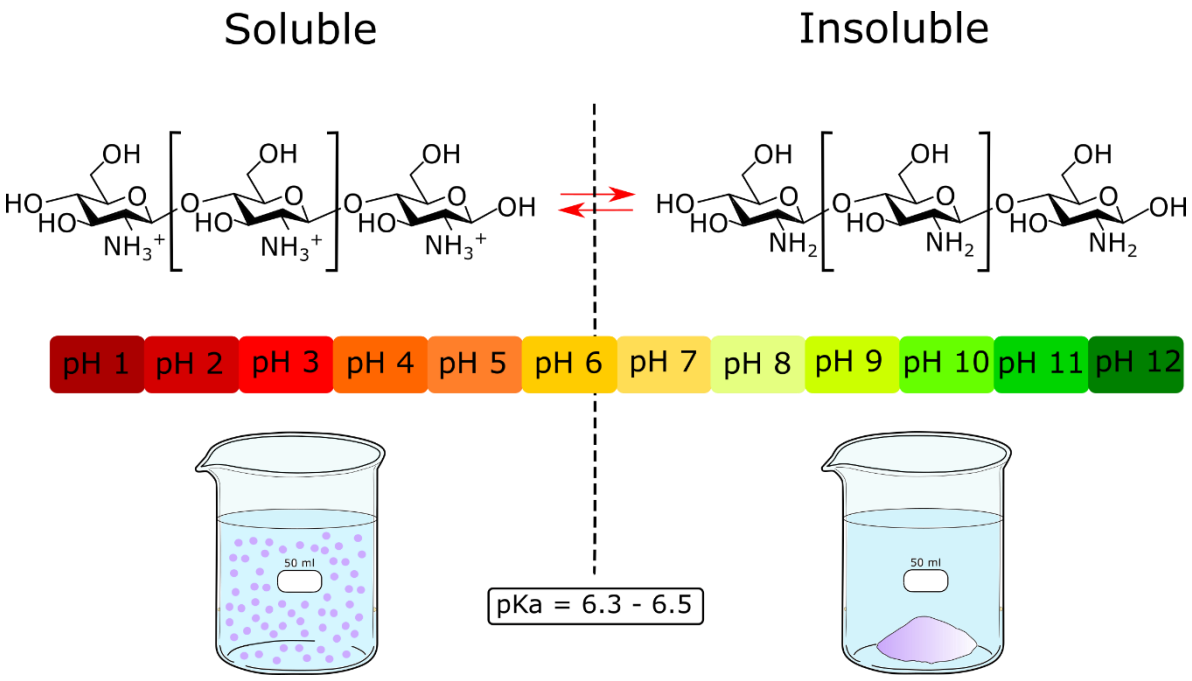

Figure 4.8. Influence of pH on the solubility of chitosan (purple). Under acidic conditions (left), chitosan is protonated, allowing the formation of nanoparticles with mucoadhesive properties. While, under conditions above its pKa value = 6.3 - 6.5, neutral or alkaline conditions (right), chitosan deprotonates and tends to become insoluble, so the nanoparticles lose their adhesive properties, and may even collapse.

In the same way, rheological synergism can be studied from the point of view of viscosity (Δη), by contrasting the viscosity of the mixture and the sum of the individual components [254]. Considering that the viscosity synergism viscosity corresponding to a mixture between a polymer dispersion and a mucous solution can be considered as a reflection of the mucoadhesive strength of the polymer - mucin system [259], due to the fact that the entanglement of the chains and the

formation of molecular bonds between the mucus and the polymeric nanoparticles alters the rheological behavior of both materials [249]. For this reason, the flow sweep tests were carried out to corroborate the presence of the positive rheological synergism previously obtained through the oscillation frequency tests. The resulting graphs (Figure 4.9) demonstrated that the mixture preserved the characteristic behavior of polymer solution, which corresponds to shear thinning behavior regardless of pH conditions.

The results of the viscosity analysis confirmed that under highly acidic media (pH = 2, 4) the mucoadhesive phenomenon occurs, since positive rheological synergism values were obtained, because the viscosity values of the mixture are considerably higher ($p < 0.05$) than the values corresponding to the sum of the individual viscosities, as observed in Figures 4.9a and 4.9b. The strong mucoadhesive interactions are a result of the cationic nature of chitosan, and of the high degree of interpenetration that was established between the glycoprotein chains of mucin and the polymeric chains, allowing the formation of several secondary chemical bonds among the chains of both materials, and hence, producing a significant increase in the viscosity of the samples [56], [260]. Whereas, as the environmental conditions approach neutral values (pH = 6), the degree of rheological synergism decreases and becomes negligible ($p < 0.05$), although it remains slightly positive, as Figure 4.9c shows. These variations are caused by the influence of the ionizable groups of chitosan, which deprotonate when approaching the pKa value (6.5), decreasing the charge density on the nanoparticles surface and, consequently, limiting the electrostatic interactions with the mucus [185], [257]. Finally, the rheological study revealed that the mixtures in a neutral environment (pH = 7) exhibit a negative synergism (Figure 4.9d), indicating that there is no presence of the mucoadhesive phenomenon, because the chitosan is deprotonated and does not establish ionic interactions with the mucus [261], and even nanoparticles tend to collapse due to the precipitation of chitosan molecules [262].

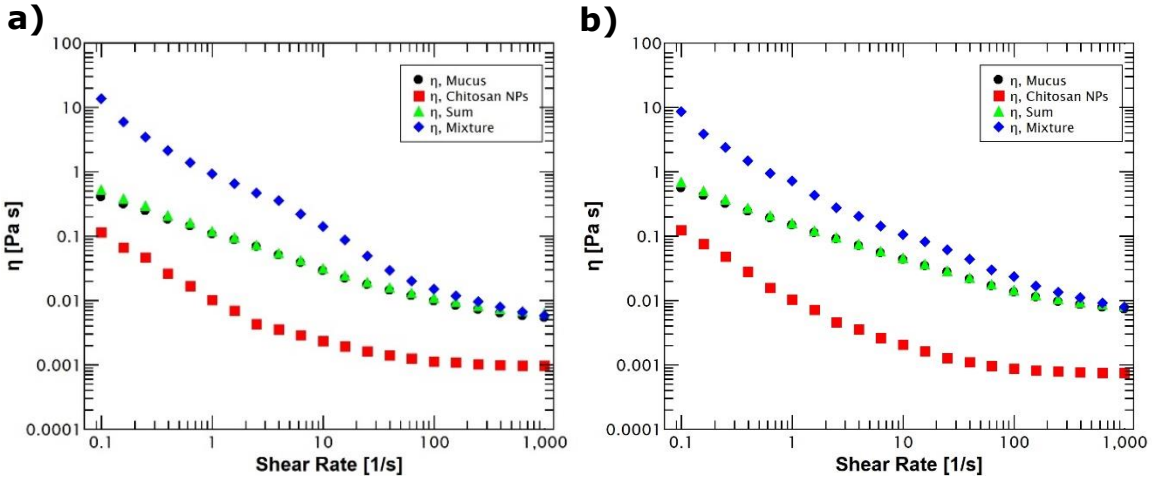

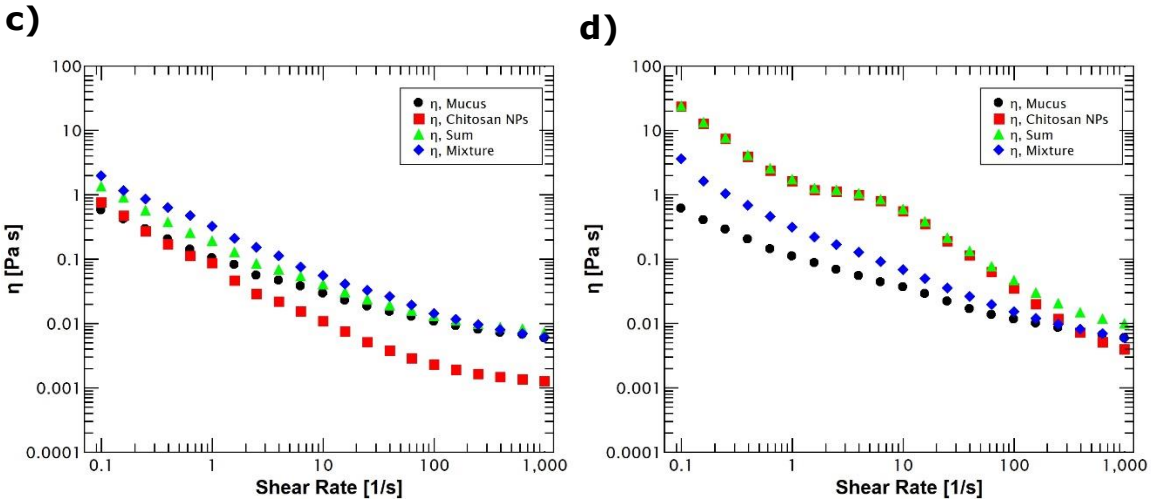

Figure 4.9. Evaluation of the mucoadhesion of chitosan:TPP nanoparticles by rheological synergism from the point of view of the apparent viscosity (Δη). Apparent viscosities (η) of the reconstituted mucus (black dots), the chitosan:TPP nanoparticles (red squares), the summation of chitosan:TPP nanoparticles - reconstituted mucus (green triangles) and the mixture of chitosan:TPP nanoparticles - reconstituted mucus (blue diamonds). The mixtures in highly acidic conditions (pH = 2 and 4) showed an evident mucoadhesive performance since their viscosity was higher than in the sums. Instead, the mixture in slightly acidity (pH=6) showed minimal mucoadhesiveness, and the mixture in a neutral environment (pH=7) did not exhibite significant difference with the sum, showing negligible or null mucoadhesion. N=5

4.3.2 Triborheological Synergism

The triborheological analysis of the mucus-nanoparticles system demonstrated that the lubricating properties of the mucus improved when the mucoadhesion phenomenon occurred, regardless of the acidity conditions, as observed in the different Stribeck curves corresponding to Figure 4.10. The samples corresponding to the mucus-nanoparticle mixture reached the boundary lubrication regime in an angular velocity range very similar to the mucus samples alone, 0.01 - 0.6 rad/s. In the case of the mixed lubrication regime, a very similar situation arose in which both the mucus-alone and mixed-lubrication samples reached the regime within the angular velocity range of 0.6 - 3.9 rad/s, with the exception of the mixture in highly acidic conditions (pH = 2), where an elongation of the regime occurred until reaching an angular velocity of 9.99 rad/s.

Finally, it was demonstrated that pH conditions exert some influence during the hydrodynamic lubrication regime. Emphasizing that the mixture under more acidic conditions showed a greater improvement in its lubricating properties, because the CoF increased in a more controlled manner than the other mixtures (Figure 4.10a, 4.10b, 4.10c and 4.10d), and presented the most significant broad

reduction in comparison to the values of reconstituted mucus alone, as can be seen in Table 3.2.

Table 3.2. Comparison of the CoF values among reconstituted mucus alone and the mixture of reconstituted mucus - chitosan:TPP nanoparticles during the different lubrication regimes (boundary lubrication, mixed lubrication and hydrodynamic lubrication) considering the variations in the pH conditions. **N = 3**

	Boundary Lubrication Stage		Mixed Lubrication Stage		Hydrodynamic lubrication Stage	
pH	Mucus	Mixture	Mucus	Mixture	Mucus	Mixture
2	0.15 ± 0.035	0.21 ± 0.081	0.04 ± 0.019	0.07 ± 0.006	0.27 ± 0.026	0.17 ± 0.024
4	0.19 ± 0.029	0.17 ± 0.037	0.05 ± 0.016	0.06 ± 0.031	0.24 ± 0.044	0.19 ± 0.008
6	0.14 ± 0.028	0.13 ± 0.049	0.03 ± 0.008	0.03 ± 0.012	0.23 ± 0.054	0.17 ± 0.030
7	0.16 ± 0.040	0.14 ± 0.008	0.05 ± 0.041	0.03 ± 0.003	0.19 ± 0.016	0.15 ± 0.049

The lubricating properties of the mixture improved significantly under high acidity conditions because the protonated chitosan acts as a physical crosslinker, inducing the entanglement of chains with mucus and the formation of electrostatic bonds, increasing the charge capacity of the mucus solution and providing greater resistance to wear generated by friction [263]. Unlike a neutral environment, where chitosan has limited solubility and few electrostatic interactions due to the low surface charge density as a consequence of the deprotonation of its amino groups, significantly reducing the formation of mucin - chitosan aggregates [264], [265]. Consequently, synergistic lubricity at neutral pH is produced mainly by hydrogen bond formation, and hence, the synergistic lubricant effects are minimum [266].

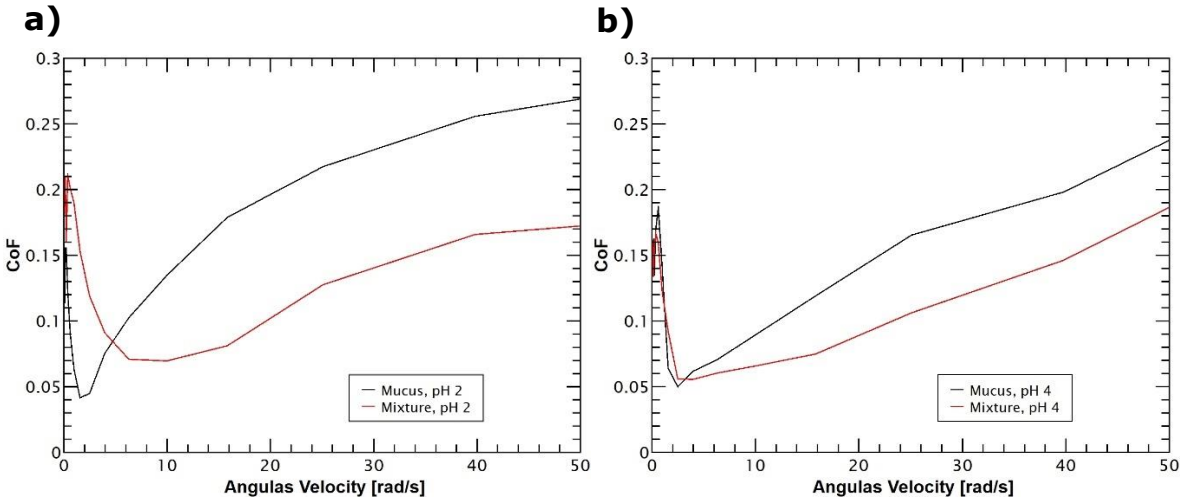

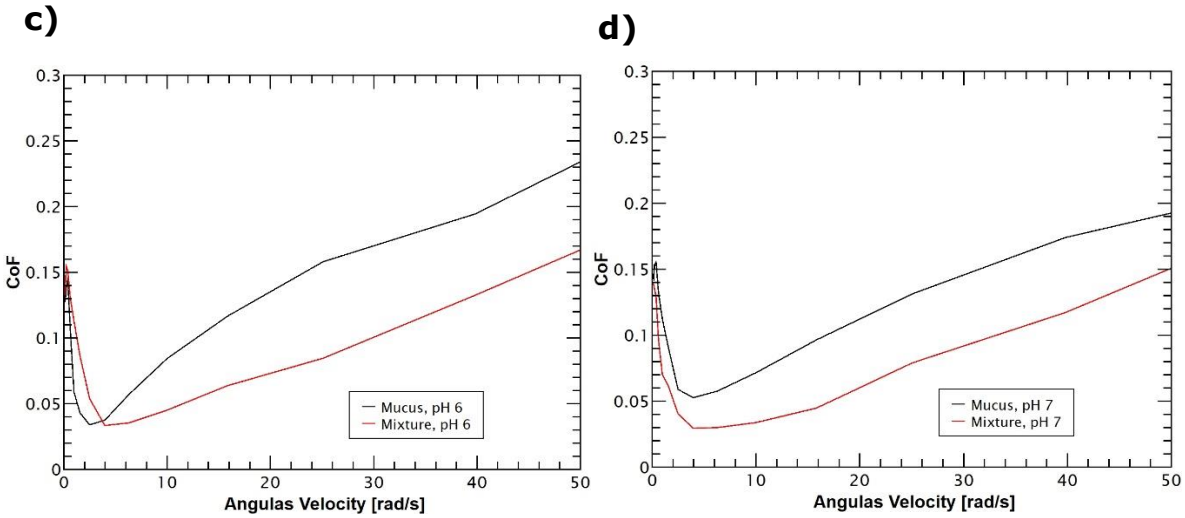

Figure 4.10. Comparative evaluation of coefficient of friction (CoF) of the reconstituted mucus alone and the mixture of reconstituted mucus – chitosan:TPP nanoparticles at 37°C under different pH conditions. a) Stribeck curve at pH 2. b) Stribeck curve at pH 4. c) Stribeck curve at pH 6. d) Stribeck curve at pH 7. All the mixtures exhibited improved lubricant properties regarding mucus samples. N=3

Chapter 5. Conclusions

Triborheological evaluation of the reconstituted mucus showed that its viscoelastic properties are dependent on pH, so they vary throughout the gastrointestinal tract as a function of the fluctuations in the acidic conditions of the environment. Under the highly acidic conditions of the stomach, the reconstituted mucus acquired an elastic performance similar to a "weak gel" that fulfills the function of protecting the stomach epithelium from gastric acids. On the contrary, under neutral conditions, the mucus shows a polymeric solution behavior with lubricating properties in order to protect the digestive tract from the shear stress generated during digestion (peristaltic movements). Moreover, triborheology demonstrated that the viscosity of the reconstituted mucus maintains a non-Newtonian shear-thinning behavior regardless of the pH variations it experiences throughout the tract. However, the lubricating properties of the reconstituted mucus showed limited behavior, mainly under acidic conditions, due to the deglycosylation and loss of minor elements that the mucin undergoes during the purification and cleansing processes, affecting their interactions on a molecular scale and, consequently, its lubricating performance.

On the other hand, chitosan:TPP nanoparticles demonstrated high sensitivity to pH variations. The nanoparticles showed a small size (171.01 ± 21.86 nm) and a highly positive zeta potential (23.55 ± 0.84 mV) under extremely acidic conditions. Whereas the size of the nanoparticles increased up to three times under neutral conditions (reaching values of 506.23 ± 49.98 nm) and showed a zeta potential close to zero (3.87 ± 0.79 nm). This performance is intimately related to the cationic nature of chitosan (pKa ~ 6.5), which experienced the protonation/deprotonation of its amino groups depending on the different acidity conditions. On the other hand, the characterization through SEM confirmed the spherical shape of the chitosan:TPP nanoparticles in solution, and an irregular shape with high agglomeration of the lyophilized nanoparticles.

The mucoadhesive profile of the chitosan:TPP nanoparticles was analyzed through the rheological synergism method from the point of view of elastic modulus ($\Delta G'$) and viscosity ($\Delta\eta$). The analysis through the elastic modulus (G') showed a positive synergism for all the samples in acidic conditions (pH 2, 4 and 6), while the sample in neutral conditions (pH = 7) exhibited a negligible synergism with a p value > 0.05. Otherwise, the synergism of the viscosity (η) only showed positive values in highly acidic conditions (pH = 2 and 4), while the samples close to the pKa of chitosan: the slightly acidic (pH = 6) and neutral (pH = 7) samples, exhibited negligible and negative synergism, respectively. Therefore, considering both rheological synergism studies as complementary, it can be established that the mucoadhesion phenomenon only occurs under acidic pH conditions, since the amino groups of chitosan are protonated and establish electrostatic interactions with

negatively charged mucin molecules. On the contrary, under neutral conditions, the amino groups of chitosan deprotonate, limiting the surface charges, and consequently, the electrostatic interactions. Thus, chitosan nanoparticles exhibit a poor mucoadhesive profile, and even tend to agglomerate and collapse.

Finally, the Stribeck curves corresponding to the reconstituted mucus-chitosan:TPP nanoparticles mixtures showed the existence of a relationship between the mucoadhesive phenomenon and an improvement in the lubricating properties of the mucus. The wear resistance and the load bearing properties of the mucus are enhanced due to the physical entanglement and the formation of electrostatic interactions between the mucin and chitosan chains.

Bibliography

[1] S. Mitragotri, P. A. Burke, and R. Langer, “Overcoming the challenges in administering biopharmaceuticals: formulation and delivery strategies,” *Nat. Rev. Drug Discov.*, vol. 13, no. 9, pp. 655–672, Sep. 2014, doi: 10.1038/nrd4363.

[2] J. Grießinger *et al.*, “Methods to determine the interactions of micro- and nanoparticles with mucus,” *Eur. J. Pharm. Biopharm.*, vol. 96, pp. 464–476, 2015, doi: https://doi.org/10.1016/j.ejpb.2015.01.005.

[3] J. G. Song, S. H. Lee, and H.-K. Han, “The stabilization of biopharmaceuticals: current understanding and future perspectives,” *J. Pharm. Investig.*, vol. 47, no. 6, pp. 475–496, Nov. 2017, doi: 10.1007/s40005-017-0341-9.

[4] B. Homayun, A. Kumar, P. T. H. Nascimento, and H.-J. Choi, “Macropored microparticles with a core–shell architecture for oral delivery of biopharmaceuticals,” *Arch. Pharm. Res.*, vol. 41, no. 8, pp. 848–860, Aug. 2018, doi: 10.1007/s12272-018-1062-y.

[5] F. Araújo, N. Shrestha, P. L. Granja, J. Hirvonen, H. A. Santos, and B. Sarmento, “Safety and toxicity concerns of orally delivered nanoparticles as drug carriers,” *Expert Opin. Drug Metab. Toxicol.*, vol. 11, no. 3, pp. 381–393, Mar. 2015, doi: 10.1517/17425255.2015.992781.

[6] J. Wang *et al.*, “Oral delivery of metformin by chitosan nanoparticles for polycystic kidney disease,” *J. Control. Release*, vol. 329, pp. 1198–1209, Jan. 2021, doi: 10.1016/j.jconrel.2020.10.047.

[7] J. Leal, H. D. C. Smyth, and D. Ghosh, “Physicochemical properties of mucus and their impact on transmucosal drug delivery,” *Int. J. Pharm.*, vol. 532, no. 1, pp. 555–572, Oct. 2017, doi: 10.1016/j.ijpharm.2017.09.018.

[8] M. D. Wilcox, L. K. Van Rooij, P. I. Chater, I. Pereira de Sousa, and J. P. Pearson, “The effect of nanoparticle permeation on the bulk rheological properties of mucus from the small intestine,” *Eur. J. Pharm. Biopharm.*, vol. 96, pp. 484–487, Oct. 2015, doi: 10.1016/j.ejpb.2015.02.029.

[9] P. C. Griffiths, B. Cattoz, M. S. Ibrahim, and J. C. Anuonye, “Probing the interaction of nanoparticles with mucin for drug delivery applications using dynamic light scattering,” *Eur. J. Pharm. Biopharm.*, vol. 97, pp. 218–222, Nov. 2015, doi: 10.1016/j.ejpb.2015.05.004.

[10] W. Shan *et al.*, “Overcoming the Diffusion Barrier of Mucus and Absorption Barrier of Epithelium by Self-Assembled Nanoparticles for Oral Delivery of Insulin,” *ACS Nano*, vol. 9, no. 3, pp. 2345–2356, Mar. 2015, doi: 10.1021/acsnano.5b00028.

[11] H. Batchelor, “Paediatric biopharmaceutics classification system: Current status and future decisions,” *Int. J. Pharm.*, vol. 469, no. 2, pp. 251–253, Aug. 2014, doi: 10.1016/j.ijpharm.2014.02.046.

[12] A. Charalabidis, M. Sfouni, C. Bergström, and P. Macheras, “The Biopharmaceutics Classification System (BCS) and the Biopharmaceutics Drug Disposition Classification System (BDDCS): Beyond guidelines,” *Int. J. Pharm.*, vol. 566, pp. 264–281, Jul. 2019, doi: 10.1016/j.ijpharm.2019.05.041.

[13] C. A. S. Bergström, S. B. E. Andersson, J. H. Fagerberg, G. Ragnarsson, and A. Lindahl, “Is the full potential of the biopharmaceutics classification system reached?,” *Eur. J. Pharm. Sci.*, vol. 57, pp. 224–231, Jun. 2014, doi: 10.1016/j.ejps.2013.09.010.

[14] S. L. J. Tan and N. Billa, “Improved Bioavailability of Poorly Soluble Drugs through Gastrointestinal Muco-Adhesion of Lipid Nanoparticles,” *Pharmaceutics*, vol. 13, no. 11, p. 1817, Oct. 2021, doi: 10.3390/pharmaceutics13111817.

[15] G. Orive, A. R. Gascón, R. M. Hernández, A. Domínguez-Gil, and J. L. Pedraz, “Techniques: New approaches to the delivery of biopharmaceuticals,” *Trends Pharmacol. Sci.*, vol. 25, no. 7, pp. 382–387, Jul. 2004, doi: 10.1016/j.tips.2004.05.006.

[16] N. Bhattarai, H. R. Ramay, S.-H. Chou, and M. Zhang, “Chitosan and lactic acid-grafted chitosan nanoparticles as carriers for prolonged drug delivery,” *Int. J. Nanomedicine*, vol. 1, no. 2, pp. 181–187, 2006.

[17] J. Reinholz, K. Landfester, and V. Mailänder, “The challenges of oral drug delivery via nanocarriers,” *Drug Deliv.*, vol. 25, no. 1, pp. 1694–1705, Jan. 2018, doi: 10.1080/10717544.2018.1501119.

[18] M. Liu, J. Zhang, W. Shan, and Y. Huang, “Developments of mucus penetrating nanoparticles,” *Asian J. Pharm. Sci.*, vol. 10, no. 4, pp. 275–282, Jul. 2015, doi: 10.1016/j.ajps.2014.12.007.

[19] K. M. El-Say and H. S. El-Sawy, “Polymeric nanoparticles: Promising platform for drug delivery,” *Int. J. Pharm.*, vol. 528, no. 1–2, pp. 675–691, Aug. 2017, doi: 10.1016/j.ijpharm.2017.06.052.

[20] B. L. Banik, P. Fattahi, and J. L. Brown, “Polymeric nanoparticles: the future of nanomedicine,” *WIREs Nanomedicine and Nanobiotechnology*, vol. 8, no. 2, pp. 271–299, Mar. 2016, doi: 10.1002/wnan.1364.

[21] A. Zielińska *et al.*, “Polymeric Nanoparticles: Production, Characterization, Toxicology and Ecotoxicology,” *Molecules*, vol. 25, no. 16, p. 3731, Aug. 2020, doi: 10.3390/molecules25163731.

[22] F. Masood, “Polymeric nanoparticles for targeted drug delivery system for cancer therapy,” *Mater. Sci. Eng. C*, vol. 60, pp. 569–578, Mar. 2016, doi: 10.1016/j.msec.2015.11.067.

[23] M. Mohammed, J. Syeda, K. Wasan, and E. Wasan, “An Overview of Chitosan Nanoparticles and Its Application in Non-Parenteral Drug Delivery,” *Pharmaceutics*, vol. 9, no. 4, p. 53, Nov. 2017, doi: 10.3390/pharmaceutics9040053.

[24] K. Divya and M. S. Jisha, “Chitosan nanoparticles preparation and applications,” *Environ. Chem. Lett.*, vol. 16, no. 1, pp. 101–112, Mar. 2018, doi: 10.1007/s10311-

017-0670-y.

[25] K. Chandra Hembram, S. Prabha, R. Chandra, B. Ahmed, and S. Nimesh, “Advances in preparation and characterization of chitosan nanoparticles for therapeutics,” *Artif. Cells, Nanomedicine, Biotechnol.*, vol. 44, no. 1, pp. 305–314, Jan. 2016, doi: 10.3109/21691401.2014.948548.

[26] J. Sharifi-Rad *et al.*, “Chitosan nanoparticles as a promising tool in nanomedicine with particular emphasis on oncological treatment,” *Cancer Cell Int.*, vol. 21, no. 1, p. 318, Dec. 2021, doi: 10.1186/s12935-021-02025-4.

[27] J. Liang, H. Yan, P. Puligundla, X. Gao, Y. Zhou, and X. Wan, “Applications of chitosan nanoparticles to enhance absorption and bioavailability of tea polyphenols: A review,” *Food Hydrocoll.*, vol. 69, pp. 286–292, Aug. 2017, doi: 10.1016/j.foodhyd.2017.01.041.

[28] J. Jhaveri, Z. Raichura, T. Khan, M. Momin, and A. Omri, “Chitosan Nanoparticles-Insight into Properties, Functionalization and Applications in Drug Delivery and Theranostics,” *Molecules*, vol. 26, no. 2, p. 272, Jan. 2021, doi: 10.3390/molecules26020272.

[29] T. M. Ways, W. Lau, and V. Khutoryanskiy, “Chitosan and Its Derivatives for Application in Mucoadhesive Drug Delivery Systems,” *Polymers (Basel).*, vol. 10, no. 3, p. 267, Mar. 2018, doi: 10.3390/polym10030267.

[30] S. Rossi *et al.*, “Rheological analysis and mucoadhesion: A 30 year-old and still active combination,” *J. Pharm. Biomed. Anal.*, vol. 156, pp. 232–238, Jul. 2018, doi: 10.1016/j.jpba.2018.04.041.

[31] R. A. Baus, F. Zahir-Jouzdani, S. Dünnhaupt, F. Atyabi, and A. Bernkop-Schnürch, “Mucoadhesive hydrogels for buccal drug delivery: In vitro-in vivo correlation study,” *Eur. J. Pharm. Biopharm.*, vol. 142, pp. 498–505, Sep. 2019, doi: 10.1016/j.ejpb.2019.07.019.

[32] M. Silva, R. Calado, J. Marto, A. Bettencourt, A. Almeida, and L. Gonçalves, “Chitosan Nanoparticles as a Mucoadhesive Drug Delivery System for Ocular Administration,” *Mar. Drugs*, vol. 15, no. 12, p. 370, Dec. 2017, doi: 10.3390/md15120370.

[33] S. Mouftah, M. M. A. Abdel-Mottaleb, and A. Lamprecht, “Buccal delivery of low molecular weight heparin by cationic polymethacrylate nanoparticles,” *Int. J. Pharm.*, vol. 515, no. 1–2, pp. 565–574, Dec. 2016, doi: 10.1016/j.ijpharm.2016.10.039.

[34] C. E. Wagner, K. M. Wheeler, and K. Ribbeck, “Mucins and Their Role in Shaping the Functions of Mucus Barriers,” *Annu. Rev. Cell Dev. Biol.*, vol. 34, no. 1, pp. 189–215, Oct. 2018, doi: 10.1146/annurev-cellbio-100617-062818.

[35] J. Kočevar-Nared, J. Kristl, and J. Šmid-Korbar, “Comparative rheological investigation of crude gastric mucin and natural gastric mucus,” *Biomaterials*, vol. 18, no. 9, pp. 677–681, Jan. 1997, doi: 10.1016/S0142-9612(96)00180-9.

[36] Z. Wang, Z. Sun, X. Ye, X. P. Li, and W. Tan, “Research on bio-tribological properties

of intestinal mucous and its mechanism analysis," *Monatshefte für Chemie - Chem. Mon.*, vol. 148, no. 7, pp. 1295–1299, Jul. 2017, doi: 10.1007/s00706-016-1870-z.

[37] K. Hyun *et al.*, "A review of nonlinear oscillatory shear tests: Analysis and application of large amplitude oscillatory shear (LAOS)," *Prog. Polym. Sci.*, vol. 36, no. 12, pp. 1697–1753, 2011.

[38] S. Cao *et al.*, "Nanoparticles: Oral Delivery for Protein and Peptide Drugs," *AAPS PharmSciTech*, vol. 20, no. 5, p. 190, Jul. 2019, doi: 10.1208/s12249-019-1325-z.

[39] G. Ruiz-Pulido and D. I. Medina, "An overview of gastrointestinal mucus rheology under different pH conditions and introduction to pH-dependent rheological interactions with PLGA and chitosan nanoparticles," *Eur. J. Pharm. Biopharm.*, vol. 159, pp. 123–136, Feb. 2021, doi: 10.1016/j.ejpb.2020.12.013.

[40] R. K. Gupta, *Polymer and composite rheology*. CRC Press, 2000.

[41] A. Abodinar, K. Tømmeraas, E. Ronander, A. M. Smith, and G. A. Morris, "The physicochemical characterisation of pepsin degraded pig gastric mucin," *Int. J. Biol. Macromol.*, vol. 87, 2016, doi: 10.1016/j.ijbiomac.2016.02.062.

[42] F. C. Godoi, B. R. Bhandari, and S. Prakash, "Tribo-rheology and sensory analysis of a dairy semi-solid," *Food Hydrocoll.*, vol. 70, pp. 240–250, Sep. 2017, doi: 10.1016/j.foodhyd.2017.04.011.

[43] M. Uribe Velasco, *Los polímeros: síntesis, caracterización, degradación y reología*, no. 547.28 U75 2007. 2010.

[44] A. Malkin and A. Isayev, *Rheology. Concepts, Methods & Applications*. Toronto: ChemTec Publishing, 2006.

[45] O. Sadiku-Agboola, E. R. Sadiku, A. T. Adegbola, and O. F. Biotidara, "Rheological Properties of Polymers: Structure and Morphology of Molten Polymer Blends," *Mater. Sci. Appl.*, vol. 02, no. 01, pp. 30–41, 2011, doi: 10.4236/msa.2011.21005.

[46] C. W. Macosko, *Rheology Principles*. VCH Publishes, 1994.

[47] G. V Marcos, E. C. P. Antonio, M. G. Vieira, and A. E. C. Peres, "Effect of Reagents on the Rheological Behavior of an Iron Ore Concentrate Slurry," *Int. J. Min. Eng. Miner. Process.*, vol. 1, no. 2, pp. 38–42, Aug. 2012, doi: 10.5923/j.mining.20120102.03.

[48] Sigma-Aldrich Inc., "Mucin from bovine submaxillary glands," 2019. [Online]. Available: https://www.sigmaaldrich.com/catalog/product/sigma/m3895?lang=es&region=MX&cm_sp=Insite-_-prodRecCold_xviews-_-prodRecCold3-1.

[49] H. S. Melito, C. R. Daubert, and E. A. Foegeding, "Validation of a large amplitude oscillatory shear protocol," *J. Food Eng.*, vol. 113, no. 1, pp. 124–135, 2012.

[50] B. Yang *et al.*, "Chitosan mediated solid lipid nanoparticles for enhanced liver delivery of zedoary turmeric oil in vivo," *Int. J. Biol. Macromol.*, vol. 149, pp. 108–115, Apr.

2020, doi: 10.1016/j.ijbiomac.2020.01.222.

[51] S. Yu, X. Xu, J. Feng, M. Liu, and K. Hu, “Chitosan and chitosan coating nanoparticles for the treatment of brain disease,” *Int. J. Pharm.*, vol. 560, pp. 282–293, Apr. 2019, doi: 10.1016/j.ijpharm.2019.02.012.

[52] S. Sudhakar, S. V. Chandran, N. Selvamurugan, and R. A. Nazeer, “Biodistribution and pharmacokinetics of thiolated chitosan nanoparticles for oral delivery of insulin in vivo,” *Int. J. Biol. Macromol.*, vol. 150, pp. 281–288, May 2020, doi: 10.1016/j.ijbiomac.2020.02.079.

[53] A. E. Caprifico, E. Polycarpou, P. J. S. Foot, and G. Calabrese, “Fluorescein Isothiocyanate Chitosan Nanoparticles in Oral Drug Delivery Studies,” *Trends Pharmacol. Sci.*, vol. 41, no. 10, pp. 686–689, Oct. 2020, doi: 10.1016/j.tips.2020.07.005.

[54] L. Ye, “Recent advances in structural integrity analysis-proceedings of the international congress (APCF/SIF-2014):(APCFS/SIF 2014),” 2015.

[55] V. V. Khutoryanskiy, “Advances in Mucoadhesion and Mucoadhesive Polymers,” *Macromol. Biosci.*, vol. 11, no. 6, pp. 748–764, Jun. 2011, doi: 10.1002/mabi.201000388.

[56] M. Hajikhani and Z. Emam-Djomeh, “Chapter Eleven - Mucoadhesive delivery systems for nanoencapsulated food ingredients,” in *Nanoencapsulation in the Food Industry*, vol. 5, S. M. B. T.-R. and B. of N. F. I. Jafari, Ed. Academic Press, 2020, pp. 395–448.

[57] D. Ding, B. Kundukad, A. Somasundar, S. Vijayan, S. A. Khan, and P. S. Doyle, “Design of Mucoadhesive PLGA Microparticles for Ocular Drug Delivery,” *ACS Appl. Bio Mater.*, vol. 1, no. 3, pp. 561–571, Sep. 2018, doi: 10.1021/acsabm.8b00041.

[58] T. Ron *et al.*, “Gastric mucus and mucuslike hydrogels: Thin film lubricating properties at soft interfaces,” *Biointerphases*, vol. 12, no. 5, p. 051001, 2017, doi: 10.1116/1.5003708.

[59] M. Boegh, S. G. Baldursdottir, M. H. Nielsen, A. Müllertz, and H. M. Nielsen, “Development and Rheological Profiling of Biosimilar Mucus,” *Nord. Rheol. Soc. Annu. Trans.*, vol. 21, pp. 233–240, 2013.

[60] J. A. Caicedo and J. E. Perilla, “Effect of pH on the rheological response of reconstituted gastric mucin,” *Ing. e Investig.*, vol. 35, no. 2, pp. 43–48, Aug. 2015, doi: 10.15446/ing.investig.v35n2.50019.

[61] R. Bansil and B. S. Turner, “The biology of mucus: Composition, synthesis and organization,” *Adv. Drug Deliv. Rev.*, vol. 124, pp. 3–15, Jan. 2018, doi: 10.1016/j.addr.2017.09.023.

[62] C. Taylor, J. Pearson, K. Draget, P. Dettmar, and O. Smidsrod, “Rheological characterisation of mixed gels of mucin and alginate,” *Carbohydr. Polym.*, vol. 59, no. 2, pp. 189–195, Jan. 2005, doi: 10.1016/j.carbpol.2004.09.009.

[63] J. Y. Lock, T. L. Carlson, and R. L. Carrier, “Mucus models to evaluate the diffusion of drugs and particles,” *Adv. Drug Deliv. Rev.*, vol. 124, pp. 34–49, Jan. 2018, doi: 10.1016/j.addr.2017.11.001.

[64] V. J. Schömiga, B. T. Käsdorfb, C. Scholza, K. Bidmonb, O. Lielegb, and S. Berensmeier, “An optimized purification process for porcine gastric mucin with preservation of its native functional properties,” *R. Soc. Chem.*, vol. 6, pp. 44932–44943, 2016, doi: 10.1039/C6RA07424C.

[65] L. Wright, P. Joyce, T. J. Barnes, and C. A. Prestidge, “Mimicking the Gastrointestinal Mucus Barrier: Laboratory-Based Approaches to Facilitate an Enhanced Understanding of Mucus Permeation,” *ACS Biomater. Sci. Eng.*, p. acsbiomaterials.1c00814, Nov. 2021, doi: 10.1021/acsbiomaterials.1c00814.

[66] L. D. Li, T. Crouzier, A. Sarkar, L. Dunphy, J. Han, and K. Ribbeck, “Spatial Configuration and Composition of Charge Modulates Transport into a Mucin Hydrogel Barrier,” *Biophys. J.*, vol. 105, no. 6, pp. 1357–1365, Sep. 2013, doi: 10.1016/j.bpj.2013.07.050.

[67] R. G. Riley *et al.*, “An investigation of mucus/polymer rheological synergism using synthesised and characterised poly(acrylic acid)s,” *Int. J. Pharm.*, vol. 217, no. 1–2, pp. 87–100, Apr. 2001, doi: 10.1016/S0378-5173(01)00592-0.

[68] TA Instruments, “An Introduction to Tribo-Rheometry: Quantifying Friction,” 2009. [Online]. Available: https://www.tainstruments.com/an-introduction-to-tribo-rheometry-quantifying-friction/?lang=es.

[69] H. P. Kavehpour and G. H. McKinley, “Tribo-Rheometry: From Gap-Dependent Rheology to Tribology,” *Tribol. Lett.*, vol. 17, no. 2, pp. 327–335, Aug. 2004, doi: 10.1023/B:TRIL.0000032471.06795.ea.

[70] J. I. Aviles Castrillo, “Synthesis and biotriborheological characterization of shea butter solid lipid nanoparticles in topical formulation.” Instituto Tecnológico y de Estudios Superiores de Monterrey, 2020.

[71] Y. Zhu, B. Bhandari, and S. Prakash, “Tribo-rheology characteristics and microstructure of a protein solution with varying casein to whey protein ratios and addition of hydrocolloids,” *Food Hydrocoll.*, vol. 89, pp. 874–884, Apr. 2019, doi: 10.1016/j.foodhyd.2018.12.005.

[72] A. Sarkar and E. M. Krop, “Marrying oral tribology to sensory perception: a systematic review,” *Curr. Opin. Food Sci.*, vol. 27, pp. 64–73, Jun. 2019, doi: 10.1016/j.cofs.2019.05.007.

[73] S. Mu, F. Ren, Q. Shen, H. Zhou, and J. Luo, “Creamy mouthfeel of emulsion-filled gels with different fat contents: Correlating tribo–rheology with sensory measurements,” *Food Hydrocoll.*, vol. 131, p. 107754, Oct. 2022, doi: 10.1016/j.foodhyd.2022.107754.

[74] Y. Zhu, B. Bhandari, and S. Prakash, “Relating the tribo-rheological properties of chocolate flavoured milk to temporal aspects of texture,” *Int. Dairy J.*, vol. 110, p.

104794, Nov. 2020, doi: 10.1016/j.idairyj.2020.104794.

[75] J. Chen and J. R. Stokes, “Rheology and tribology: Two distinctive regimes of food texture sensation,” *Trends Food Sci. Technol.*, vol. 25, no. 1, pp. 4–12, May 2012, doi: 10.1016/j.tifs.2011.11.006.

[76] Z. Pang, R. Xu, Y. Zhu, N. Bansal, and X. Liu, “Tribo-rheology and kinetics of soymilk gelation with different types of milk proteins,” *Food Chem.*, vol. 311, p. 125961, May 2020, doi: 10.1016/j.foodchem.2019.125961.

[77] B. Bhushan, *Handbook of Micro/Nano Tribology*, 2nd ed. CRC Press, 1999.

[78] L. C. Duque-Ossa, “Evaluación de Sistemas Triboreológicos con Aplicaciones Médicas,” Instituto Tecnológico y de Estudios Superiores de Monterrey, 2019.

[79] P. A. Janmey and M. Schliwa, “Rheology,” *Curr. Biol.*, vol. 18, no. 15, pp. R639–R641, Aug. 2008, doi: 10.1016/j.cub.2008.05.001.

[80] T. Eliades, S. Zinelis, D.-G. Kim, and W. Brantley, “Structure/property relationships in orthodontic polymers,” in *Orthodontic Applications of Biomaterials*, Elsevier, 2017, pp. 39–59.

[81] D. T. N. Chen, Q. Wen, P. A. Janmey, J. C. Crocker, and A. G. Yodh, “Rheology of Soft Materials,” *Annu. Rev. Condens. Matter Phys.*, vol. 1, no. 1, pp. 301–322, Aug. 2010, doi: 10.1146/annurev-conmatphys-070909-104120.

[82] E. Fröhlich and E. Roblegg, “Mucus as Barrier for Drug Delivery by Nanoparticles,” *J. Nanosci. Nanotechnol.*, vol. 14, no. 1, pp. 126–136, 2014, doi: 10.1166/jnn.2014.9015.

[83] G. Tabilo-Munizaga and G. V. Barbosa-Cánovas, “Rheology for the food industry,” *J. Food Eng.*, vol. 67, no. 1–2, pp. 147–156, Mar. 2005, doi: 10.1016/j.jfoodeng.2004.05.062.

[84] A. Malkin, S. Ilyin, T. Roumyantseva, and V. Kulichikhin, “Rheological Evidence of Gel Formation in Dilute Poly(acrylonitrile) Solutions,” *Macromolecules*, vol. 46, no. 1, pp. 257–266, Jan. 2013, doi: 10.1021/ma301423u.

[85] Malvern Instruments, “A Basic Introduction to Rheology,” Worcestershire, 2016.

[86] G. D. Han, *Rheology and Processing of Polymeric Materials*. New York: Oxford University Press, 2007.

[87] E. Baloglu, S. Y. Karavana, Z. A. Senyigit, and T. Guneri, “Rheological and mechanical properties of poloxamer mixtures as a mucoadhesive gel base,” *Pharm. Dev. Technol.*, vol. 16, no. 6, pp. 627–636, 2011, doi: 10.3109/10837450.2010.508074.

[88] H. F. George and F. Qureshi, “Newton’s Law of Viscosity, Newtonian and Non-Newtonian Fluids,” in *Encyclopedia of Tribology*, Boston, MA: Springer US, 2013, pp. 2416–2420.

[89] T. Sochi, “Non-Newtonian flow in porous media,” *Polymer (Guildf).*, vol. 51, no. 22, pp. 5007–5023, Oct. 2010, doi: 10.1016/j.polymer.2010.07.047.

[90] R. P. Chhabra, “Non-Newtonian Fluids: An Introduction,” in *Rheology of Complex Fluids*, New York, NY: Springer New York, 2010, pp. 3–34.

[91] E. Mitsoulis and R. R. Huilgol, “Entry flows of Bingham plastics in expansions,” *J. Nonnewton. Fluid Mech.*, vol. 122, no. 1–3, pp. 45–54, Sep. 2004, doi: 10.1016/j.jnnfm.2003.10.007.

[92] M. Zarei and J. Aalaie, “Application of shear thickening fluids in material development,” *J. Mater. Res. Technol.*, vol. 9, no. 5, pp. 10411–10433, Sep. 2020, doi: 10.1016/j.jmrt.2020.07.049.

[93] Anton Paar, “Internal structures of samples and shear-thinning behavior,” 2022. [Online]. Available: https://wiki.anton-paar.com/en/internal-structures-of-samples-and-shear-thinning-behavior/.

[94] J. Aho, J. P. Boetker, S. Baldursdottir, and J. Rantanen, “Rheology as a tool for evaluation of melt processability of innovative dosage forms,” *Int. J. Pharm.*, vol. 494, no. 2, pp. 623–642, Oct. 2015, doi: 10.1016/j.ijpharm.2015.02.009.

[95] P. Sunthar, “Polymer Rheology,” in *Rheology of Complex Fluids*, New York, NY: Springer New York, 2010, pp. 171–191.

[96] B. Bhushan, *Introduction to Tribology*, 2nd ed. John Wiley & Sons, 2013.

[97] P. L. Menezes, M. Nosonovsky, S. P. Ingole, S. V. Kailas, and M. R. Lovell, Eds., *Tribology for Scientists and Engineers*. New York, NY: Springer New York, 2013.

[98] P. L. Menezes, M. Nosonovsky, S. V. Kailas, and M. R. Lovell, “Friction and Wear,” in *Tribology for Scientists and Engineers*, New York, NY, NY: Springer New York, 2013, pp. 43–91.

[99] G. Straffelini, *Friction and Wear*. Cham: Springer International Publishing, 2015.

[100] Z. Chen, X. He, C. Xiao, and S. Kim, “Effect of Humidity on Friction and Wear—A Critical Review,” *Lubricants*, vol. 6, no. 3, p. 74, Aug. 2018, doi: 10.3390/lubricants6030074.

[101] M. Sedlaček, B. Podgornik, and J. Vižintin, “Influence of surface preparation on roughness parameters, friction and wear,” *Wear*, vol. 266, no. 3–4, pp. 482–487, Feb. 2009, doi: 10.1016/j.wear.2008.04.017.

[102] N. K. Myshkin, M. I. Petrokovets, and A. V. Kovalev, “Tribology of polymers: Adhesion, friction, wear, and mass-transfer,” *Tribol. Int.*, vol. 38, no. 11–12, pp. 910–921, Nov. 2005, doi: 10.1016/j.triboint.2005.07.016.

[103] N. K. Myshkin and I. G. Goryacheva, “Tribology: Trends in the half-century development,” *J. Frict. Wear*, vol. 37, no. 6, pp. 513–516, Nov. 2016, doi: 10.3103/S106836661606009X.

[104] G. Ramsey and R. Homer, *Fundamentals of Tribology*, 3rd ed. World Scientific, 2018.

[105] A. Moshkovich, V. Perfilyev, I. Lapsker, and L. Rapoport, “Stribeck Curve Under Friction of Copper Samples in the Steady Friction State,” *Tribol. Lett.*, vol. 37, no. 3, pp. 645–653, Mar. 2010, doi: 10.1007/s11249-009-9562-z.

[106] S. Akbarzadeh and M. M. Khonsari, “Effect of Surface Pattern on Stribeck Curve,” *Tribol. Lett.*, vol. 37, no. 2, pp. 477–486, Feb. 2010, doi: 10.1007/s11249-009-9543-2.

[107] M. Kalin, I. Velkavrh, and J. Vižintin, “The Stribeck curve and lubrication design for non-fully wetted surfaces,” *Wear*, vol. 267, no. 5–8, pp. 1232–1240, Jun. 2009, doi: 10.1016/j.wear.2008.12.072.

[108] J. W. Robinson *et al.*, “Probing the molecular design of hyper-branched aryl polyesters towards lubricant applications,” *Sci. Rep.*, vol. 6, no. 1, p. 18624, May 2016, doi: 10.1038/srep18624.

[109] M. Woydt and R. Wäsche, “The history of the Stribeck curve and ball bearing steels: The role of Adolf Martens,” *Wear*, vol. 268, no. 11–12, pp. 1542–1546, May 2010, doi: 10.1016/j.wear.2010.02.015.

[110] K. Michael M. and B. E. Richard, *Recent Developments in Wear Prevention, Friction and Lubrication*. Kerala, 2010.

[111] I. D. Marinescu, W. B. Rowe, B. Dimitrov, and I. Inasaki, “Process Fluids for Abrasive Machining,” in *Tribology of Abrasive Machining Processes*, Elsevier, 2004, pp. 531–585.

[112] H. Zhang, M. Hua, G. Dong, D. Zhang, and K.-S. Chin, “A mixed lubrication model for studying tribological behaviors of surface texturing,” *Tribol. Int.*, vol. 93, pp. 583–592, Jan. 2016, doi: 10.1016/j.triboint.2015.03.027.

[113] D. A. Garrec and I. T. Norton, “The influence of hydrocolloid hydrodynamics on lubrication,” *Food Hydrocoll.*, vol. 26, no. 2, pp. 389–397, Mar. 2012, doi: 10.1016/j.foodhyd.2011.02.017.

[114] P. Sahoo, S. K. Das, and J. Paulo Davim, “Tribology of materials for biomedical applications,” in *Mechanical Behaviour of Biomaterials*, Elsevier, 2019, pp. 1–45.

[115] Z. R. Zhou and Z. M. Jin, “Biotribology: Recent progresses and future perspectives,” *Biosurface and Biotribology*, vol. 1, no. 1, pp. 3–24, Mar. 2015, doi: 10.1016/j.bsbt.2015.03.001.

[116] *Characterization and Analysis of Polymers*. John Wiley & Sons, 2008.

[117] R. P. Chhabra and J. F. Richardson, “Rheometry for non-Newtonian fluids**This chapter has been written by Dr. P.R. Williams, Reader, Department of Chemical and Biological Process Engineering, University of Wales Swansea.,” in *Non-Newtonian Flow in the Process Industries*, Elsevier, 1999, pp. 37–72.

[118] Y.-J. Cho and S. Kang, *Emerging Technologies for Food Quality and Food Safety*

Evaluation. 2011.

[119] B. G. Lipták, *Instrument Engineers' Handbook, Volume One: Process Measurement and Analysis*, 4th ed. CRC Press, 2003.

[120] S. Bucak and D. Rende, *Colloid and Surface Chemistry: A Laboratory Guide for Exploration of the Nano World*. CRC Press, 2013.

[121] T. Crouzier *et al.*, "Modulating Mucin Hydration and Lubrication by Deglycosylation and Polyethylene Glycol Binding," *Adv. Mater. Interfaces*, vol. 2, no. 18, p. 1500308, Dec. 2015, doi: 10.1002/admi.201500308.

[122] C. Liu, X. Jiang, Y. Gan, and M. Yu, "Engineering nanoparticles to overcome the mucus barrier for drug delivery: Design, evaluation and state-of-the-art," *Med. Drug Discov.*, vol. 12, p. 100110, Dec. 2021, doi: 10.1016/j.medidd.2021.100110.

[123] M. Faderl, M. Noti, N. Corazza, and C. Mueller, "Keeping bugs in check: The mucus layer as a critical component in maintaining intestinal homeostasis," *IUBMB Life*, vol. 67, no. 4, pp. 275–285, Apr. 2015, doi: 10.1002/iub.1374.

[124] M. Herath, S. Hosie, J. C. Bornstein, A. E. Franks, and E. L. Hill-Yardin, "The Role of the Gastrointestinal Mucus System in Intestinal Homeostasis: Implications for Neurological Disorders," *Front. Cell. Infect. Microbiol.*, vol. 10, May 2020, doi: 10.3389/fcimb.2020.00248.

[125] A. Macierzanka, A. R. Mackie, B. H. Bajka, N. M. Rigby, F. Nau, and D. Dupont, "Transport of Particles in Intestinal Mucus under Simulated Infant and Adult Physiological Conditions: Impact of Mucus Structure and Extracellular DNA," *PLoS One*, vol. 9, no. 4, p. e95274, Apr. 2014, doi: 10.1371/journal.pone.0095274.

[126] A. M. Duraj-Thatte, P. Praveschotinunt, T. R. Nash, F. R. Ward, and N. S. Joshi, "Modulating bacterial and gut mucosal interactions with engineered biofilm matrix proteins," *Sci. Rep.*, vol. 8, no. 1, p. 3475, Dec. 2018, doi: 10.1038/s41598-018-21834-8.

[127] M. A. McGuckin, S. K. Lindén, P. Sutton, and T. H. Florin, "Mucin dynamics and enteric pathogens," *Nat. Rev. Microbiol.*, vol. 9, no. 4, pp. 265–278, Apr. 2011, doi: 10.1038/nrmicro2538.

[128] I. R. Dubbelboer *et al.*, "Gastrointestinal mucus in dog: Physiological characteristics, composition, and structural properties," *Eur. J. Pharm. Biopharm.*, vol. 173, pp. 92–102, Apr. 2022, doi: 10.1016/j.ejpb.2022.02.019.

[129] L. M. Ensign, R. Cone, and J. Hanes, "Oral drug delivery with polymeric nanoparticles: The gastrointestinal mucus barriers," *Adv. Drug Deliv. Rev.*, vol. 64, no. 6, pp. 557–570, May 2012, doi: 10.1016/j.addr.2011.12.009.

[130] E. L. Mitchell *et al.*, "Reduced intestinal motility, mucosal barrier function, and inflammation in aged monkeys," *J. Nutr. Health Aging*, vol. 21, no. 4, pp. 354–361, Apr. 2017, doi: 10.1007/s12603-016-0725-y.

[131] A. Mackie, B. Bajka, and N. Rigby, "Roles for dietary fibre in the upper GI tract: The

importance of viscosity," *Food Res. Int.*, vol. 88, pp. 234–238, Oct. 2016, doi: 10.1016/j.foodres.2015.11.011.

[132] X. Qin and E. A. Deitch, "Dissolution of lipids from mucus: A possible mechanism for prompt disruption of gut barrier function by alcohol," *Toxicol. Lett.*, vol. 232, no. 2, pp. 356–362, Jan. 2015, doi: 10.1016/j.toxlet.2014.11.027.

[133] L. Berkowitz *et al.*, "Impact of Cigarette Smoking on the Gastrointestinal Tract Inflammation: Opposing Effects in Crohn's Disease and Ulcerative Colitis," *Front. Immunol.*, vol. 9, Jan. 2018, doi: 10.3389/fimmu.2018.00074.

[134] G. Capurso and E. Lahner, "The interaction between smoking, alcohol and the gut microbiome," *Best Pract. Res. Clin. Gastroenterol.*, vol. 31, no. 5, pp. 579–588, Oct. 2017, doi: 10.1016/j.bpg.2017.10.006.

[135] M. Elderman *et al.*, "The effect of age on the intestinal mucus thickness, microbiota composition and immunity in relation to sex in mice," *PLoS One*, vol. 12, no. 9, p. e0184274, Sep. 2017, doi: 10.1371/journal.pone.0184274.

[136] M. E. V. Johansson, H. Sjövall, and G. C. Hansson, "The gastrointestinal mucus system in health and disease," *Nat. Rev. Gastroenterol. Hepatol.*, vol. 10, no. 6, pp. 352–361, Jun. 2013, doi: 10.1038/nrgastro.2013.35.

[137] K. Netsomboon and A. Bernkop-Schnürch, "Mucoadhesive vs. mucopenetrating particulate drug delivery," *Eur. J. Pharm. Biopharm.*, vol. 98, pp. 76–89, 2016, doi: https://doi.org/10.1016/j.ejpb.2015.11.003.

[138] J. Ahn, T. Crouzier, K. Ribbeck, M. F. Rubner, and R. E. Cohen, "Tuning the Properties of Mucin via Layer-by-Layer Assembly," *Biomacromolecules*, vol. 16, no. 1, pp. 228–235, Jan. 2015, doi: 10.1021/bm5014475.

[139] K. Bowman and K. W. Leong, "Chitosan nanoparticles for oral drug and gene delivery," *Int. J. Nanomedicine*, vol. 1, no. 2, pp. 117–128, 2006.

[140] S. P. Bandi, Y. S. Kumbhar, and V. V. K. Venuganti, "Effect of particle size and surface charge of nanoparticles in penetration through intestinal mucus barrier," *J. Nanoparticle Res.*, vol. 22, no. 3, p. 62, Mar. 2020, doi: 10.1007/s11051-020-04785-y.

[141] M. Boegh and H. M. Nielsen, "Mucus as a Barrier to Drug Delivery - Understanding and Mimicking the Barrier Properties," *Basic Clin. Pharmacol. Toxicol.*, vol. 116, no. 3, pp. 179–186, Mar. 2015, doi: 10.1111/bcpt.12342.

[142] E. Y. T. Chen, Y.-C. Wang, C.-S. Chen, and W.-C. Chin, "Functionalized Positive Nanoparticles Reduce Mucin Swelling and Dispersion," *PLoS One*, vol. 5, no. 11, p. e15434, Nov. 2010, doi: 10.1371/journal.pone.0015434.

[143] V. M. de Oliveira Cardoso, M. P. D. Gremião, and B. S. F. Cury, "Mucin-polysaccharide interactions: A rheological approach to evaluate the effect of pH on the mucoadhesive properties," *Int. J. Biol. Macromol.*, vol. 149, pp. 234–245, 2020, doi: https://doi.org/10.1016/j.ijbiomac.2020.01.235.

[144] J. Witten, T. Samad, and K. Ribbeck, “Selective permeability of mucus barriers,” *Curr. Opin. Biotechnol.*, vol. 52, pp. 124–133, Aug. 2018, doi: 10.1016/j.copbio.2018.03.010.

[145] A. Runnsjö, A. P. Dabkowska, E. Sparr, V. Kocherbitov, T. Arnebrant, and J. Engblom, “Diffusion through Pig Gastric Mucin: Effect of Relative Humidity,” *PLoS One*, vol. 11, no. 6, p. e0157596, Jun. 2016, doi: 10.1371/journal.pone.0157596.

[146] N. Juge, “Microbial adhesins to gastrointestinal mucus,” *Trends Microbiol.*, vol. 20, no. 1, pp. 30–39, Jan. 2012, doi: 10.1016/j.tim.2011.10.001.

[147] J. S. Crater and R. L. Carrier, “Barrier Properties of Gastrointestinal Mucus to Nanoparticle Transport,” *Macromol. Biosci.*, vol. 10, no. 12, pp. 1473–1483, Dec. 2010, doi: 10.1002/mabi.201000137.

[148] F. J. O. Varum, F. Veiga, J. S. Sousa, and A. W. Basit, “An investigation into the role of mucus thickness on mucoadhesion in the gastrointestinal tract of pig,” *Eur. J. Pharm. Sci.*, vol. 40, no. 4, pp. 335–341, Jul. 2010, doi: 10.1016/j.ejps.2010.04.007.

[149] C. B. Morrison, M. R. Markovetz, and C. Ehre, “Mucus, mucins, and cystic fibrosis,” *Pediatr. Pulmonol.*, vol. 54, no. S3, Nov. 2019, doi: 10.1002/ppul.24530.

[150] S. K. Lai, Y.-Y. Wang, D. Wirtz, and J. Hanes, “Micro- and macrorheology of mucus,” *Adv. Drug Deliv. Rev.*, vol. 61, no. 2, pp. 86–100, Feb. 2009, doi: 10.1016/j.addr.2008.09.012.

[151] K. Peng *et al.*, “Modulation of Gastrointestinal Mucus Properties with Ionic Liquids for Drug Delivery,” *Adv. Healthc. Mater.*, vol. 10, no. 13, p. 2002192, Jul. 2021, doi: 10.1002/adhm.202002192.

[152] E. Y. Chen, D. Daley, Y.-C. Wang, M. Garnica, C.-S. Chen, and W.-C. Chin, “Functionalized carboxyl nanoparticles enhance mucus dispersion and hydration,” *Sci. Rep.*, vol. 2, no. 1, p. 211, Dec. 2012, doi: 10.1038/srep00211.

[153] O. W. Meldrum, G. E. Yakubov, M. R. Bonilla, O. Deshmukh, M. A. McGuckin, and M. J. Gidley, “Mucin gel assembly is controlled by a collective action of non-mucin proteins, disulfide bridges, Ca2+-mediated links, and hydrogen bonding,” *Sci. Rep.*, vol. 8, 2018, doi: https://doi.org/10.1038/s41598-018-24223-3.

[154] R. A. Cone, “Barrier properties of mucus,” *Adv. Drug Deliv. Rev.*, vol. 61, no. 2, pp. 75–85, Feb. 2009, doi: 10.1016/j.addr.2008.09.008.

[155] G. Rajput, F. Majmudar, J. Patel, R. Thakor, and N. Rajgor, “Stomach-specific mucoadhesive microsphere as a controlled drug delivery system,” *Syst. Rev. Pharm.*, vol. 1, no. 1, p. 70, 2010, doi: 10.4103/0975-8453.59515.

[156] J. P. Celli *et al.*, “Rheology of Gastric Mucin Exhibits a pH-Dependent Sol−Gel Transition,” *Biomacromolecules*, vol. 8, no. 5, pp. 1580–1586, May 2007, doi: 10.1021/bm0609691.

[157] M. Ahmad, C. Ritzoulis, and J. Chen, “Shear and extensional rheological characterisation of mucin solutions,” *Colloids Surfaces B Biointerfaces*, vol. 171, no.

1, pp. 614–621, 2018, doi: https://doi.org/10.1016/j.colsurfb.2018.07.075.

[158] B. B. Demouveaux, V. Gouyer, F. Gottrand, T. Narita, and J.-L. Desseyn, “Gel-forming mucin interactome drives mucus viscoelasticity,” *Adv. Colloid Interface Sci.*, vol. 252, pp. 69–82, Feb. 2018, doi: https://doi.org/10.1016/j.cis.2017.12.005.

[159] H. M. Yildiz, L. Speciner, C. Ozdemir, D. E. Cohen, and R. L. Carrier, “Food-associated stimuli enhance barrier properties of gastrointestinal mucus,” *Biomaterials*, vol. 54, pp. 1–8, Jun. 2015, doi: 10.1016/j.biomaterials.2015.02.118.

[160] M. M. Badran, A. H. Alomrani, G. I. Harisa, A. E. Ashour, A. Kumar, and A. E. Yassin, “Novel docetaxel chitosan-coated PLGA/PCL nanoparticles with magnified cytotoxicity and bioavailability,” *Biomed. Pharmacother.*, vol. 106, pp. 1461–1468, Oct. 2018, doi: 10.1016/j.biopha.2018.07.102.

[161] A. Lechanteur, J. das Neves, and B. Sarmento, “The role of mucus in cell-based models used to screen mucosal drug delivery,” *Adv. Drug Deliv. Rev.*, vol. 124, pp. 50–63, Jan. 2018, doi: 10.1016/j.addr.2017.07.019.

[162] M. Abdulkarim, P. K. Sharma, and M. Gumbleton, “Self-emulsifying drug delivery system: Mucus permeation and innovative quantification technologies,” *Adv. Drug Deliv. Rev.*, vol. 142, pp. 62–74, Mar. 2019, doi: 10.1016/j.addr.2019.04.001.

[163] M. Abdulkarim *et al.*, “Nanoparticle diffusion within intestinal mucus: Three-dimensional response analysis dissecting the impact of particle surface charge, size and heterogeneity across polyelectrolyte, pegylated and viral particles,” *Eur. J. Pharm. Biopharm.*, vol. 97, pp. 230–238, Nov. 2015, doi: 10.1016/j.ejpb.2015.01.023.

[164] J. Rohrer *et al.*, “Mucus permeating thiolated self-emulsifying drug delivery systems,” *Eur. J. Pharm. Biopharm.*, vol. 98, pp. 90–97, Jan. 2016, doi: 10.1016/j.ejpb.2015.11.004.

[165] M. García-Díaz, D. Birch, F. Wan, and H. M. Nielsen, “The role of mucus as an invisible cloak to transepithelial drug delivery by nanoparticles,” *Adv. Drug Deliv. Rev.*, vol. 124, pp. 107–124, Jan. 2018, doi: 10.1016/j.addr.2017.11.002.

[166] H. Zhang, M.-A. Shahbazi, P. V. Almeida, and H. A. Santos, “Mucus as a Barrier for Biopharmaceuticals and Drug Delivery Systems,” in *Mucosal Delivery of Biopharmaceuticals*, Boston, MA: Springer US, 2014, pp. 59–97.

[167] J. Griesser, G. Hetényi, H. Kadas, F. Demarne, V. Jannin, and A. Bernkop-Schnürch, “Self-emulsifying peptide drug delivery systems: How to make them highly mucus permeating,” *Int. J. Pharm.*, vol. 538, no. 1–2, pp. 159–166, Mar. 2018, doi: 10.1016/j.ijpharm.2018.01.018.

[168] L. Taina-González and M. de la Fuente, “The Potential of Nanomedicine to Unlock the Limitless Applications of mRNA,” *Pharmaceutics*, vol. 14, no. 2, p. 460, Feb. 2022, doi: 10.3390/pharmaceutics14020460.

[169] S. Kashyap, A. Singh, A. Mishra, and V. Singh, “Enhanced sustained release of furosemide in long circulating chitosan-conjugated PLGA nanoparticles,” *Res. Pharm. Sci.*, vol. 14, no. 2, pp. 93–106, 2019, doi: 10.4103/1735-5362.253356.

[170] N. K. Al-Nemrawi, A. R. Okour, and R. H. Dave, “Surface modification of PLGA nanoparticles using chitosan: Effect of molecular weight, concentration, and degree of deacetylation,” *Adv. Polym. Technol.*, vol. 37, no. 8, pp. 3066–3075, Dec. 2018, doi: 10.1002/adv.22077.

[171] K. McNamara and S. A. M. Tofail, “Nanoparticles in biomedical applications,” *Adv. Phys. X*, vol. 2, no. 1, pp. 54–88, Jan. 2017, doi: 10.1080/23746149.2016.1254570.

[172] M. Elsabahy and K. L. Wooley, “Design of polymeric nanoparticles for biomedical delivery applications,” *Chem. Soc. Rev.*, vol. 41, no. 7, p. 2545, 2012, doi: 10.1039/c2cs15327k.

[173] C. I. C. Crucho and M. T. Barros, “Polymeric nanoparticles: A study on the preparation variables and characterization methods,” *Mater. Sci. Eng. C*, vol. 80, pp. 771–784, Nov. 2017, doi: 10.1016/j.msec.2017.06.004.

[174] T. Patel, J. Zhou, J. M. Piepmeier, and W. M. Saltzman, “Polymeric nanoparticles for drug delivery to the central nervous system,” *Adv. Drug Deliv. Rev.*, vol. 64, no. 7, pp. 701–705, May 2012, doi: 10.1016/j.addr.2011.12.006.

[175] M. M. Badran, G. I. Harisa, S. A. AlQahtani, F. K. Alanazi, and K. M. A. Zoheir, “Pravastatin-loaded chitosan nanoparticles: Formulation, characterization and cytotoxicity studies,” *J. Drug Deliv. Sci. Technol.*, vol. 32, pp. 1–9, Apr. 2016, doi: 10.1016/j.jddst.2016.01.004.

[176] F. Bruinsmann *et al.*, “Chitosan-Coated Nanoparticles: Effect of Chitosan Molecular Weight on Nasal Transmucosal Delivery,” *Pharmaceutics*, vol. 11, no. 2, p. 86, Feb. 2019, doi: 10.3390/pharmaceutics11020086.

[177] S.-M. Jung *et al.*, “Thermodynamic Insights and Conceptual Design of Skin-Sensitive Chitosan Coated Ceramide/PLGA Nanodrug for Regeneration of Stratum Corneum on Atopic Dermatitis,” *Sci. Rep.*, vol. 5, no. 1, p. 18089, Dec. 2015, doi: 10.1038/srep18089.

[178] G. Ruiz-Pulido *et al.*, “Nanomaterials for the Diagnosis and Treatment of Head and Neck Cancers: A Review,” *Materials (Basel).*, vol. 14, no. 13, p. 3706, Jul. 2021, doi: 10.3390/ma14133706.

[179] B. Lu, X. Lv, and Y. Le, “Chitosan-Modified PLGA Nanoparticles for Control-Released Drug Delivery,” *Polymers (Basel).*, vol. 11, no. 2, p. 304, Feb. 2019, doi: 10.3390/polym11020304.

[180] J. Bassi da Silva, S. Ferreira, A. Reis, M. Cook, and M. Bruschi, “Assessing Mucoadhesion in Polymer Gels: The Effect of Method Type and Instrument Variables,” *Polymers (Basel).*, vol. 10, no. 3, p. 254, Mar. 2018, doi: 10.3390/polym10030254.

[181] C. Feng *et al.*, “Surface charge effect on mucoadhesion of chitosan based nanogels for local anti-colorectal cancer drug delivery,” *Colloids Surfaces B Biointerfaces*, vol. 128, pp. 439–447, Apr. 2015, doi: 10.1016/j.colsurfb.2015.02.042.

[182] M. T. Cook and V. V. Khutoryanskiy, “Mucoadhesion and mucosa-mimetic

materials—A mini-review," *Int. J. Pharm.*, vol. 495, no. 2, pp. 991–998, Nov. 2015, doi: 10.1016/j.ijpharm.2015.09.064.

[183] K. Maisel, L. Ensign, M. Reddy, R. Cone, and J. Hanes, "Effect of surface chemistry on nanoparticle interaction with gastrointestinal mucus and distribution in the gastrointestinal tract following oral and rectal administration in the mouse," *J. Control. Release*, vol. 197, pp. 48–57, Jan. 2015, doi: 10.1016/j.jconrel.2014.10.026.

[184] S. L. . Cook, S. P. . Bull, L. Methven, J. K. . Parker, and V. V. Khutoryanskiy, "Mucoadhesion: A food perspective," *Food Hydrocoll.*, vol. 72, pp. 281–296, 2017, doi: 10.1016/j.foodhyd.2017.05.043.

[185] R. Shaikh, R. Singh, T. Raghu, M. J. Garland, A. D. Woolfson, and R. F. Donnelly, "Mucoadhesive drug delivery systems," *J. Pharm. Bioallied Sci.*, vol. 3, no. 1, pp. 89–100, 2011, doi: 10.4103/0975-7406.76478.

[186] T. Yu, G. P. Andrews, and D. S. Jones, "Mucoadhesion and Characterization of Mucoadhesive Properties," in *Mucosal Delivery of Biopharmaceuticals*, Boston, MA: Springer US, 2014, pp. 35–58.

[187] J. J. Carreras, P. Canales, and A. Melero, "Mucoadhesion of Polymeric Drug Delivery Systems: Polymeric Nanoparticles and its Interactions with the Intestinal Barrier," *JSM Nanotechnol Nanomed*, vol. 4, no. 1, p. 1041, 2016.

[188] D. Chenthamara *et al.*, "Therapeutic efficacy of nanoparticles and routes of administration," *Biomater. Res.*, vol. 23, no. 1, p. 20, Dec. 2019, doi: 10.1186/s40824-019-0166-x.

[189] C. Menzel *et al.*, "Covalently binding mucoadhesive polymers: N-hydroxysuccinimide grafted polyacrylates," *Eur. J. Pharm. Biopharm.*, vol. 139, pp. 161–167, Jun. 2019, doi: 10.1016/j.ejpb.2019.02.017.

[190] J. Hombach, A. Bernkop-Schnürch, F. C. Carvalho, M. L. Bruschi, R. C. Evangelista, and M. P. D. Gremião, "Mucoadhesive Drug Delivery Systems," in *Brazilian Journal of Pharmaceutical Sciences*, vol. 46, no. 1, 2010, pp. 251–266.

[191] S. Alaei and H. Omidian, "Mucoadhesion and Mechanical Assessment of Oral Films," *Eur. J. Pharm. Sci.*, vol. 159, p. 105727, Apr. 2021, doi: 10.1016/j.ejps.2021.105727.

[192] S. Rajindra, S. Deepak, and G. Rajeev, "Review on Mucoadhesive Drug Delivery System with Special Emphasis on Buccal Route: An Important Tool in Designing of Novel Controlled Drug Delivery System for the Effective Delivery of Pharmaceuticals," *J. Dev. Drugs*, vol. 06, no. 01, 2017, doi: 10.4172/2329-6631.1000169.

[193] P. Schattling, E. Taipaleenmäki, Y. Zhang, and B. Städler, "A Polymer Chemistry Point of View on Mucoadhesion and Mucopenetration," *Macromol. Biosci.*, vol. 17, no. 9, p. 1700060, Sep. 2017, doi: 10.1002/mabi.201700060.

[194] E. Meng-Lund, C. Muff-Westergaard, C. Sander, P. Madelung, and J. Jacobsen, "A mechanistic based approach for enhancing buccal mucoadhesion of chitosan," *Int. J. Pharm.*, vol. 461, no. 1–2, pp. 280–285, Jan. 2014, doi: 10.1016/j.ijpharm.2013.10.047.

[195] J. D. Smart, “Theories of Mucoadhesion,” in *Mucoadhesive materials and drug delivery system*, V. V. Khutoryanskiy, Ed. John Wiley & Sons, 2014, pp. 159–170.

[196] A. Amit, S. Sharad, K. M. Ajazuddin, and J. Swarna, “Theories and factors affecting mucoadhesive drug delivery systems: A review,” *Int. J. Res. Ayurveda Pharm.*, vol. 2, no. 4, 2011.

[197] S. Rhushikesh and S. Suresh, “A Review on Mucoadhesive Drug Delivery System,” *Int. J. Res. Anal. Rev.*, vol. 7, no. 1, pp. 793–808, 2020.

[198] V. Puri, A. Sharma, P. Maman, N. Rathore, S. Inderbir, and I. Singh, “Overview of mucoadhesive biopolymers for buccal drug delivery systems,” *Int. J. Appl. Pharm.*, vol. 11, no. 6, pp. 18–29, Oct. 2019, doi: 10.22159/ijap.2019v11i6.35438.

[199] A. P. Nikalje, S. Tiwari, and S. Kamble, “Mucoadhesive: As Oral Controlled Gastroretentive Drug Delivery System,” *Int. J. Res. Pharm. Sci.*, vol. 2, no. 3, 2012.

[200] S. Ali, Modh F.; Bakalis, “Mucoadhesive polymers for food formulations,” *Porc. Food Sci.*, vol. 1, pp. 68–75, 2011, doi: 10.1016/j.profoo.2011.09.012.

[201] P. Sriamornsak, N. Wattanakorn, and H. Takeuchi, “Study on the mucoadhesion mechanism of pectin by atomic force microscopy and mucin-particle method,” *Carbohydr. Polym.*, vol. 79, no. 1, pp. 54–59, Jan. 2010, doi: 10.1016/J.CARBPOL.2009.07.018.

[202] E. Hagesaether, M. Hiorth, and S. A. Sande, “Mucoadhesion and drug permeability of free mixed films of pectin and chitosan: An in vitro and ex vivo study,” *Eur. J. Pharm. Biopharm.*, vol. 71, no. 2, pp. 325–331, Feb. 2009, doi: 10.1016/j.ejpb.2008.09.002.

[203] S. Mansuri, P. Kesharwani, K. Jain, R. K. . Tekade, and N. K. . Jain, “Mucoadhesion: A promising approach in drug delivery system,” *React. Funct. Polym.*, vol. 100, pp. 151–172, Mar. 2016, doi: 10.1016/j.reactfunctpolym.2016.01.011.

[204] P. Subramanian, “Mucoadhesive Delivery System: A Smart Way to Improve Bioavailability of Nutraceuticals,” *Foods*, vol. 10, no. 6, p. 1362, Jun. 2021, doi: 10.3390/foods10061362.

[205] J. D. Smart, “The basics and underlying mechanisms of mucoadhesion,” *Adv. Drug Deliv. Rev.*, vol. 57, no. 11, pp. 1556–1568, Nov. 2005, doi: 10.1016/j.addr.2005.07.001.

[206] D. M. Shinkar, A. S. Dhake, and C. M. Setty, “Drug Delivery from the Oral Cavity: A Focus on Mucoadhesive Buccal Drug Delivery Systems,” *PDA J. Pharm. Sci. Technol.*, vol. 66, no. 5, pp. 466–500, Sep. 2012, doi: 10.5731/pdajpst.2012.00877.

[207] B. M. Boddupalli, Z. N. K. Mohammed, R. A. Nath, and D. Banji, “Mucoadhesive drug delivery system: An overview.,” *J. Adv. Pharm. Technol. Res.*, vol. 1, no. 4, pp. 381–7, Oct. 2010, doi: 10.4103/0110-5558.76436.

[208] N. Kumari, G. Aggarwal, and S. L. Harikumar, “MUCOADHESIVE MICROSPHERES: A REVIEW,” *J. Drug Deliv. Ther.*, vol. 4, no. 5, pp. 48–54, Sep. 2014, doi: 10.22270/JDDT.V4I5.953.

[209] P. Sriamornsak and N. Wattanakorn, “Rheological synergy in aqueous mixtures of pectin and mucin,” *Carbohydr. Polym.*, vol. 74, no. 3, pp. 474–481, Nov. 2008, doi: 10.1016/j.carbpol.2008.03.021.

[210] F. Madsen, K. Eberth, and J. D. Smart, “A rheological assessment of the nature of interactions between mucoadhesive polymers and a homogenised mucus gel,” *Biomaterials*, vol. 19, no. 11–12, pp. 1083–1092, Jun. 1998, doi: 10.1016/S0142-9612(98)00037-4.

[211] F. Madsen, K. Eberth, and J. Smart, “A rheological examination of the mucoadhesive/mucus interaction: the effect of mucoadhesive type and concentration,” *J. Control. Release*, vol. 50, no. 1–3, pp. 167–178, 1998, doi: https://doi.org/10.1016/S0168-3659(97)00138-7.

[212] G. Sandri, S. Rossi, M. C. Bonferoni, F. Ferrari, M. Mori, and C. Caramella, “The role of chitosan as a mucoadhesive agent in mucosal drug delivery,” *J. Drug Deliv. Sci. Technol.*, vol. 22, no. 4, pp. 275–284, Jan. 2012, doi: 10.1016/S1773-2247(12)50046-8.

[213] J. Bassi da Silva, S. B. de S. Ferreira, O. de Freitas, and M. L. Bruschi, “A critical review about methodologies for the analysis of mucoadhesive properties of drug delivery systems,” *Drug Dev. Ind. Pharm.*, vol. 43, no. 7, pp. 1053–1070, Jul. 2017, doi: 10.1080/03639045.2017.1294600.

[214] H. Hägerström and K. Edsman, “Limitations of the rheological mucoadhesion method: The effect of the choice of conditions and the rheological synergism parameter,” *Eur. J. Pharm. Sci.*, vol. 18, no. 5, pp. 349–357, Apr. 2003, doi: 10.1016/S0928-0987(03)00037-X.

[215] S. B. De Souza Ferreira, J. B. Da Silva, F. B. Borghi-Pangoni, M. V. Junqueira, and M. L. Bruschi, “Linear correlation between rheological, mechanical and mucoadhesive properties of polycarbophil polymer blends for biomedical applications,” *J. Mech. Behav. Biomed. Mater.*, vol. 68, pp. 265–275, Apr. 2017, doi: 10.1016/j.jmbbm.2017.02.016.

[216] R. Hamed, A. AbuRezeq, and O. Tarawneh, “Development of hydrogels, oleogels, and bigels as local drug delivery systems for periodontitis,” *Drug Dev. Ind. Pharm.*, vol. 44, no. 9, pp. 1488–1497, Sep. 2018, doi: 10.1080/03639045.2018.1464021.

[217] S. Rossi, F. Ferrari, M. C. Bonferoni, and C. Caramella, “Characterization of chitosan hydrochloride–mucin rheological interaction: influence of polymer concentration and polymer:mucin weight ratio,” *Eur. J. Pharm. Sci.*, vol. 12, no. 4, pp. 479–485, Feb. 2001, doi: 10.1016/S0928-0987(00)00194-9.

[218] I. Singh and V. Rana, “Techniques for the Assessment of Mucoadhesion in Drug Delivery Systems: An Overview,” *J. Adhes. Sci. Technol.*, vol. 26, no. 18–19, pp. 2251–2267, Oct. 2012, doi: 10.1163/156856111X610171.

[219] P. García-Guzmán *et al.*, “Rheological mucoadhesion and cytotoxicity of montmorillonite clay mineral/hybrid microparticles biocomposite,” *Appl. Clay Sci.*, vol. 180, p. 105202, Nov. 2019, doi: 10.1016/j.clay.2019.105202.

[220] A. Račić, B. Čalija, J. Milić, N. Milašinović, and D. Krajišnik, “Development of polysaccharide-based mucoadhesive ophthalmic lubricating vehicles: The effect of different polymers on physicochemical properties and functionality,” *J. Drug Deliv. Sci. Technol.*, vol. 49, pp. 50–57, Feb. 2019, doi: 10.1016/j.jddst.2018.10.034.

[221] A. Curnutt, K. Smith, E. Darrow, and K. B. Walters, “Chemical and Microstructural Characterization of pH and [Ca2+] Dependent Sol-Gel Transitions in Mucin Biopolymer,” *Sci. Rep.*, vol. 10, no. 1, p. 8760, Dec. 2020, doi: 10.1038/s41598-020-65392-4.

[222] Collado-González, González Espinosa, and Goycoolea, “Interaction Between Chitosan and Mucin: Fundamentals and Applications,” *Biomimetics*, vol. 4, no. 2, p. 32, Apr. 2019, doi: 10.3390/biomimetics4020032.

[223] P. Georgiades, P. D. A. Pudney, D. J. Thornton, and T. A. Waigh, “Particle tracking microrheology of purified gastrointestinal mucins,” *Biopolymers*, vol. 101, no. 4, pp. 366–377, 2015, doi: 10.1002/bip.22372.

[224] B. Menchicchi *et al.*, “Biophysical Analysis of the Molecular Interactions between Polysaccharides and Mucin,” *Biomacromolecules*, vol. 16, no. 3, pp. 924–935, Mar. 2015, doi: 10.1021/bm501832y.

[225] G. Ruiz-Pulido, D. Quintanar-Guerrero, L. E. Serrano-Mora, and D. I. Medina, “Triborheological Analysis of Reconstituted Gastrointestinal Mucus/Chitosan:TPP Nanoparticles System to Study Mucoadhesion Phenomenon under Different pH Conditions,” *Polymers*, vol. 14, no. 22. 2022, doi: 10.3390/polym14224978.

[226] J. M. Coles, D. P. Chang, and S. Zauscher, “Molecular mechanisms of aqueous boundary lubrication by mucinous glycoproteins,” *Curr. Opin. Colloid Interface Sci.*, vol. 15, no. 6, pp. 406–416, Dec. 2010, doi: 10.1016/j.cocis.2010.07.002.

[227] J. An, C. Jin, A. Dėdinaitė, J. Holgersson, N. G. Karlsson, and P. M. Claesson, “Influence of Glycosylation on Interfacial Properties of Recombinant Mucins: Adsorption, Surface Forces, and Friction,” *Langmuir*, vol. 33, no. 18, pp. 4386–4395, May 2017, doi: 10.1021/acs.langmuir.7b00030.

[228] G. Ruiz-Pulido and D. Medina, “Tribo-rheological analysis of reconstituted gastrointestinal porcine mucus under different pH conditions.,” in *Proceedings of the Virtual 2021 AOCS Annual Meeting & Expo*, 2021, doi: 10.21748/am21.543.

[229] G. E. Yakubov, J. McColl, J. H. H. Bongaerts, and J. J. Ramsden, “Viscous Boundary Lubrication of Hydrophobic Surfaces by Mucin,” *Langmuir*, vol. 25, no. 4, pp. 2313–2321, Feb. 2009, doi: 10.1021/la8018666.

[230] J. H. H. Bongaerts, K. Fourtouni, and J. R. Stokes, “Soft-tribology: Lubrication in a compliant PDMS–PDMS contact,” *Tribol. Int.*, vol. 40, no. 10–12, pp. 1531–1542, Oct. 2007, doi: 10.1016/j.triboint.2007.01.007.

[231] C. T. Nordgård and K. I. Draget, “Dynamic responses in small intestinal mucus: Relevance for the maintenance of an intact barrier,” *Eur. J. Pharm. Biopharm.*, vol. 95, pp. 144–150, Sep. 2015, doi: 10.1016/j.ejpb.2015.01.024.

[232] A. Alishahi *et al.*, “Shelf life and delivery enhancement of vitamin C using chitosan nanoparticles,” *Food Chem.*, vol. 126, no. 3, pp. 935–940, Jun. 2011, doi: 10.1016/j.foodchem.2010.11.086.

[233] A. Barbosa, S. Costa Lima, and S. Reis, “Application of pH-Responsive Fucoidan/Chitosan Nanoparticles to Improve Oral Quercetin Delivery,” *Molecules*, vol. 24, no. 2, p. 346, Jan. 2019, doi: 10.3390/molecules24020346.

[234] A. Makhlof, Y. Tozuka, and H. Takeuchi, “Design and evaluation of novel pH-sensitive chitosan nanoparticles for oral insulin delivery,” *Eur. J. Pharm. Sci.*, vol. 42, no. 5, pp. 445–451, Apr. 2011, doi: 10.1016/j.ejps.2010.12.007.

[235] T. Takei, H. Nakahara, H. Ijima, and K. Kawakami, “Synthesis of a chitosan derivative soluble at neutral pH and gellable by freeze–thawing, and its application in wound care,” *Acta Biomater.*, vol. 8, no. 2, pp. 686–693, Feb. 2012, doi: 10.1016/j.actbio.2011.10.005.

[236] W. Fan, W. Yan, Z. Xu, and H. Ni, “Formation mechanism of monodisperse, low molecular weight chitosan nanoparticles by ionic gelation technique,” *Colloids Surfaces B Biointerfaces*, vol. 90, pp. 21–27, Feb. 2012, doi: 10.1016/j.colsurfb.2011.09.042.

[237] A. R. Dudhani and S. L. Kosaraju, “Bioadhesive chitosan nanoparticles: Preparation and characterization,” *Carbohydr. Polym.*, vol. 81, no. 2, pp. 243–251, Jun. 2010, doi: 10.1016/j.carbpol.2010.02.026.

[238] D. J. Sullivan, M. Cruz-Romero, T. Collins, E. Cummins, J. P. Kerry, and M. A. Morris, “Synthesis of monodisperse chitosan nanoparticles,” *Food Hydrocoll.*, vol. 83, pp. 355–364, Oct. 2018, doi: 10.1016/j.foodhyd.2018.05.010.

[239] C. Mattu, R. Li, and G. Ciardelli, “Chitosan nanoparticles as therapeutic protein nanocarriers: The effect of ph on particle formation and encapsulation efficiency,” *Polym. Compos.*, vol. 34, no. 9, pp. 1538–1545, Sep. 2013, doi: 10.1002/pc.22415.

[240] Z.-X. Tang, J.-Q. Qian, and L.-E. Shi, “Preparation of chitosan nanoparticles as carrier for immobilized enzyme,” *Appl. Biochem. Biotechnol.*, vol. 136, no. 1, pp. 77–96, Jan. 2007, doi: 10.1007/BF02685940.

[241] M. Hadidi, S. Pouramin, F. Adinepour, S. Haghani, and S. M. Jafari, “Chitosan nanoparticles loaded with clove essential oil: Characterization, antioxidant and antibacterial activities,” *Carbohydr. Polym.*, vol. 236, p. 116075, May 2020, doi: 10.1016/j.carbpol.2020.116075.

[242] M. R. de Moura, F. A. Aouada, and L. H. C. Mattoso, “Preparation of chitosan nanoparticles using methacrylic acid,” *J. Colloid Interface Sci.*, vol. 321, no. 2, pp. 477–483, May 2008, doi: 10.1016/j.jcis.2008.02.006.

[243] R. Athavale *et al.*, “Tuning the surface charge properties of chitosan nanoparticles,” *Mater. Lett.*, vol. 308, p. 131114, Feb. 2022, doi: 10.1016/j.matlet.2021.131114.

[244] G. Thandapani, S. P. P., S. P.N., and A. Sukumaran, “Size optimization and in vitro biocompatibility studies of chitosan nanoparticles,” *Int. J. Biol. Macromol.*, vol. 104,

pp. 1794–1806, Nov. 2017, doi: 10.1016/j.ijbiomac.2017.08.057.

[245] Y. Gokce, B. Cengiz, N. Yildiz, A. Calimli, and Z. Aktas, “Ultrasonication of chitosan nanoparticle suspension: Influence on particle size,” *Colloids Surfaces A Physicochem. Eng. Asp.*, vol. 462, pp. 75–81, Nov. 2014, doi: 10.1016/j.colsurfa.2014.08.028.

[246] K. Edsman and H. Hägerström, “Pharmaceutical applications of mucoadhesion for the non-oral routes,” *J. Pharm. Pharmacol.*, vol. 57, no. 1, pp. 3–22, Feb. 2010, doi: 10.1211/0022357055227.

[247] J. B. da Silva, R. S. dos Santos, M. B. da Silva, G. Braga, M. T. Cook, and M. L. Bruschi, “Interaction between mucoadhesive cellulose derivatives and Pluronic F127: Investigation on the micelle structure and mucoadhesive performance,” *Mater. Sci. Eng. C*, vol. 119, p. 111643, Feb. 2021, doi: 10.1016/j.msec.2020.111643.

[248] M. Davidovich-Pinhas and H. Bianco-Peled, “Mucoadhesion: a review of characterization techniques,” *Expert Opin. Drug Deliv.*, vol. 7, no. 2, pp. 259–271, Feb. 2010, doi: 10.1517/17425240903473134.

[249] D. Dodou, P. Breedveld, and P. A. Wieringa, “Mucoadhesives in the gastrointestinal tract: revisiting the literature for novel applications,” *Eur. J. Pharm. Biopharm.*, vol. 60, no. 1, pp. 1–16, May 2005, doi: 10.1016/j.ejpb.2005.01.007.

[250] M. C. Bonferoni *et al.*, “Comparison of different in vitro and ex vivo methods to evaluate mucoadhesion of glycol-palmitoyl chitosan micelles,” *J. Drug Deliv. Sci. Technol.*, vol. 20, no. 6, pp. 419–424, 2010, doi: 10.1016/S1773-2247(10)50073-X.

[251] M. Jelkmann, C. Leichner, C. Menzel, V. Kreb, and A. Bernkop-Schnürch, “Cationic starch derivatives as mucoadhesive and soluble excipients in drug delivery,” *Int. J. Pharm.*, vol. 570, p. 118664, Oct. 2019, doi: 10.1016/j.ijpharm.2019.118664.

[252] A. Bernkop-Schnürch, A. Weithaler, K. Albrecht, and A. Greimel, “Thiomers: Preparation and in vitro evaluation of a mucoadhesive nanoparticulate drug delivery system,” *Int. J. Pharm.*, vol. 317, no. 1, pp. 76–81, Jul. 2006, doi: 10.1016/j.ijpharm.2006.02.044.

[253] P. M. Raj, R. Raj, A. Kaul, A. K. Mishra, and A. Ram, “Biodistribution and targeting potential assessment of mucoadhesive chitosan nanoparticles designed for ulcerative colitis via scintigraphy,” *RSC Adv.*, vol. 8, no. 37, pp. 20809–20821, 2018, doi: 10.1039/C8RA01898G.

[254] R. S. Dave, T. C. Goostrey, M. Ziolkowska, S. Czerny-Holownia, T. Hoare, and H. Sheardown, “Ocular drug delivery to the anterior segment using nanocarriers: A mucoadhesive/mucopenetrative perspective,” *J. Control. Release*, vol. 336, pp. 71–88, Aug. 2021, doi: 10.1016/j.jconrel.2021.06.011.

[255] F. Sami El-banna, M. E. Mahfouz, S. Leporatti, M. El-Kemary, and N. A. N. Hanafy, “Chitosan as a Natural Copolymer with Unique Properties for the Development of Hydrogels,” *Appl. Sci.*, vol. 9, no. 11, p. 2193, May 2019, doi: 10.3390/app9112193.

[256] C.-A. Lee, B.-S. Kim, and C.-W. Cho, “Quantitative evaluation of mucoadhesive

polymers to compare the mucoadhesion," *J. Pharm. Investig.*, vol. 46, no. 2, pp. 189–194, 2016, doi: 10.1007/s40005-016-0233-4.

[257] A. J. Coutinho, S. A. Costa Lima, C. M. M. Afonso, and S. Reis, "Mucoadhesive and pH responsive fucoidan-chitosan nanoparticles for the oral delivery of methotrexate," *Int. J. Biol. Macromol.*, vol. 158, pp. 180–188, 2020, doi: https://doi.org/10.1016/j.ijbiomac.2020.04.233.

[258] P. Mukhopadhyay, R. Mishra, D. Rana, and P. P. Kundu, "Strategies for effective oral insulin delivery with modified chitosan nanoparticles: A review," *Prog. Polym. Sci.*, vol. 37, no. 11, pp. 1457–1475, Nov. 2012, doi: 10.1016/j.progpolymsci.2012.04.004.

[259] N. Thirawong, R. A. Kennedy, and P. Sriamornsak, "Viscometric study of pectin–mucin interaction and its mucoadhesive bond strength," *Carbohydr. Polym.*, vol. 71, no. 2, pp. 170–179, Jan. 2008, doi: 10.1016/j.carbpol.2007.05.026.

[260] N. Sahatsapan, T. Rojanarata, T. Ngawhirunpat, P. Opanasopit, and P. Tonglairoum, "6-Maleimidohexanoic acid-grafted chitosan: A new generation mucoadhesive polymer," *Carbohydr. Polym.*, vol. 202, pp. 258–264, 2018, doi: https://doi.org/10.1016/j.carbpol.2018.08.119.

[261] C.-H. Chen, Y.-S. Lin, S.-J. Wu, and F.-L. Mi, "Mutlifunctional nanoparticles prepared from arginine-modified chitosan and thiolated fucoidan for oral delivery of hydrophobic and hydrophilic drugs," *Carbohydr. Polym.*, vol. 193, pp. 163–172, Aug. 2018, doi: 10.1016/j.carbpol.2018.03.080.

[262] Y.-H. Lin, C.-H. Chang, Y.-S. Wu, Y.-M. Hsu, S.-F. Chiou, and Y.-J. Chen, "Development of pH-responsive chitosan/heparin nanoparticles for stomach-specific anti-Helicobacter pylori therapy," *Biomaterials*, vol. 30, no. 19, pp. 3332–3342, Jul. 2009, doi: 10.1016/j.biomaterials.2009.02.036.

[263] N. Nikogeorgos, P. Efler, A. B. Kayitmazer, and S. Lee, "'Bio-glues' to enhance slipperiness of mucins: improved lubricity and wear resistance of porcine gastric mucin (PGM) layers assisted by mucoadhesion with chitosan," *Soft Matter*, vol. 11, no. 3, pp. 489–498, 2015, doi: 10.1039/C4SM02021A.

[264] N. Nikogeorgos, N. J. Patil, B. Zappone, and S. Lee, "Interaction of porcine gastric mucin with various polycations and its influence on the boundary lubrication properties," *Polymer (Guildf).*, vol. 100, pp. 158–168, Sep. 2016, doi: 10.1016/j.polymer.2016.08.030.

[265] M. Ahmad, C. Ritzoulis, W. Pan, and J. Chen, "Biologically-relevant interactions, phase separations and thermodynamics of chitosan–mucin binary systems," *Process Biochem.*, vol. 94, pp. 152–163, Jul. 2020, doi: 10.1016/j.procbio.2020.04.003.

[266] B. Á. Szilágyi, A. Mammadova, B. Gyarmati, and A. Szilágyi, "Mucoadhesive interactions between synthetic polyaspartamides and porcine gastric mucin on the colloid size scale," *Colloids Surfaces B Biointerfaces*, vol. 194, p. 111219, Oct. 2020, doi: 10.1016/j.colsurfb.2020.111219.

Published Papers

1. **Ruiz-Pulido, G.**, & Medina, D. I. (2021). An overview of gastrointestinal mucus rheology under different pH conditions and introduction to pH-dependent rheological interactions with PLGA and chitosan nanoparticles. *European Journal of Pharmaceutics and Biopharmaceutics*, 159, 123–136. doi:10.1016/j.ejpb.2020.12.013

2. **Ruiz-Pulido, G.**, Quintanar-Guerrero, D., Serrano-Mora, L. E., & Medina, D. I., Triborheological Analysis of Reconstituted Gastrointestinal Mucus / Chitosan:TPP Nanoparticles System to Study Mucoadhesion Phenomenon under Different pH Conditions. *Polymers*, *14*(22), 4978. doi: 10.3390/polym14224978.

3. **Ruiz-Pulido, G.**, Medina, D. I., Barani, M., Rahdar, A., Sargazi, G., Baino, F., & Pandey, S. (2021). Nanomaterials for the Diagnosis and Treatment of Head and Neck Cancers: A Review. *Materials*, *14*(13), 3706. doi:10.3390/ma14133706

Collaborations

1. Aguilar-Pérez, K.M., Avilés-Castrillo, J. I., & **Ruiz-Pulido, G**. (2020). Nano-sorbent materials for pharmaceutical-based wastewater effluents - An overview. *Case Studies in Chemical and Environmental Engineering*, *2*(10.1016/j.cscee.2020.100028), 100028. doi:10.1016/j.cscee.2020.100028
2. Aguilar-Pérez, K.M., Avilés-Castrillo, J. I., **Ruiz-Pulido, G.**, Medina, D. I., Parra-Saldivar, R., & Iqbal, H. M. N. (2021). Nanoadsorbents in focus for the remediation of environmentally-related contaminants with rising toxicity concerns. *Science of The Total Environment*, *779*, 146465. doi:10.1016/j.scitotenv.2021.146465

3. Aguilar-Pérez, Katya M., **Ruiz-Pulido, G.**, Medina, D. I., Parra-Saldivar, R., & Iqbal, H. M. N. (2021). Insight of nanotechnological processing for nano-fortified functional foods and nutraceutical—opportunities, challenges, and future scope in food for better health. Critical Reviews in Food Science and Nutrition, 1–18. doi:10.1080/10408398.2021.2004994

4. Duque-Ossa, L. C., **Ruiz-Pulido, G.**, & Medina, D. I. (2021). Triborheological Study under Physiological Conditions of PVA Hydrogel/HA Lubricant as Synthetic System for Soft Tissue Replacement. *Polymers*, *13*(5), 746. doi:10.3390/polym13050746

5. Parsons, R. B., Kocinaj, A., **Ruiz Pulido, G.**, Prendergast, S. A., Parsons, A. E., Facey, P. D., & Hirth, F. (2022). Alpha-synucleinopathy reduces NMNAT3 protein levels and neurite formation that can be rescued by targeting the NAD+ pathway. *Human Molecular Genetics*, *31*(17), 2918–2933. doi:10.1093/hmg/ddac077

Conference Papers

1. **Ruiz-Pulido, G.**, & Medina, D. (2021). *Tribo-rheological analysis of reconstituted gastrointestinal porcine mucus under different pH conditions.* In *Proceedings of the Virtual 2021 AOCS Annual Meeting & Expo*. American Oil Chemists' Society (AOCS). doi:10.21748/am21.543

2. **Ruiz, G.**, & Medina, D. (2022). *Triborheological Analysis of Reconstituted Gastrointestinal Porcine Mucus / Polymeric Nanoparticles System for Studying Mucoadhesion*. In *Proceedings of 2022 AOCS Annual Meeting & Expo*. American Oil Chemists' Society (AOCS). doi:10.21748/KHSF3022

Curriculum Vitae

Dr. Gustavo Ruiz-Pulido earned his B.S. in Biotechnology Engineering in the concentration of Molecular Diagnostics from Tecnológico de Monterrey – Campus Estado de México (2016). The next year, Dr. Gustavo received a ‘CONACYT - Gobierno del Estado de Veracruz 2017’ scholarship to pursue a master’s degree abroad (2017) to study in London, United Kingdom. He obtained his Master's in Biopharmaceuticals with Merit from King's College London (2018) with the dissertation entitled 'Analysis of the effect of α-synuclein upon the expression profile of NAD+ biosynthesis pathway enzymes using an in vitro cell-line model'. Then, he moved to Mexico City to enrolled in the PhD at Tecnológico de Monterrey – Campus Estado de México with a scholarship received by ‘CONACYT’ and Tecnológico de Monterrey. He obtained his PhD degree in Nanotechnology with the dissertation entitled 'Triborheological Analysis of Reconstituted Gastrointestinal Porcine Mucus / Chitosan:TPP Nanoparticles System for studying mucoadhesion under different pH conditions'.